SIMULATION OF LAKES AND SURFACE WATER HEAT EXCHANGERS FOR DESIGN OF SURFACE WATER HEAT PUMP SYSTEMS

By

KRISHNA CONJEEVARAM BASHYAM

Bachelor of Engineering in Mechanical Engineering

Anna University

Chennai, Tamil Nadu, India

2009

Submitted to the Faculty of the
Graduate College of the
Oklahoma State University
in partial fulfillment of
the requirements for
the Degree of
MASTER OF SCIENCE
May, 2013

SIMULATION OF LAKES AND SURFACE WATER HEAT EXCHANGERS FOR DESIGN OF SURFACE WATER HEAT PUMP SYSTEMS

Thesis Approved:

Dr. Jeffrey D. Spitler

Thesis Adviser

Dr. Daniel E. Fisher

Dr. David G. Lilley

ACKNOWLEDGEMENTS

I would first like to extend my sincere gratitude to my advisor and mentor Dr. Jeffrey D. Spitler, for his support, encouragement and constructive guidance that he offered throughout my Graduate program. I could not simply express how much I have learnt from your technical expertise and your profound knowledge. I thank you very much for your advice, which enabled me to think critically and 'approach' a research problem. I consider it as a great privilege to have worked under your supervision.

My sincere appreciation also extends to my advisory committee members Dr. Daniel E. Fisher and Dr. David G. Lilley. Their coursework, guidance and discussions have helped a lot with my research work. I would also to like to acknowledge the financial support from the US Department of Energy, American Society of Heating, Refrigerating and Air-Conditioning Engineers (ASHRAE) and the School of Mechanical and Aerospace Engineering, OSU.

I would like to extend my thanks to my colleague and project teammate Manojkumar Selvakumar. The many an hour we have spent working together on this project will be greatly cherished. I would also like to thank Lu Xing for initially helping me with my design tool, Matt Mitchel for providing the required experimental data, Edwin Lee and James Cullin for their help and guidance with my research work. My, thanks to all my friends here in OSU, the BETSRG group, my roommates and my friends back in India. Special thanks to Anand Govindarajan, Kumar, Ram, Veera, Naren, Sridhar, Fazal, Renold and Bala. I appreciate their friendship, motivation and constant help.

My heartfelt thanks to my entire family, who are always there to advice and motivate me whenever I am in need. I would like to recognize my family members Dr. Devanathan, A.J. Raghavan, A.J. Murali, C.S. Sripadarajan, C.R. Kamala, Rema and Venakatesh for their constant encouragement and advice.

I am forever grateful to my parents Shri. C.R. Bashyam and Smt. A.J. Radhabai Bashyam for their unconditional love and support. I am thankful to all the values and lessons, which they have instilled into me, and I wish to dedicate this thesis to them. I would also like to thank my brother C.B. Sriram for his support and encouragement.

Finally, I thank God Almighty for His blessings, which made everything possible.

Name: KRISHNA CONJEEVARAM BASHYAM

Date of Degree: MAY 2013

Title of Study: SIMULATION OF LAKES AND SURFACE WATER HEAT EXCHANGERS FOR DESIGN OF SURFACE WATER HEAT PUMP SYSTEMS

Major Field: MECHANICAL ENGINEERING

Abstract:

Surface Water Heat Pump (SWHP) system utilize surface water bodies, such as ponds, lakes, rivers, and the sea, as heat sources and/or sinks. These systems may be open-loop, circulating water between the surface water body and a heat exchanger on dry land, or closed-loop, utilizing a submerged surface water heat exchanger (SWHE). Both types of SWHP systems have been widely used, but little in the way of design data, design procedures, or energy calculation procedures is available to aid engineers in the design and analysis of these systems. For either type of SWHP system, the ability to predict the evolution of lake temperature with time is an important aspect of needed design and energy analysis procedures. This thesis describes the development and validation of a lake model that is coupled with a surface water heat exchanger model to predict both the lake dynamics (temperature, stratification, ice/snow cover) and the heat transfer performance of different types of SWHE. This one-dimensional model utilizes a detailed surface heat balance model at the upper boundary, a sediment conduction heat transfer model at the lower boundary, and an eddy diffusion model to predict transport within the lake. The lake model is implemented as part of the developed software design tool, which can be used as an aid in the sizing of SWHE used in closed loop SWHP systems.

TABLE OF CONTENTS

Chapter Page

Chapter Page

Chapter Page

LIST OF TABLES

Table Page

Table Page

Table Page

LIST OF FIGURES

Figure Page

Figure Page

Figure Page

NOMENCLATURE

A = lake horizontal area, [m^2]

C_d = drag coefficient [-]

C_p = specific heat capacity, [J/kg·°C]

d = heat exchanger tube diameter, [m]

d_{c_o} = heat exchanger outside coil diameter, [m]

De = Dean number [-]

EFT = heat exchanger entering fluid temperature, [°C]

$ExFT$ = heat exchanger exit fluid temperature, [°C]

g = acceleration due to gravity, [m/s^2]

H_{ice} = ice thickness, [m]

$H_{ice,\ new}$ = New ice thickness due to congelation ice growth, [m]

H_{snow} = Snow thickness, [m]

$H_{snow\text{-}ice}$ = Thickness of snow ice, [m]

h_c = surface convective heat transfer coefficient, [$W/m^2 \cdot K$]

h_{fg} = Latent heat of vaporization, [J/kg]

h_{lw} = long wave radiative heat transfer coefficient, [$W/m^2 \cdot K$]

K = thermal conductivity, [$W/m \cdot K$]

k_z = vertical eddy diffusion coefficient, [m^2/day]

k_{zmax} = the maximum hypolimnion eddy diffusion coefficient, [m^2/day]

L_{freeze} = latent heat of freezing of ice, [J/kg]

$\dot{m}$ = mass flow rate, [kg/s]

m_{ice} = mass of ice surrounding the heat exchanger tube, [kg]

m_{water} = mass of water melted from ice surrounding the heat exchanger tube, [kg]

N = stability frequency or the Brunt Vaisala frequency, [s^{-1}]

$N_{circuit}$ = the number of heat exchanger circuits placed in the lake [-]

Nu = Nusselt number [-]

PE = Potential energy, [J]

$Pitch_{ratio}$ = Coil pitch ratio [-]

Pr = Prandtl number [-]

Q = internal distribution of heat to each water layer due to the absorption of solar radiation, sediments heat transfer from heat exchangers in the water column, [W/m^3]

q_{coil} = heat transfer between the heat exchanger fluid and ice/water interface, [W]

$q_{deficit}$ = sensible heat deficit in the sub-cooled water layer converted into latent heat of ice, [W]

q_{lat} = latent heat to freeze the water or melt the ice formed at each segment, [W]

q_{sc} = sensible heat to sub-cool the ice during freezing at each segment, [W]

q_{sh} = sensible heat to superheat the water during the melting period at each segment, [W]

q_{wat} = heat transfer between the surrounding lake water and the ice/water interface, [W]

q''_{c} = convective heat flux from the lake surface to the atmosphere, [W/m^2]

q''_{e} = evaporative heat flux from the lake surface, [W/m^2]

q_{hx} = heat transfer from the heat exchanger to the surface water body, [W]

q''_{lw} = net long wave radiation incident on the lake surface, [W/m^2]

$q''_{net\text{-}surface}$ = net heat flux on the lake surface, [W/m^2]

$q''_{net}(z)$ = net heat flux at the depth z inside the water column, [W/m^2]

$q''_{sediment}$ = heat flux from sediment to water, [W/m^2]

$q''_{sw}(z)$ = incoming short wave radiative heat flux absorbed at the depth z, [W/m^2]

$q''_{sw\text{-}surface}$ = heat flux due to short wave radiation incident on the lake surface, [W/m^2]

r = radius of the heat exchanger tube, [m]

ρ' = surface reflectivity coefficient [-]

R, Res = Thermal resistances, [1/K]

Ra^* = modified Rayleigh number [-]

t = time, [s]

T = temperature, [°C]

TKE = Total kinetic energy, [J]

UA = global heat transfer coefficient, [W/K]

V_{epi} = Volume of the epilimnion, [m^3]

V_z = Volume of the layer below the epilimnion, [m^3]

$V_{p,air}$ = Vapor pressure at air temperature [Pa]

$V_{p,surface}$ = Vapor pressure at water surface temperature [Pa]

W = Wind speed, [m/s]

W_{str} = Wind sheltering coefficient [-]

w_{air} = humidity ratio of air, [kg water/kg dry air]

$w_{surface}$ = humidity ratio of saturated air at the lake surface, [kg water/kg dry air]

z = lake depth, [m]

z_{epi} = Thickness of the epilimnion layer, [m]

$z_{M, epi}$ = Depth of the center of mass of the epilimnion, [m]

$\Delta z_{M, z}$ = Distance from the layers center of mass to the bottom of the epilimnion, [m]

Δx = horizontal center to center distance between adjacent heat exchanger tubes, [mm]

Δy = vertical center to center distance between adjacent heat exchanger tubes, [mm]

α_{sed} = sediment thermal diffusivity, [m^2/day]

β = thermal expansion coefficient, [K^{-1}]

β_w = water surface absorption coefficient = 0.4 [-]

ε = effectiveness of the heat exchanger [-]

ε_{water} = emissivity coefficient of water = 0.97 [-]

σ = Stefan Boltzmann constant, [$5.67 * 10^{-8}$ $W/m^2 \cdot K^4$]

μ = extinction coefficient of water, [m^{-1}]

ρ = density, [Kg/m^3]

θ = ice/water overlapping angle, [radians]

τ = Wind shear stress, [N/m^2]

Subscripts

fluid = heat exchanger fluid

freeze = freezing point

hx = Heat exchanger

i = inside

o = outside

sed = sediment

weq = water equivalent

ws = water-sediment layer

CHAPTER 1

INTRODUCTION

1.1 Overview

Surface Water Heat Pump (SWHP) system utilize surface water bodies, such as ponds, lakes, rivers, and the sea, as heat sources and/or sinks. These systems may be open-loop, circulating water between the surface water body and a heat exchanger on dry land, or closed-loop, utilizing a submerged surface water heat exchanger (SWHE). Open-loop surface water heat pump (SWHP) systems utilizing surface water bodies as a heat source or sink for heat pump applications have been in use since the 1940s (Mitchell and Spitler 2013). Open-loop systems circulate water between the surface water body and a heat exchanger on dry land. Conversely, closed loop SWHP systems use surface water heat exchangers (SWHE) submerged in the water body. SWHE are most commonly coils of high-density polyethylene (HDPE) piping and metal flat plate heat exchangers. Closed loop SWHP systems have been installed for commercial purposes since the 1970s (Johansson 1983). Though the value and efficiency of SWHP systems are recognized, there is a paucity of standard design procedures, guidelines and energy calculation procedures to aid engineers to efficiently design and analyze the system.

The temperature characteristics of a surface water body are of prime interest for an engineer designing a SWHP system, as the water temperatures have a direct effect on the heat transfer performance of an SWHE, and, hence, its required size. Due to variations in morphology[1] and local climatic conditions, temperature and stratification characteristics of every surface water body are different. Furthermore, temperatures may vary significantly from year to year depending on yearly variations in weather conditions. Unlike surface weather conditions, for which statistical temperature and humidity data, based on 30 years of measurements are readily available (ASHRAE 2009) there is no equivalent data available for surface water bodies. Only very limited water temperature data sets are available and year-to-year variations further complicate the use of such historical data for design purposes. A possible alternative approach is to use a lake simulation model coupled with either typical meteorological year-type weather data, or historical meteorological data, which, by comparison, are much more widely available.

In a closed-loop SWHP system, the actual performance of SWHEs submerged in the lake depend not only on the lake temperatures to which they are exposed, but also on the overall heat transfer coefficient of the heat exchanger. Unlike a conventional heat exchanger, the exterior convective resistance is buoyancy-driven, and so depends on the density difference between the water at the heat exchanger surface and the surrounding lake. Because the water density varies non-linearly with temperature and will usually pass through the maximum density point (3.8°C (38.8°F)) under heating conditions, the exterior convective resistance will usually vary significantly over the year. In addition, ice formation may occur under low temperature conditions and high heat extraction rates. The ice formation affects the heat transfer, and creates a buoyant force against which the heat exchangers must be anchored. Both of these phenomena can be treated with a simulation, but may be difficult to treat with other simpler methods.

[1] Morphology refers to the geometric characteristics of the lake – shape, depth, lake bottom roughness. When quantified, this is sometimes referred to as lake morphometry. (Håkanson 1981).

It may also be necessary to assess the effects of the SWHP system on the surface water body. Although in almost all cases, SWHP systems will have negligible effects on the surface water body, it is possible that excessive heat extraction or heat rejection by the SWHP system relative to the lake size could adversely affect the lake ecosystem or adversely affect the capacity and performance of the SWHP system. Again, a simulation-based approach has the possibility of estimating these effects.

A lake model that can predict the evolution of lake temperature with time and depth, the time-varying performance of the SWHE, and the effects of the SWHP system on the lake will facilitate design and energy analysis of SWHP systems. For such a model to be useful to practicing engineers, the amount of effort that can be spent in characterizing a specific lake is necessarily limited, as is the amount of computing time that can be spent.

1.2 Objectives and organization:

This thesis has two main objectives,

1. To develop an experimentally validated lake model that treats both the lake and the surface water heat exchanger but which has reasonable levels of required input data and computational effort. The developed model should have the ability to be used in lakes of various sizes.
2. To develop a software design tool which utilizes the developed lake model to aid engineers in sizing of SWHE in the design of SWHP systems

Part of this project, which includes the development of the lake model has been developed in collaboration with my colleague Manojkumar Selvakumar. Hence, most of the sections in Chapter 2 of this thesis will be similar to the lake model development chapter in Selvakumar (2013) thesis documentation. Chapter 2 presents the detailed development of the one-dimensional numerical lake model complete with detailed background and literature review. Validation results of the lake model against the experimental results from Ice Lake in Minnesota and a research

pond maintained by Oklahoma State University are analyzed. Chapter 3 presents a detailed discussion on the surface water heat exchanger (SWHE) model development and the validation of the model with the experimental data from a spiral-helical coil heat exchanger. Chapter 3 has been written in collaboration with my colleague Manojkumar Selvakumar, hence, this chapter will be identical to the SWHE model development chapter in Selvakumar (2013). Chapter 4 presents a literature about eleven eddy diffusion and seven surface convection/evaporation sub-models, and their sensitivity analysis on lake temperature prediction. Chapter 5 describes the model limitations for both the lake model and the surface water heat exchanger model. Chapter 6 provides an overview of the developed design tool for surface water heat pump systems. Chapter 7 presents the conclusions and identifies the possible areas for future research.

CHAPTER 2

DEVELOPMENT OF A ONE DIMENSIONAL LAKE SIMULATION MODEL

The development of the one-dimensional lake model has been performed in collaboration with my colleague Manojkumar Selvakumar. Hence, several sections of this chapter will be similar to the lake model development chapter in Selvakumar (2013) thesis documentation.

2.1 Background

The thermal structure of a surface water body is determined by carefully estimating the available heat energy input and losses through the water body and the distribution of that heat within the water column (Hondzo and Stefan 1993b). Hence, a good understanding of different heat fluxes and stratification dynamics is necessary in order to predict good temperature characteristics of a surface water body. The different heat transfer and transport mechanisms are discussed in the sections below.

2.1.1 Heat transfer mechanisms in surface water bodies

In unfrozen lakes, solar irradiation is usually the main heating mechanism. Some of the incident solar radiation is absorbed at the water body surface; the remaining energy is transmitted through the water body, where it is absorbed in the water or at the bottom. Penetration of the solar radiation through the depth depends on the transmissivity of the water, which in turn depends on its turbidity. Evaporation is the main cooling mechanism for ponds and lakes. Surface convection heat transfer and longwave radiation may heat or cool the water body depending on the relative temperatures of the water body surface and the surroundings.

Heat transfer from the ground below the water body (referred to as sediment heat transfer) can become highly significant in winter especially during the times when the water body freezes at the surface (Fang and Stefan 1996).Though often negligible, heat transfer to/from surface water heat exchangers may also be important. Heat transfer mechanisms within the lake are discussed in the next section.

2.1.2 Heat transport mechanisms in surface water bodies

The distribution of mass, energy and momentum in a surface water body are due to different hydrodynamic transport processes including advection and diffusion. Advection refers to the transport of mass, momentum and energy by fluid's bulk motion. Diffusion in surface water bodies takes place by mixing of water mass due to turbulent mixing (turbulent diffusion) and molecular diffusion. Molecular diffusion is a transport process at microscopic scales due the scattering of particles by random molecular motion. Turbulent diffusion results from the random motion of water parcels in a turbulent flow. Diffusion by turbulent mixing is of several orders magnitude greater than molecular diffusion. Turbulent diffusion is characterized by irregular, random fluctuations due to turbulent eddies in the water system. Hence, turbulent diffusion can also be referred as eddy diffusion. Several mixing mechanisms responsible for the hydrodynamic transport in a surface water body includes surface wind stress, internal waves, shear waves, inflows, outflows and various other mixing mechanisms. The formation and cause of these different mixing mechanisms on the surface water body and their effects on the water temperatures are discussed in detail by Imberger (1985). Figure 2-1 illustrates some of the heat transfer and mixing mechanisms for a typical surface water body with a heat exchanger installation.

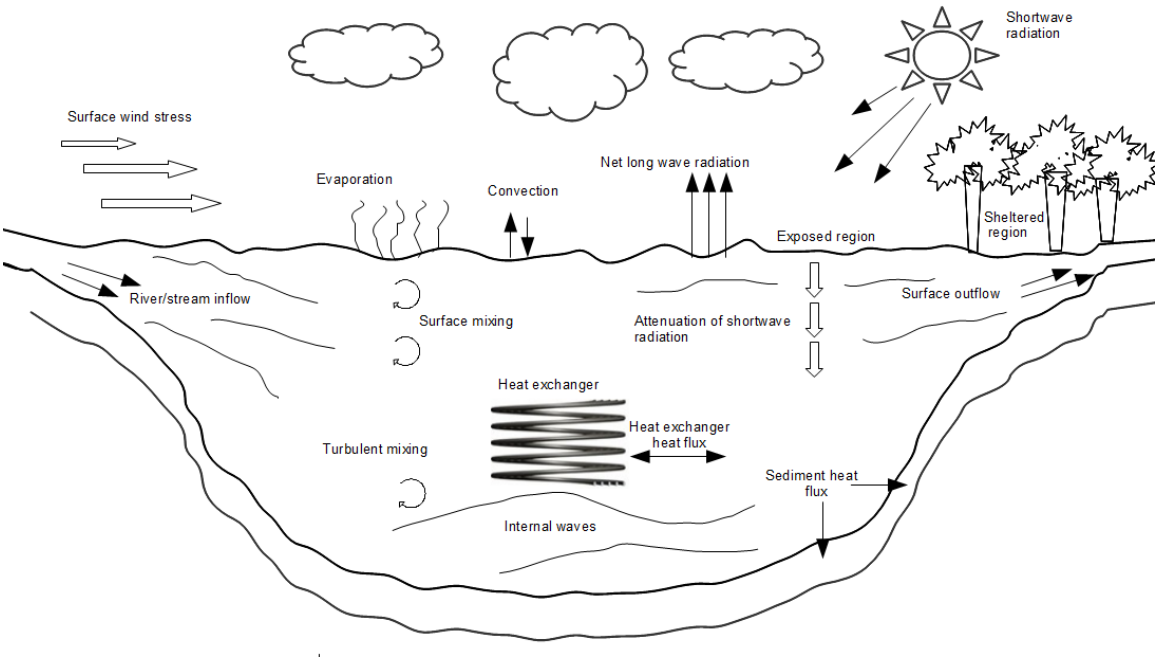

Figure 2- 1: Heat and temperature transport mechanism for a typical surface water body with a heat exchanger

2.1.3 Thermal stratification

For a lake during summer conditions, the formation of stratification is controlled by the balance between two phenomena: heat input at the surface leads to naturally stabilizing temperature and density gradients, and, surface wind generates turbulent energy that is destabilizing. Surface winds over a shallow water body may completely overwhelm the naturally occurring temperature-density gradients in the water column and cause it to mix completely. Hence, shallow ponds are often un-stratified for most of the year. Stratification is most commonly observed in deeper ponds and lakes where the wind induced mixing is restricted to a certain depth near the surface. This gives rise to a temperature profile with three distinct regions as illustrated with experimental data for a 16.6-hectare (41 acres) lake with maximum depth of 16 m (52.5 ft) in Figure 2-2:

- The epilimnion or upper mixed region characterized by well-mixed and relatively high water temperatures.

- Metalimnion or thermocline region: This transition region between the warm surface water and cooler bottom water is characterized by large temperature and density gradients.
- Hypolimnion or lower mixed region: This relatively cold, well-mixed region below the thermocline extends to the bottom of the surface water body. It tends to be undisturbed by the surface winds. Figure 2-2, shows the temperature variation along the depth for Ice Lake, a small lake (surface area 41 acres; maximum depth 16 m) situated in Minnesota on a summer day. The experimental temperature data for Ice Lake is obtained from an online source (WOW 2012).

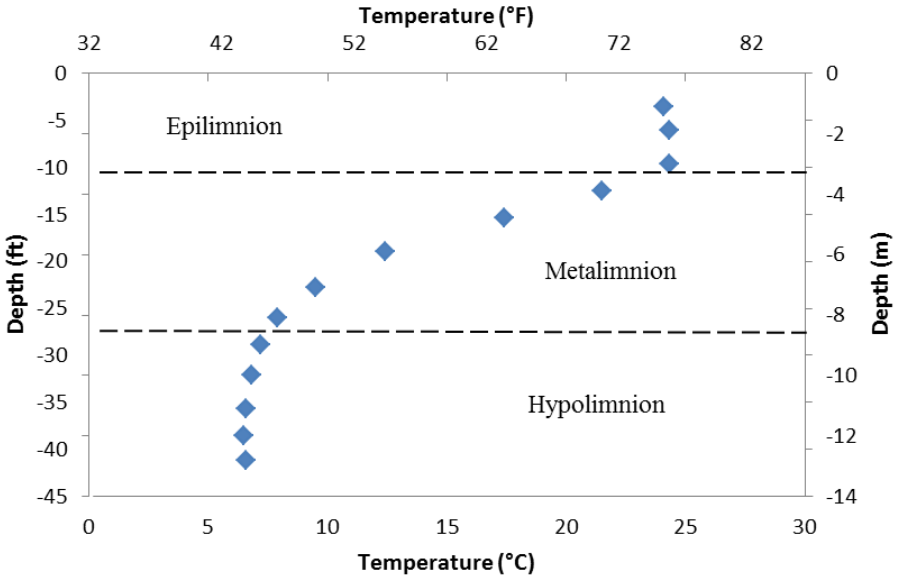

Figure 2- 2: Temperature profile for Ice Lake in Minnesota on July 31, 2002

Most lakes exhibit such distinct temperature stratification regions throughout the summer and most of the fall season. By late fall season, the lake surface temperature cools down, and the density gradient in the water column slowly diminishes. At this time, the turbulent energy from the surface wind is sufficient to completely de-stabilize or mix the entire water column. This phenomenon is called as turnover and during the turnover period, the temperature of the lakes

remains the same from the surface to the bottom. Lakes that develop surface ice cover exhibit the same phenomenon in the spring when the surface ice melts and as the temperature of the epilimnion approaches 3.8 °C (38.8 °F) (maximum density of water). Based on the period of occurrence they are called as spring/fall turnovers and most stratified lakes exhibit such turnover conditions at least once or twice annually.

2.2. Existing pond and lake models

Modeling of lakes and reservoirs to predict their temperature variations and water quality for environmental purposes has been a subject of research for many years. Numerous one-dimensional (Imberger, et al. 1978; Ford and Stefan 1980; Saloranta and Andersen 2007), two-dimensional (Hayter, et al. 1998; Ji, et al. 2001) and three-dimensional (Blumberg and Mellor 1987; Hamrick 1992) numerical models to name a few have been developed over the years to predict the water temperature and hence the water quality of different surface water bodies. Although two and three-dimensional lake models can potentially more accurately assess and determine the temperature distribution in a lake, given the inherent constraints on both engineer time and computational time, a one-dimensional lake model was deemed more practical, and hence only literature describing one-dimensional lake models are discussed here.

In addition to the one-dimensional models listed in the last paragraph, work has been carried out by a number of other authors (Tucker and Green 1977; Imberger, et al. 1978; McCormick and Scavia 1981; Sengupta, et al. 1981). Saloranta and Andersen (2004, 2007) have provided a detailed and readable account of one such comprehensive model. However, a lengthy research program directed by Professor H.G. Stefan at the University of Minnesota perhaps best illustrates the incremental developments in the field and will be discussed further below, as it and the Saloranta and Andersen (2004) work were heavily utilized for the development of the lake model. All of the lake models discretizes the lake into several depth layers to numerically calculate the

temperature profile and assumes the vertical temperature transport by eddy diffusion except for Ford and Stefan (1980) which assumes temperature transport by molecular diffusion.

Ford and Stefan (1980) initially developed a model to simulate temperatures and stratification in small lakes using an integral energy approach. This approach finds the depth where the turbulent kinetic energy from the wind balances the potential energy available from the natural stratification. This depth represents the upper mixed or epilimnion region and below this depth are the stratified metalimnion and hypolimnion regions. The model allowed only molecular diffusion in the thermocline and hypolimnion regions, but was able to predict the temperatures reasonably when validated against three lakes whose surface areas vary from (72- 447 acres) and depths from (9.1 – 27.4 m).

Riley and Stefan (1988) developed the MINLAKE program which utilizes a one-dimensional lake model based on the integral energy approach by Ford and Stefan (1980) to simulate temperatures and water quality to predict eutrophication in lakes. The model considers the effect of eddy diffusion for temperature transport and calculates separate eddy diffusion coefficients for the epilimnion and hypolimnion layers. The MINLAKE program was developed with an intention to be applicable in predicting both water temperatures and water quality for temperate lakes with different bathymetries. The model considers the effect of mixing, stratification, inflow and outflow in lakes but does not consider the formation of ice/snow cover on the lake surface.

Gu and Stefan (1990) enhanced the existing MINLAKE program to predict the lake temperature characteristics under ice and snow conditions. They considered the importance of sediment heat transfer, which were not previously considered in the earlier version of the MINLAKE models. They also calculated the new heat transfer rates between the lake surface and the atmosphere when the surface of the lake is frozen, thus extending the MINLAKE program to simulate year round lake temperatures. Gu and Stefan (1990) validated the enhanced MINLAKE model with the experimental temperatures from Lake Calhoun in Minnesota (surface area 403 acres; maximum depth 27m) with a very good level of accuracy. Ellis, et al. (1991) calculated the

eddy diffusion coefficients for lakes under ice/snow cover based on their measurements from a small lake in Minnesota. Fang and Stefan (1996) developed a correlation to predict the eddy diffusion coefficients for lakes under ice/snow cover based on the results from Ellis, et al. (1991).

The lake models discussed to this point does not consider the effects of surface water heat exchangers (SWHE) on surface water body temperatures. There have also been some less comprehensive lake models, which also model the performance and effects of SWHP system. Pezent and Kavanaugh (1990) developed a model to simulate lakes as heat sources/sinks for heat exchangers with water source heat pump systems based on the solar pond model by Srinivasan and Guha (1987) and river/reservoir model by Raphael (1962). The model was developed to predict lake temperatures in the southern warm climatic regions. Hence, it does not consider the formation of surface ice on the water body. The lake is initially divided into three stratification regions (epilimnion, metalimnion and hypolimnion) with a pre-defined region thickness. The model does not consider the effects of wind stress on stratification and the mechanism of temperature transport by turbulent diffusion. The seasonal variation in the stratification is calculated based on experimental observations of certain lakes in Alabama. With all these assumptions, the model could only match the temperature profile for a lake in Alabama in the epilimnion and hypolimnion regions. It could not follow the experimental temperature profile in the thermocline region reasonably and had a maximum temperature difference of around 7 °C in the thermocline region.

Chiasson, et al. (2000) developed a one dimensional shallow pond model as a supplemental heat rejecter for ground source heat pump systems. The model includes the heat transfer effects by the heat exchanger in calculating the pond temperatures. The model was developed for shallow ponds that were assumed to be well mixed, thus there was no need to determine stratification. The pond heat exchangers were “slinky” configurations of HDPE pipe placed either horizontally or vertically in the pond.

2.3 Lake model development

As discussed above, one-dimensional lake models have been the subject of research for some years. The lake model developed in this paper follows the model structure outlined by Saloranta and Andersen (2007) and Riley and Stefan (1988). Unlike the models developed by previous authors, this lake model has a different intended application, which has had some impact on the approach taken.

When considering the appropriate level of detail for the lake model, there are two primary considerations – the availability of validation data and the intended application. As noted by Riley and Stefan (1988) when developing a daily time step one-dimensional model, development of multi-dimensional models with much shorter time steps was not supported by available data (typically consisting, at best, of daily temperature profiles measured when the lake surface is not frozen). That remains the situation today, and there are surprisingly few lakes for which continuous daily measurements are available. In no case have the authors found anything approaching a grid of measurements that might help establish actual horizontal distributions of temperature at any time in a lake.

With regard to intended application, the model is developed for use by HVAC design engineers to both design and perform energy analysis on SWHP systems. The actual users of the model are expected to have limited knowledge of lake limnology and the bathymetry of specific lakes. In addition, the model must have reasonable computational speed in order to be used as part of the overall design and energy analysis tasks faced by the design engineer. The model should have reasonable accuracy, but assessing the accuracy for a model that calculates an average temperature vs. depth using temperature measurements made from a single spot on the lake surface is inherently difficult.

Therefore, the following approximations have been made in order to provide reasonable computational speed and reasonable accuracy, given the constraints discussed above:

1. The lake model is one-dimensional with a daily time step. Surface water heat exchangers in the lake may be modeled on shorter time steps, using the daily average lake temperature at a specific depth as a boundary condition.
2. Inflows and ouflows are neglected.
3. The effects of local wind sheltering and solar shading due to vegetation or buildings are neglected.
4. The lake surface level is approximated as being constant; changes due to evaporation, precipitation, and varying inflows and outflows are not considered.
5. Turbidity in the lake, which may change over the year in a real lake is assumed to have a constant user-specified value.

2.3.1 Governing equations

The one dimensional vertical advection-diffusion equation to predict the temperature distribution for a horizontally mixed and vertically stratified lake can be written as (Saloranta and Andersen 2007),

$$A\frac{\partial T}{\partial t} = \frac{\partial}{\partial z}\left(k_z A\frac{\partial T}{\partial z}\right) + A\frac{Q}{\rho_w C_p} \qquad (2.1)$$

Where,

A is the horizontal area of the lake in [m^2]

T is the water temperature, which is a function of both depth and time in [°C]

k_z is the vertical eddy diffusion coefficient in [m^2/day]

Q is the heating rate of a surface water body at a depth z by solar radiation, sediments and heat exchangers in [W/m^3]

ρ_w is the density of water in [kg/m^3] and

C_p is the specific heat capacity of water [J/kg·°C]

The governing equation was developed to its final form by considering constant values for water density and specific heat (Dake and Harleman 1969). Later authors (Saloranta and Andersen 2007) have used this formulation with temperature-varying water properties. Use of temperature-dependent water properties with this form results in a slight energy imbalance. The effect of water temperatures due to this energy imbalance is explained in Appendix D.

The net heat energy input to a surface water body includes the heat exchange with the atmosphere and within the water column. Hence, the heating rate (Q) for the surface water body has to be calculated separately at the water body surface and within the water column. The net heat added at the surface of the water body is,

$$Q = \frac{q"_{net-surface} * A_{surface}}{V_{surface}} \quad (2.2)$$

Where,

$q"_{net\text{-}surface}$ is the net heat flux available at the surface of the water body in [W/m^2]

$A_{surface}$ is the surface area of the water body in [m^2] and

$V_{surface}$ is the volume of the surface layer of the water body in [m^3].

Description on lake surface, surface layer and volume of the surface layer are described under the "spatial discretization" section. The net heat flux on the lake surface during open water conditions $(q"_{net\text{-}surface})$ is calculated by the surface heat balance between the incoming shortwave and long wave radiation heat fluxes on the water surface and the outgoing convection, evaporation and back radiation heat fluxes from the water surface to the atmosphere. The net heat flux is then treated as a volumetric heat gain in the top layer. When the lake surface is frozen, the surface heat balance is modified described in the "modeling of ice and snow" section.

$$q"_{net-surface} = q"_{sw-surface} + q"_{lw} + q"_{conv} - q"_{e} \quad (2.3)$$

Where,

$q"_{net\text{-}surface}$ is the net heat flux on the lake surface in [W/m^2]

$q''_{sw\text{-}surface}$ is the heat flux due to short wave radiation incident on the pond surface in [W/m^2]

q''_{lw} is the heat flux due to net long wave radiation on the pond surface in [W/m^2]

q''_{conv} is the convective heat flux from the pond surface to the atmosphere in [W/m^2]

q''_{e} is the evaporative heat flux from the pond surface to the atmosphere in [W/m^2]

The mechanism of heat exchange with the atmosphere at the lake surface differs when the surface of the water body is frozen or covered with snow. The calculation of the net surface heat flux during surface freezing conditions is described in the "modeling of ice and snow" section.

The heating rate at a particular depth z_1 inside the water body is calculated as,

$$Q = \frac{q''_{sw-abs}(z_1) * A(z_1) + q''_{sediment}(z_1) * A(z_1) + q_{hx}}{V(z_1)} \qquad (2.4)$$

Where,

$q''_{sw\text{-}abs}(z_1)$ is the short wave radiative heat flux absorbed at a depth z_1 in [W/m^2]

$q''_{sediment}(z_1)$ is the heat flux from the sediment associated with the water body at the depth z_1 in [W/m^2]

q_{hx} is the heat transfer from the heat exchanger in [W]

$A(z_1)$ is the horizontal area of the water body at the depth z_1 in [m^2]

$V(z_1)$ volume of the water column between two consecutive depths z_1 and z_2 in [m^3].

z_1 and z_2 are the depths measured from the surface of the water body in [m] ($z_2 > z_1$)

As implemented here, the heat transfer to/from the SWHE is distributed uniformly among the water layers. This approximation neglects the distribution of heat by local buoyant plumes.

The turbulent diffusion process predominantly controls the heat and temperature transport mechanism in a surface water body. This turbulent diffusion in the lake can be parameterized by the eddy diffusion coefficient. The accuracy of temperature prediction is highly dependent on the effective prediction of the eddy diffusion coefficient (k_z). It is generally expressed as a form which can be written as (McCormick and Scavia 1981),

$$k_z = k_o f(s) \tag{2.5}$$

Where, k_o is the eddy diffusion coefficient in the absence of stratification [m^2/day] and s is the stability parameter [-].

2.3.2 Shortwave radiation

Heat flux due to shortwave radiation is the heat gain in the lake due to the absorbed solar radiation. The heat flux due to incident solar radiation absorbed by the lake surface ($Q''_{sw\text{-}surface}$) is calculated as

$$q''_{sw-surface} = q''_{solar}\,(1 - \rho'_w)\alpha_w \tag{2.6}$$

Where, q''_{solar} is the incident solar radiation on the lake in [W/m^2], ρ'_w is the water surface reflectivity coefficient [-] and α_w is the water surface absorption coefficient [-]. The amount of radiation reflected from the surface of the water body varies with the reflectivity coefficient (ρ'_w). The reflectivity of water surface during open water season varies with time of day, latitude, cloud cover, solar altitude angle, turbidity of water body and surface wave actions. However, it is largely dependent on solar altitude angle. The approach used to calculate reflectivity averaged over a day is adopted from Hamilton and Schladow (1997).

$$\rho'_w = 0.08 + 0.02\left[\frac{2\pi n}{365} \pm \frac{\pi}{2}\right] \tag{2.7}$$

Where, n is the day of the year $1 \leq n \leq 365$, and the term $\pi/2$ added for the northern hemisphere and subtracted for southern hemisphere. The ratio of absorbed to the transmitted radiation at the surface of the water body is surface absorption coefficient for water (α_w). The surface absorption coefficient is assumed to be equal for all lakes and is taken as 0.4 (Dake and Harleman 1969; Hondzo and Stefan 1993a).

The penetration of the solar radiation and the amount of absorption of the incident solar radiation in the water column is highly dependent on the lake water clarity. The penetration of solar radiation in the water column is measured by the solar attenuation or extinction coefficient,

which is dependent on the lake turbidity. The radiative heat flux incident at a depth z inside the water column is calculated as,

$$q"_{sw}(z) = q"_{solar}(1 - \rho'_w)(1 - \alpha_w)\exp(-\mu z) \quad (2.8)$$

Where, μ is the extinction coefficient of water in [m^{-1}], which is a function of lake turbidity. The amount of radiative heat flux absorbed at a particular depth is calculated by the difference in the incident radiative heat flux at consecutive depths.

$$q"_{sw-abs}(z_1) = q"_{sw}(z_1) - q"_{sw}(z_2) \quad (2.9)$$

The extinction coefficient is calculated as, (Hondzo and Stefan 1993a)

$$\mu = \frac{1.84}{z_{Secchi}} \quad (2.10)$$

Where, z_{secchi} is the secchi depth of the lake in [m], which is a measure of lake turbidity.

2.3.3 Long wave radiation

The approach to calculate the amount of heat transfer on the surface of the water body due to long wave radiation using a linearized radiation coefficient (h_{lw}) is based on Chiasson, et al. (2000). The net long wave radiative heat flux on the lake surface ($q"_{lw}$) is calculated as,

$$q"_{lw} = h_{lw}(T_{sky} - T_{surface}) \quad (2.11)$$

Where, h_{lw} is the linearized long wave radiation coefficient [$W/m^2 \cdot K$], $T_{surface}$ is the lake surface temperature in [K] and T_{sky} is the sky temperature in [K]. T_{sky} is computed from the relationship given by Swinbank (1963). The linearized long wave radiation coefficient is calculated using Equation 2.12.

$$h_{lw} = 4\varepsilon_{water}\sigma\left(\frac{T_{surface} + T_{sky}}{2}\right)^3 \quad (2.12)$$

Where, ε_{water} is the emissivity coefficient of water taken as 0.97 (Omstedt 1990) and σ is the Stefan-Boltzmann constant [$5.67 * 10^{-8}$ $W/m^2 \cdot K^4$].

2.3.4 Surface Convection

Convective heat flux or sensible heat flux on the lake surface accounts for heat transfer due to wind (forced convection) and air-surface water temperature difference (free convection). Several empirical correlations exist to determine the convective heat transfer coefficient and hence to calculate the convective heat flux over the lake surface. Those correlations are based on the experimental results from swimming pools, cooling ponds, small lakes and horizontal flat plates. The lake model contains seven different correlations to calculate the surface convective and evaporative heat fluxes. The accuracy of each correlation in predicting the temperatures different surface water bodies are studied. Based on our validation and sensitivity studies on 14 different lakes, the surface convection correlation by Molineaux, et al. (1994) has been identified to predict lake temperatures with a good level of accuracy. The study and the validation details of the different surface convection and evaporation correlations are presented in detail in Chapter 4 of this thesis. The correlation by Molineaux, et al. (1994) to calculate the convective heat transfer coefficient is given below,

$$h_c = 3.1 + 2.1W \tag{2.13}$$

Where, h_c is the convective heat transfer coefficient in [W/m^2·K] and W is the wind speed over the lake surface in [m/s]. Finally, the heat flux due to convection at the lake surface can be computed by

$$q''_{conv} = h_c(T_{air} - T_{surface}) \tag{2.14}$$

Where, $A_{surface}$ is the surface area of the lake in [m^2] and T_{air} is the ambient air temperature in [°C].

2.3.5 Surface evaporation

Heat transfer due to evaporation is the dominant lake cooling mechanism. The equation to calculate the evaporative heat flux (q''_e) based on the convective heat transfer coefficient from Molineaux, et al. (1994) can be written as,

$$q''_e = \frac{h_{fg} h_c}{c_{p,air}} (w_{surface} - w_{air}) \quad (2.15)$$

Where, h_{fg} is the latent heat of vaporization [J/kg], w_{air} is the humidity ratio of the ambient air in [kg water/kg dry air], and $w_{surface}$ is the humidity ratio of the saturated air at the lake surface in [kg water/kg dry air].

2.3.6 Sediment heat flux

Heat transfer from the ground (sediments) is a significant source of heat gain to a surface water body during ice cover period (Gu and Stefan 1990). Lake simulation model incorporates the theory of sediment heat transfer from Fang and Stefan (1996) and the solution methodology from Saloranta and Andersen (2004). A one-dimensional, unsteady heat conduction equation to calculate the sediment temperatures is given in Equation 2.16. The sediment and the water column are discretized into a number of layers and the partial differential equation is solved by implicit finite difference method using Tri-diagonal matrix algorithm (TDMA). The procedure for solving the one-dimensional sediment heat conduction equation is similar to the solution methodology of the one-dimensional temperature transport equation discussed in section 2.4.2.

$$\frac{\partial T_{sed}}{\partial t} = \alpha_{sed} \frac{\partial^2 T_{sed}}{\partial {z_{sed}}^2} \quad (2.16)$$

Where, T_{sed} is the sediment temperature in [°C], z_{sed} is the depth of the sediment column in [m] and α_{sed} is the thermal diffusivity of the sediments [m^2/day]. The ground temperature is assumed to remain constant at 10 m (33 ft) below the lake bottom and hence the sediment temperature profiles are solved in 10 m (33 ft) thick sediment columns. The temperature of the sediment surface in contact with water (topmost sediment layer) is assumed to be equal to the water temperature at that depth. The heat flux at the water-sediment (*ws*) interface depends on the temperature gradient $\left(\frac{\partial T_{sed}}{\partial z_{sed}}\right)_{ws}$ and the interface area.

$$q''_{sediment}(z_1) = -k_{sed} \left(\frac{\partial T_{sed}}{\partial z_{sed}}\right)_{ws} \left(\frac{A_{sed}(z_1)}{A(z_1)}\right) \quad (2.17)$$

Where, k_{sed} is the thermal conductivity of the sediments = 1.01 [W/m·K] (Fang and Stefan 1996), $A(z_1)$ is the horizontal area of the surface water body at a particular depth in [m^2], $A_{sed}(z_1)$ is the water-sediment interface area in [m^2]. The water-sediment interface area at a particular depth is approximately calculated from the difference in the horizontal area of the surface water body at consecutive depths.

2.3.7 Heat transfer from a surface water heat exchanger

The amount of heat transferred to the surface water body from the heat exchanger depends on the thermal load supplied to the surface water heat exchangers, type of the heat exchanger, temperature of the surface water body at the depth where the heat exchanger is placed and the mass flow rate of the heat exchanger fluid. The heat exchanger fluid is usually water or an antifreeze mixture. The calculation of heat transfer due to a heat exchanger is explained in detail in Chapter 3 of this thesis. The extraction and rejection of heat by the SWHE directly affects the layers, at which the heat is being extracted or rejected. Under heat rejection conditions, the buoyant plume transports the heat upwards in the lake. Under heat extraction conditions, depending on which side of the maximum density point the lake and the plume are, it is possible that the plume might go upwards or downwards. The lake model currently distributes the heat transfer energy from the SWHE uniformly (proportionally to the volume) of each water layer.

2.3.8 Formulation of eddy diffusion coefficient

Mixing dynamics by eddy diffusion for a surface water body varies with the surface area and other lake physiological factors. Correlations to predict the eddy diffusion coefficient are calculated on the experimental observation either on a single surface water body or on water bodies of similar characteristics. The lake model contains eleven different correlations to calculate the eddy diffusion coefficients for surface water bodies of varying sizes (shallow ponds, small, medium and large lakes). Based on validation and sensitivity studies the eddy diffusion

correlation by Gu and Stefan (1995) is found to predict the temperatures of shallow ponds with good level of accuracy. The study of different eddy diffusion models, their validation results and the criteria used in selecting the best models are discussed in detail in Chapter 4 of this thesis. The eddy diffusion coefficient (k_z) determined by Gu and Stefan (1995) for shallow wastewater ponds is,

$$k_z = \min[k_{zmax}, k_{zmax} C N^{-1}] \tag{2.18}$$

Where, k_{zmax} is the maximum hypolimnion eddy diffusion coefficient [m^2/day], N is the stability or the Brunt Vaisala frequency[$1/s^2$] , C is a constant taken as $8.66*10^{-3}$ [s^{-1}](Jassby and Powell 1975). The stability frequency is estimated by Hondzo and Stefan (1993a) as,

$$N = \sqrt{\left(\frac{g}{\rho_w}\right)\left(\frac{\partial \rho_w}{\partial z}\right)} \tag{2.19}$$

Where, g is the acceleration due to gravity in [m/s^2] and ρ_w is the density of the water [kg/m^3]. The maximum hypolimnion eddy diffusion coefficient (k_{zmax}) represents the diffusion coefficient that in a lake observed during weakly stratified or un-stratified conditions. This occurs due to extensive turbulent mixing of water layers. Hondzo and Stefan (1993a) derived the relationship between k_{zmax} and the surface area of the lake as,

$$k_{zmax} = 0.048\left(A_{surface}\right)^{0.56} \tag{2.20}$$

The expression for k_{zmax} holds good for large ponds and lakes. In case of shallow ponds, which tend to stratify and un-stratify many times in a day, there does not appear to be a standard procedure to estimate the value of k_{zmax}. Gu and Stefan (1995) estimated the k_{zmax} value of 0.1 m^2/day for their 1.8 acre rectangular wastewater pond in Minnesota with a maximum depth of 1.8 m.

2.4 Model solution

2.4.1 Spatial discretization

The lake model solves the governing equations by using a series of discretized horizontal layers characterized by depth from the surface. The model uses a constant and a fixed layer thickness for the entire depth of the lake. The area and volume of each layer is calculated based on the morphometry of the lake basin from the equations given by Johansson, et al. (2007). Temperature and heat flux calculations are performed separately for each water layer. The layer thickness, horizontal area and eddy diffusion coefficient are evaluated at the layer interfaces, while the layer temperature and volume represent the mean value of the layer and hence can be assumed to be in the middle of a layer. The illustration of the spatial discretization is shown in Figure 2-3.

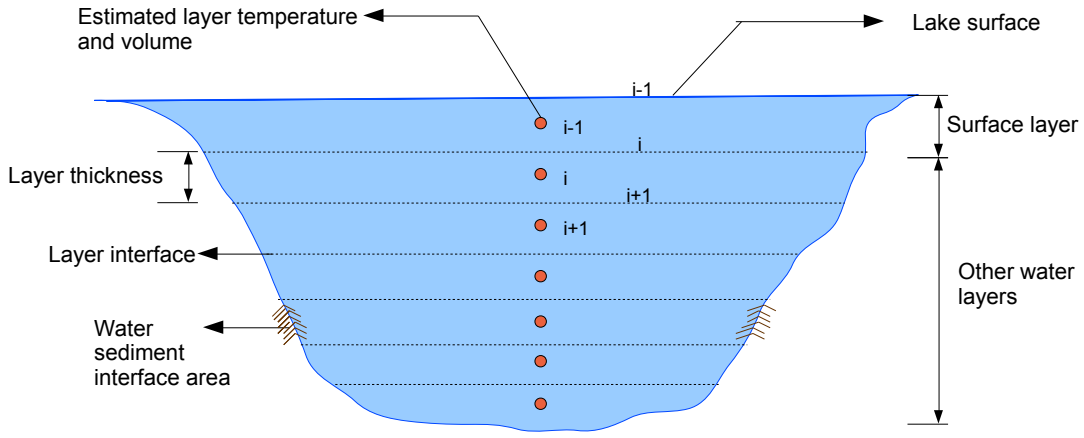

Figure 2- 3: Illustration of the model spatial discretization

2.4.2 Formulation of TDMA coefficients

The discretization of a lake into set of one-dimensional layers results in a set of linear equations, one for each layer. Since the concentration of a variable in a layer is dependent on its concentration in the adjacent layers, the set of equations are arranged in tri-diagonal matrix form

and solved simultaneously. Integrating the one dimensional advection diffusion equation (Equation 2.1) between z_i and z_{i+1}, where i is the layer number, gives

$$\int_{z_i}^{z_{i+1}} A\frac{\partial T}{\partial t}dz = \int_{z_i}^{z_{i+1}} \frac{\partial}{\partial z}\left[k_z A\frac{\partial T}{\partial t}\right]dz + \int_{z_i}^{z_{i+1}} A\frac{Q}{\rho_w C_p}dz \tag{2.21}$$

$$V_i\frac{dT_i^*}{dt} = \left[k_z A\frac{\partial T}{\partial t}\right]_{z_{i+1}} - \left[k_z A\frac{\partial T}{\partial t}\right]_{z_i} + V_i\frac{Q_i^*}{\rho_w C_p} \tag{2.22}$$

Where, V_i is the volume of the layer i, $T_i^* = V_i^{-1}\int ATdz$ is the volume averaged temperature for the layer i, and $Q_i^* = V_i^{-1}\int AQdz$ is the layer averaged heating rate. The heat balance terms in Equation 2.3 are transformed to a set of linear derivatives over the time and depth increments Δt and Δz. Since, the lake model operates on a daily time step the time increment Δt is taken to be 24 hours.

$$\begin{aligned}\frac{V_i}{\Delta t}[T_i^*(t) - T_i^*(t-\Delta t)] \\ = k_{z(i+1)}A_{i+1}\frac{1}{\Delta z}[T_{i+1}^*(t) - T_i^*(t)] \\ - k_{z(i)}A_i\frac{1}{\Delta z}[T_i^*(t) - T_{i-1}^*(t)] + V_i\frac{Q_i^*}{\rho_w C_p}\end{aligned} \tag{2.23}$$

Simplifying the equation by dividing with $V_i/\Delta t$ and introducing the notations

$$\alpha_i = \frac{\Delta t}{\Delta z}\frac{A_i}{V_i}k_{z(i)}$$

$$\beta_i = \frac{\Delta t}{\Delta z}\frac{A_{i+1}}{V_i}k_{z(i+1)}$$

$$\gamma_i = 1 + \alpha_i + \beta_i$$

Equation 2.23 can be rearranged to get a generalized TDMA equation for a layer i.

$$-\alpha_i T_i^*(t) + \gamma_i T_i^*(t) - \beta_i T_{i+1}^*(t) = T_i^*(t-\Delta t) + \frac{Q_i^*}{\rho_w C_p}\Delta t \tag{2.24}$$

Assuming zero diffusion between the air-water interface and zero bottom area of the lowermost layer we get $\alpha_1 = \beta_n = 0$. Therefore, for the surface the TDMA equation transforms into

$$(1+\beta_1)T_1^*(t) - \beta_i T_2^*(t) = T_1^*(t-\Delta t) + \frac{Q^*_{surface}}{\rho_w C_p}\Delta t \qquad (2.25)$$

Where, $Q^*_{surface}$ is the heat added at the surface layer from the surface heat flux terms. The lake model uses the temperature of the previous time step and the local heating of the layers of the current time step to calculate the current time step temperature values.

Since, many of the terms in the heat flux equations require the water temperature term for the current time step to be known, an iterative method is employed to calculate the water layer temperatures. At the start of every time step the lake model assumes the previous day temperature profile and surface ice thickness value (if ice is predicted on the lake surface) to calculate the current day heat flux terms. From the heat flux terms, the current day temperature profiles and surface ice thickness are calculated. Once again, the heat flux terms for the current time step are computed from the calculated temperature profiles and ice thickness values. This procedure is repeated until both the temperature and ice thickness values of the current time step converges. Separate convergence criteria are set up for water layer temperature and surface ice thickness terms.

2.5 Formulation of convective mixing and wind induced mixing

Once the water temperatures are calculated, the lake model checks for the presence of an unstable density condition (i.e.) the presence of higher density water layer(s) above the lower density layers. If such condition occurs, water layer(s) with unstable density profiles are mixed completely with the first stable layer below the unstable layers. The complete mixing is achieved by calculating the volume weighted average temperature for the unstable water column. This procedure is repeated until the temperatures in the water column becomes neutral or stable.

The wind induced stress on the lake surface is mainly responsible for the complete mixing of surface layers resulting in the formation of epilimnion region. The lake model calculates this epilimnion layer thickness by performing an energy balance between the available total kinetic

energy from the wind with the potential energy of each layer. The total kinetic energy of the wind (*TKE*) in [J] is calculated as

$$TKE = W_{str} A_{surface} \sqrt{\frac{\tau^3}{\rho_w}} \Delta t \tag{2.26}$$

Where, τ is the wind stress [N/m^2] and W_{str} is the wind sheltering coefficient [-].

$$\tau = \rho_{air} c_d W^2 \tag{2.27}$$

$$W_{str} = 1.0 - \exp(-0.3 A_{surface}) \tag{2.28}$$

Where, C_d is the drag coefficient [-], which is dependent of the surface wind speed. During, the period of ice cover on the surface of the lake, the effect of wind on the lake surface is neglected and hence, the total kinetic energy (*TKE*) is taken as zero. The algorithm to calculate the epilimnion layer thickness (i.e.) the depth of the water layer from the surface which is completely mixed is based on Ford and Stefan (1980) and Saloranta and Andersen (2004). The surface layer is always assumed to be well mixed it is considered to the first epilimnion layer. The potential energy (*PE*) in Joules required for lifting the immediate water layer below the epilimnion to the center of the epilimnion layer is calculated.

$$PE = g \Delta \rho_w \frac{V_{epi} V_z}{V_{epi} + V_z} (z_{epi} + \Delta z_{M-z} - z_{M-epi}) \tag{2.29}$$

Where, g is the acceleration due to gravity in [m/s^2], $\Delta\rho_w$ is the density difference between the current water layer and the epilimnion layer in [kg/m^3], z_{epi} is the thickness of the epilimnion layer in [m], $\Delta z_{M\text{-}z}$ is the distance from the layer's center of mass to the bottom of the epilimnion layer in [m], and $z_{M\text{-}epi}$ is the depth where the center of mass of the epilimnion layer is present in [m]. V_{epi} is the total volume of the epilimnion layers in [m^3]. V_z is the volume of the water layer at depth z in [m^3]. The *TKE* available is compared with the *PE* of the layer. If $TKE \geq PE$ of the water layer, it is considered that, the energy from the wind is sufficient to create enough turbulence to "mix the water layer" completely with the surface layer. The term "mixing of water layers" means, that the temperature and densities of those water layers are same and the

temperature density gradient is zero. The total *PE* to mix the water layer is subtracted from the available *TKE*. Now the *PE* of the next layer is compared with the resultant *TKE,* and the procedure is repeated until the net resultant *TKE* is less than the *PE* required for new layer to mix with the epilimnion.

2.6 Modeling of turnover

During spring/autumn seasons, most surface water bodies undergo a large-scale inversion of water mass from the surface until the lake bottom, which destroys the existing stratification. This phenomenon is called as turnover and it occurs once or twice annually for most lakes. The lake model follows the algorithm given by Saloranta and Andersen (2004) to handle the turnover conditions. Turnover algorithm is initiated whenever the surface temperature crosses the temperature of maximum density (T_{maxrho} = 3.98 °C). The water layers including the surface layer that has crossed T_{maxrho}, are set to T_{maxrho}. The energy gained by this temperature difference (i.e. the energy difference relative to T_{maxrho}) is exponentially distributed to cool/warm the water column. The surface temperature is maintained at T_{maxrho} until the entire water column has been cooled/warmed to T_{maxrho}. If the entire water column is cooled/warmed to T_{maxrho} the remaining energy is used to cool/warm the surface layers.

2.7 Modeling of ice and snow cover

Some surface water bodies tend to freeze near the surface during the cold winter climates. The one-dimensional lake model assumes the ice or snow thickness formed on the surface is constant throughout the water body. There are three processes involved in modeling of ice cover on the water body surface.

a. Ice formation on the lake surface during the start of the freeze-up period.
b. Congelation of ice due to continuous freezing
c. Melting of ice during warm-up period

2.7.1 Surface ice formation

Whenever the lake model encounters the water layer temperatures below the freezing point of water, it predicts the formation and growth ice/snow cover on the lake surface. The sub-cooled water layers are set to the freezing point temperature (T_{freeze}= 0°C) and the resultant heat deficit is converted to initial surface ice thickness.

$$q_{deficit,i} = \frac{\rho_{water} V_i c_{p,water} \left(T_{freeze} - T_{water,i}\right)}{\Delta t} \tag{2.30}$$

Where, $q_{deficit,i}$ is the sensible heat deficit in the i^{th} sub-cooled water layer converted to latent heat of ice in [W], $T_{water,i}$ and V_i are the temperature in [°C] and volume of the i^{th} water layer in [m^3] respectively, $c_{p,water}$ is the specific heat capacity of water [J/kg·°C] and Δt is the model time step in [s]. The initial ice thickness (H_{ice}) in [m] is calculated from the total heat deficit calculated from all the sub-cooled water layers.

$$m_{ice} = \frac{q_{deficit\ ,sum} \Delta t}{L_{freeze}} \tag{2.31}$$

$$H_{ice} = \frac{m_{ice}}{\rho_{ice} A} \tag{2.32}$$

Where, m_{ice} is the mass of ice formed on the lake surface in [kg], $q_{deficit,sum}$ is the sum of heat deficit in all the sub-cooled water layers in [W], and L_{freeze} is the latent heat of freezing of ice in [J/kg] and ρ_{ice} is the density of ice in [kg/m^3].

2.7.2 Surface snow-ice growth

After the initial ice formation on the lake surface, whenever the air temperature (T_{air}) falls below the freezing temperature (T_{freeze}) ice thickness is increased due to congelation of ice. The newly formed ice thickness ($H_{ice,new}$) as a result of congelation is calculated based on Stefan's law (Lepparanta 1993).

$$H_{ice,new} = \sqrt{H_{ice}^2 + \frac{2k_{ice}}{\rho_{ice} L_{freeze}} \left(T_{freeze} - T_{ice}\right) \Delta t} \tag{2.33}$$

Where, k_{ice} is the thermal conductivity of ice in [W/m·K] and T_{ice} is the temperature of ice formed on the surface of the water body in [°C]. The temperature of ice (T_{ice}) is calculated as,

$$T_{ice} = \frac{p\,T_{freeze} + T_{air}}{1 + p} \tag{2.34}$$

Where, p is a parameter calculated for snow-free or snow-cover conditions.

$$p = \frac{1}{10\,H_{ice}} \text{ (snow-free conditions)} \tag{2.35}$$

$$p = \frac{k_{ice}\,H_{snow}}{k_{snow}\,H_{ice}} \text{ (snow-cover conditions)} \tag{2.36}$$

Where, k_{snow} is the thermal conductivity of snow [W/m·K] and H_{snow} is the snow thickness [m]. Large amount snowfall potentially increases the weight of snow. If it exceeds the buoyancy capacity of ice then the lower part of snow, might mix with the underlying water layers. This eventually causes the formation of slush layer at ice-snow interface, which becomes a snow-ice when frozen (Saloranta 2000). This snow-ice formed is superimposed on ice growth and it is subtracted from the total snow thickness. The amount of snow-ice thickness formed which favors the additional ice growth is calculated as,

$$H_{snow-ice} = \max\left[0, \quad \left\{H_{ice}\left(\frac{\rho_{ice}}{\rho_{water}} - 1\right) + H_{snow,weq}\right\}\right] \tag{2.37}$$

Where, $H_{snow\text{-}ice}$ is the thickness of snow-ice in [m] and $H_{snow,weq}$ is the water equivalents of snow thickness in [m] and it is calculated as,

$$H_{snow,weq} = H_{snow}\left(\frac{\rho_{snow}}{\rho_{water}}\right) \tag{2.38}$$

Where, ρ_{snow} is the simulated bulk density of the snow cover in [kg/m^3]. The bulk density of snow has an initial value of 250 kg/m^3. If the air temperature is below the freezing temperature, snow density increases due to compaction of snow and the increased snow density is calculated using the equation given by Yen (1981).

$$\rho_{snow} = C_1\,\rho_{snow}\frac{H_{snow,weq}}{2}.\exp(-C_2\,\rho_{snow}).\exp\left\{-0.08\left(T_{freeze} - \frac{T_{ice}+T_{air}}{2}\right)\right\}.\Delta t \quad (2.39)$$

Where, C_1 and C_2 are empirical coefficients taken as 7.0 $m^{-1}h^{-1}$ and 0.021 m^3/kg respectively (Yen 1981; Saloranta 2000). If air temperature is above the freezing temperature then the bulk density of snow is set to a maximum value of 450 kg/m^3.

The water layer beneath the ice tends to reduce the ice thickness by melting the ice from the bottom. The heat flux between the ice-water interface, which tends to reduce the ice growth is calculated from the temperature difference between ice and water layer temperatures just beneath the ice. The net ice growth for the time step is calculated from the difference between the total ice thickness formed at the surface and the amount of ice melted from the bottom.

2.7.3 Snow-ice melt

Whenever the air temperature is above the freezing temperature, ice and snow on the surface of the water body begins to melt. Snow if present on the water body surface will melt completely before the melting of surface ice could begin. The energy required for melting is determined from the net heat flux available at the surface of the water body. The incident shortwave radiation is assumed to be completely absorbed by the snow-ice layer before it could penetrate into the water column. The equations to predict the different surface heat flux terms during surface snow-ice conditions are obtained from Saloranta (2000).

The net shortwave radiation at the surface during surface snow-ice conditions is calculated as,

$$q''_{sw-surface} = q''_{solar}(1-\rho'_{ice,snow})(1-\alpha_{ice}) \quad (2.40)$$

Where, $\rho'_{ice,snow}$ is the surface reflectivity coefficient for a water body when it is covered by snow or ice. Surface reflectivity coefficient values are assumed to be constant and taken as 0.77 for snow and 0.3 for ice respectively (Perovich 1996; Saloranta 2000). α_{ice} is the percentage of penetration of solar radiation inside the water column under ice cover. If there is a presence of snow cover, the percentage of shortwave radiation penetrated through the snow layers is taken as

zero. As for the ice, the penetration of the shortwave radiation is calculated as a function of the cloud cover.

$$\alpha_{ice} = 0.18(1 - N) + 0.35N \tag{2.41}$$

Where, N is the cloudiness for a particular day [-]. The net long wave radiative heat flux on the lake surface during the snow-ice period becomes,

$$q"_{lw} = \varepsilon_{water}\sigma(T_{air}^4\left(a + b\sqrt{e}\right)(1 + cN^2) - T_{surface}^4) \tag{2.42}$$

Where, a, b, c are empirical constants whose values are 0.68, 0.0036 and 0.18 and 'e' is the air water vapor pressure in [N/m^2]. Finally, the convective and the evaporative heat fluxes during ice-snow period is calculated as

$$q"_{conv} = \rho_{air}C_{p,air}C_h\left(T_{air} - T_{surface}\right)W \tag{2.43}$$

$$q"_{e} = h_{fg}\rho_{air}C_e(w_{surface} - w_{air})W \tag{2.44}$$

Where, ρ_{air} is the air density in [kg/m^3], $C_{p,air}$ is the specific heat capacity of air [J/kg·K] and C_h and C_e = 0.00175 are the convective and evaporative heat exchange coefficients between air and ice surface (Crocker and Wadhams 1989). The net surface heat flux first melts the snow, if the snow is completely melted during the time step, the remaining energy is used to melt the ice layers. Similarly, the remaining energy after melting all the ice layers is used to heat the water column.

2.8 Model Validation

The validation of the lake model with the experimental data from Ice Lake Minnesota and a research pond maintained by Oklahoma State University is presented in this Chapter.

2.8.1 Experimental site description and data collection

Ice Lake is a small lake located in Grand Rapids, Minnesota (surface area of 41 acres (16.6 Ha); maximum depth of 16m (52.5 ft)). The historical experimental temperature data is obtained from an online database "Water on the Web" (WOW 2012).

The research pond maintained by OSU in Stillwater OK is a small shallow pond with a surface area of 3 acres (1.2 Ha). The maximum depth of the pond at its full capacity is 3.81 m (12.5 ft). Two thermistor trees located in the deepest part of the pond continuously record temperature data along the depth for every 15 minute intervals.

2.8.2 Lake temperature and ice thickness validation

Figure 2- 4 shows the temperature comparison between the model and the experimental data along the depth for Ice Lake for the months between June-September 2003. Ice Lake exhibits a definitive stratification profile throughout the summer period. The simulation temperatures closely match with the experimental temperature profiles. A maximum error in the order of 3 °C (5.5 °F) is observed in comparison with the experimental temperatures in the metalimnion region during the month of August.

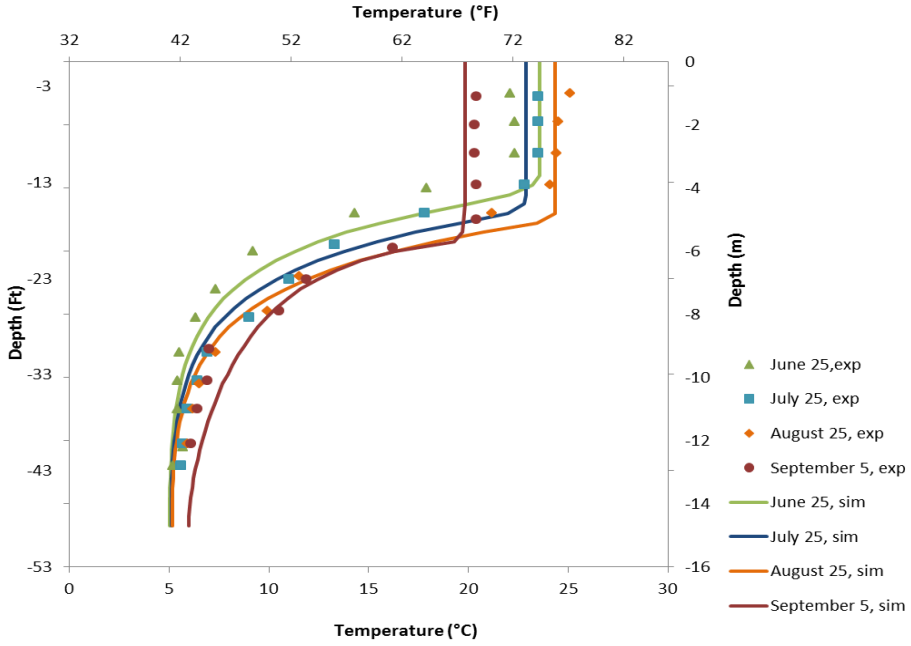

Figure 2- 4: Comparison between the experimental and simulated temperatures for Ice Lake MN

Ice thickness validation on the research pond maintained by OSU is shown in Figure 2- 5. The model gives a reasonable match for the four experimental ice thickness measurements measured during the month of January and February 2011. The ice thickness shows a decreasing trend during the end of January and reaches a maximum value of 5.2 in. (0.017 m) on January 30, 2011. This is due to warm air temperatures observed during the end of January (9 °C on January 28, 10 °C on January 29). This is followed by a sudden dip to negative temperatures on January 31 (-0.5 °C) accompanied by a snowfall of 2.4 in. (0.06 m) and much colder temperatures on February 1 (-12°C). Hence, the simulation considered the snow to mix with water over the day to form ice (slush) and predicted a sudden increase in surface ice thickness.

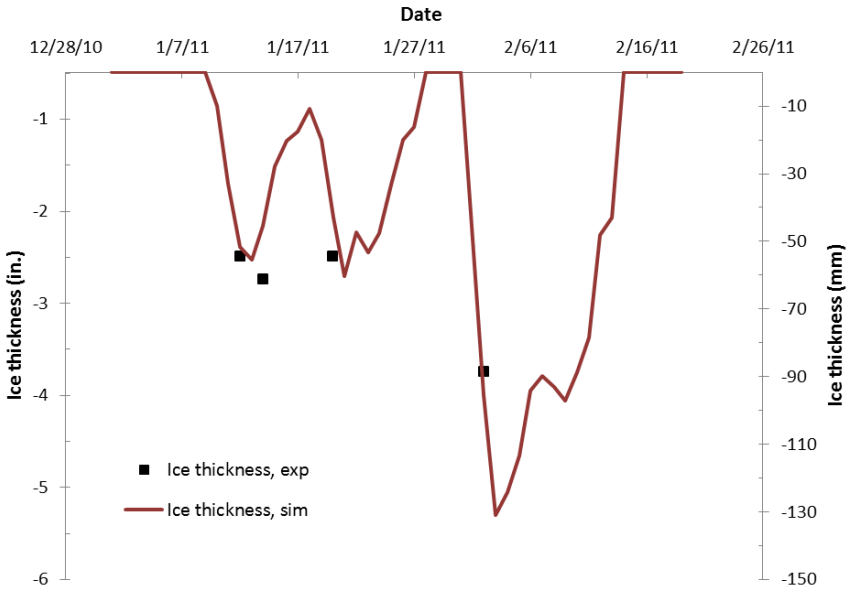

Figure 2- 5: Ice thickness measurements compared with simulation results

CHAPTER 3

DEVELOPMENT OF A SURFACE WATER HEAT EXCHANGER MODEL

This chapter has been written in collaboration with my colleague Manojkumar Selvakumar. Hence, several sections in this chapter will be identical with the SWHE model development chapter discussed in Selvakumar (2013) thesis.

Surface water heat exchangers (SWHE) may take a number of forms. Many SWHE have been formed from HDPE or other piping. These include piping laid flat on the bottom of the lake or embedded in the lake bottom (Svensson and Sörman 1983), slinky coils (Chiasson, et al. 2000), spiral-helical coils and flat spiral coils (Hansen 2011) Another common SWHE is the vertical flat plate. Other more innovative SWHE have been proposed such as the helical HDPE coil combined with a submersible motor and axial propeller described by Sjöberg (2004).

In current practice, the most commonly used SWHE seem to be spaced bundles and vertical flat plates, and these are the only configurations treated in the current model. The spaced bundles might be called “stacked spiral” or “spiral-helical” heat exchangers as each horizontal layer is a spiral connected either at the outside or inside to the layer above. Other than the work by Hansen (2011), there have been no published studies on such configurations, though Prabhanjan, et al. (2004) and Ali (2006) presented measurements and correlations for submersed helical coils.

Hansen (2011) conducted experimental tests in a 1.2-hectare (3 acre) pond, measuring overall thermal resistance and then deriving correlations to calculate outside heat transfer coefficients for heat exchanger types which include spiral-helical coils, flat spiral coils, vertical and horizontal slinky coils, loose coils and metal flat plate heat exchangers. In order to estimate the outside convective resistance, the inside convective resistance for the coils was estimated with convection correlations (Rogers and Mayhew 1964; Salimpour 2009) that considered the effect of tubing curvature. Flat plate heat exchangers are commonly constructed from spot-welding two panels together, welding the edges and expanding the gap between the plates. The resulting gap between the panels forms one or more flow paths or non-circular and irregular cross-section. For the flat plate heat exchangers, inside Nusselt number is calculated based on the Dittus-Boelter (Incropera and DeWitt 1996) correlation for straight pipes.

Ice formation around the heat exchanger occurs when the heat extraction rate is high enough to drive the outside surface temperature below freezing. Although there is no literature available that describes modeling of freezing of spiral-helical coils, there is some similarity with ice-on-coil models developed for thermal storage systems. (Silver, et al. 1989, Jekel, et al. 1993 and Neto and Krarti 1997) .

This chapter provides a detailed discussion about the model and correlations used for a spiral-helical coil heat exchanger.

3.1 Heat exchanger model

To predict the heat exchanger heat transfer it is necessary to predict the inside and outside heat transfer coefficients. The model uses the outside Nusselt number correlation developed by Hansen (2011) for spiral-helical coils to calculate the outside heat transfer coefficient. Hansen (2011) outside Nusselt number correlation is calculated at the film temperature surrounding the heat exchanger and is also dependent on the outside tube diameter and the vertical and horizontal spacing between the adjacent tubes.

$$Nu_o = 0.16(Ra_o^*)^{0.264}\left(\frac{\Delta y}{d_o}\right)^{0.078}\left(\frac{\Delta x}{d_o}\right)^{0.223} \quad (3.1)$$

Where, Nu_o is the outside Nusselt number and Ra_o^* is the modified Rayleigh number calculated at the outside film temperature ($T_{film\text{-}o}$). $T_{film\text{-}o}$ is the average temperature value between the heat exchanger tube and the surrounding water in [°C]. Δy and Δx are the vertical center-to-center distance and horizontal center-to-center distance between the adjacent heat exchanger tubes in [mm] and d_o is the heat exchanger outside tube diameter in [mm].

The modified Rayleigh number is calculated as,

$$Ra_o^* = \frac{g\beta q"_c L^4 Pr}{k_{f,o}\upsilon_{f,o}^2} \quad (3.2)$$

Where, g is the acceleration due to gravity in [m/s^2], β is the thermal expansion coefficient in [1/K], $k_{f,o}$ is the thermal conductivity of the surface water in [W/m·K] and $\upsilon_{f,o}$ is the water kinematic viscosity in [m^2/s], all calculated at the outside film temperature ($T_{film\text{-}o}$). $q"_c$ is the coil heat flux in [W/m^2], L is the characteristic length of the heat exchanger coil in [m] and Pr is the Prandtl number.

The outside convection coefficient is calculated based on the outside Nusselt number as shown in Equation 3.3.

$$h_o = (Nu_o * k_{f,o})/d_o \quad (3.3)$$

The inside Nusselt number correlation for spiral-helical is obtained from Salimpour (2009). The thermal parameters are calculated based on the inside fluid temperature (T_{fluid}) which is the average temperature value between the heat exchanger EFT and ExFT for the time step.

$$Nu_i = 0.152\, De^{0.431}\, \mathrm{Pr}^{1.06}\, Pitch_{ratio}{}^{-0.277} \quad (3.4)$$

$$De = Re\sqrt{\frac{d_i}{d_{c_o}}} \quad (3.5)$$

$$Pitch_{ratio} = \frac{\Delta y}{\pi d_{c_o}} \tag{3.6}$$

Where, Nu_i is the inside Nusselt number, De is the Dean number, $Pitch_{ratio}$ is the dimensionless pitch ratio, d_i is the inside tube diameter in [mm], d_{c_o} is the heat exchanger outside coil diameter in [mm] and Re is the Reynolds number. The inside convection coefficient is calculated from the inside Nusselt number.

$$h_i = (Nu_i * k_{f,i})/d_i \tag{3.7}$$

Where, $k_{f,i}$ is the thermal conductivity of the heat exchanger fluid in [W/m·K]. The global heat transfer coefficient (UA_{hx}) for the heat exchanger is then calculated.

$$UA_{hx} = \frac{1}{R_i + R_{tube} + R_o} \tag{3.8}$$

Where, R_i, R_{tube} and R_o are the inside, heat exchanger tube and outside convection resistances in [°C/W] respectively.

The heat transfer between the heat exchangers and the surrounding water body is calculated as,

$$q_{hx} = \varepsilon\, \dot{m}_{hx}\, c_{p,hx} (EFT_i - T_{lake})(N_{circuits}) \tag{3.9}$$

Where, q_{hx} is the heat exchanger heat transfer in [W], ε is the effectiveness of the heat exchanger calculated based on the NTU formulation, $\dot{m}_{hx}$ is the mass flow rate of the heat exchanger fluid [kg/s] and $c_{p,hx}$ is the specific heat capacity of the heat exchanger fluid [J/kg·°C], EFT_i is the heat exchanger entering fluid temperature for the i^{th} time step, T_{lake} is the daily average lake temperature for the depth range where the heat exchangers are placed in [°C] and $N_{circuits}$ is the number of SWHE circuits placed in the lake.

Finally, the heat exchanger entering and exiting fluid temperatures for the i^{th} time step are calculated by the following equations.

$$EFT_i = T_{lake} - \frac{q_{Hx}}{(\varepsilon\, \dot{m}_{hx}\, c_{p,hx})} \tag{3.10}$$

$$ExFT_i = EFT_i + \frac{q_{Hx}}{(\dot{m}_{hx}\, c_{p,hx})} \tag{3.11}$$

3.2 Ice-on-coil model

Conditions such as high heat extraction rates along with low lake water temperatures might cause the formation of ice around the SWHE's. The formation of ice reduces the heat transfer, and as this condition prevails, the ice around the heat exchangers gradually builds up, creating a buoyant force, which tends to lift the heat exchangers to the surface of the lake. Excessive formation of ice around the heat exchanger coils could cause the overlapping of ice between adjacent coils. This phenomenon completely limits the exterior convection, which further reduces the heat transfer. A numerical model to simulate the development, growth and melting of ice around the SWHE's and thereby to calculate the resultant heat transfer during freezing and melting conditions has been developed. The model also simulates ice-overlapping phenomenon for spiral-helical coil heat exchangers. This model follows the approach based on the ice-on-coil model for a thermal storage tank by Neto and Krarti (1997).

The rate of formation, growth and melting of ice varies along the length of a SWHE. For coil type SWHE configurations (spiral-helical, flat spiral and slinky coil), the model divides the coil into a number of segments along the length and the ice thickness is calculated for each segment at every time step. In the case of vertical flat plate heat exchangers, the model considers it as a single entity.

This section discusses the ice-on-coil model development for a coil type SWHE. Energy balance is performed at every coil segment to calculate the ice thickness. Figure 3-1 shows a cross sectional view of a coil segment and a thermal network diagram during ice formation period.

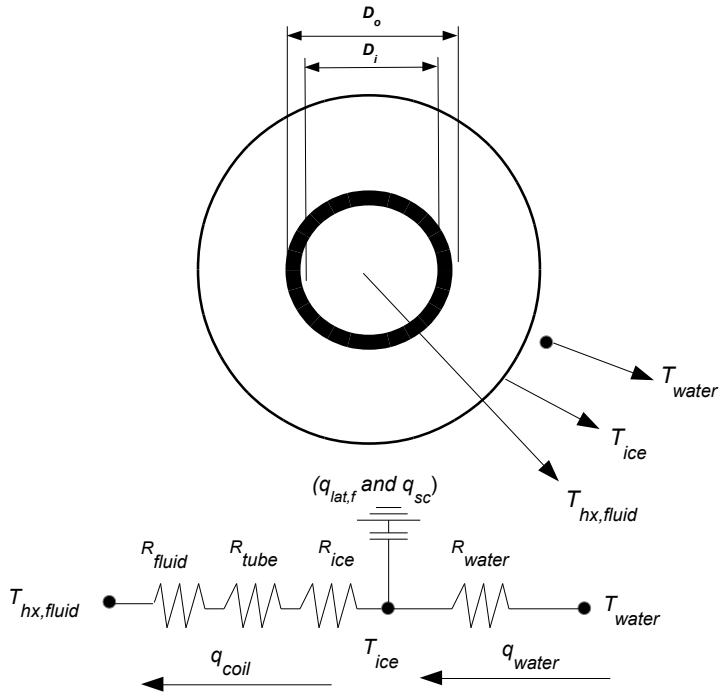

Figure 3- 1: Cross-sectional view of a heat exchanger coil segment and thermal network for ice formation period

The coil heat transfer is dependent on the ice thickness and vice-versa. Hence, the ice-on-coil model iteratively calculates the segment ice thickness until an energy balance is achieved. The following energy balance equation is applied to each coil segment '*j*'.

$$q_{coil,j} = q_{water,j} + q_{lat,f,j} + q_{sc,j} \tag{3.12}$$

Where,

$q_{coil,j}$ is the heat transfer between the heat exchanger fluid and the ice/water interface in [W]

$q_{water,j}$ is the heat transfer between water surrounding the heat exchanger segments and the ice/water interface on the heat exchanger in [W]

$q_{lat,f,j}$ is the latent heat to freeze the water or melt the ice formed at each segment in [W] and

$q_{sc,j}$ is the sensible heat to sub-cool the ice during freezing at each segment in [W]

The heat transfer between the ice/water interface and the heat exchanger fluid for every heat exchanger segment during the freezing period is calculated as,

$$q_{coil,j} = UA_{f,j}(T_{ice} - EFT_j) \tag{3.13}$$

T_{ice} is the temperature of ice at the ice-water interface (0°C (32°F)), *EFTj* is the heat exchanger entering fluid temperature for the j^{th} segment and UA_f is the overall heat transfer coefficient for the segment in [W/°C], which is calculated as,

$$UA_{f,j} = \frac{1}{(R_{fluid} + R_{tube} + R_{ice})} \tag{3.14}$$

Where, R_{fluid}, R_{tube} and R_{ice} are the thermal resistances of the heat exchanger fluid, tube and the surrounding ice in [°C/W] respectively. The thermal resistances are given by the following equations.

$$R_{fluid} = \frac{1}{\left[(2\pi - \theta_j) r_i \, L_{tube} \, h_{fluid}\right]} \tag{3.15}$$

$$R_{tube} = \frac{ln\frac{r_o}{r_i}}{(2\pi - \theta_j) k_{tube} L_{tube}} \tag{3.16}$$

$$R_{ice} = \frac{ln\frac{r_{ice}}{r_o}}{(2\pi - \theta_j) k_{ice} L_{tube}} \tag{3.17}$$

Where, r_i, r_o and r_{ice} are the heat exchanger inside tube radius, outside tube radius and radius of the ice in [m] respectively. h_{fluid} is the fluid convective heat transfer coefficient in [W/m^{2}K] and θ is the overlapping angle of ice in [radians] between the coil segments which are adjacent to each other. For a spiral helical coil, a coil segment could have a maximum of four adjacent segments depending on the location of the segment in the coil. The model currently exercises a simple algorithm in the calculation of the overlapping angle for the spiral-helical coil configuration. It specifically assumes that every 'turn' of the coil as one segment. Since, the ice-overlapping angle is also dependent on the location of the coil segment; the model also assumes a pre-defined segment configuration. Though the definition and the assumption a typical coil segment is different between the overlapping angle algorithm and the rest of the model, the ice radius predicted in the ith segment by the ice-on-coil model is taken in as the ith segment value in the overlapping algorithm. The calculation of the overlapping angle based on adjacent coil ice thickness is discussed in Neto and Krarti (1997). The model does not consider the ice overlapping

in the flat spiral and slinky coils due to the complicate geometry structure of the coils and due to the lack of experimental data.

The heat transfer between the surrounding water around the ice to the ice/water interface ($q_{wat,i}$) can be calculated as,

$$q_{wat,j} = (2\pi - \theta_j) r_{ice} L_{tube} h_{wat-ice} (T_{water,j} - 0°C) \quad (3.18)$$

Where, $h_{wat\text{-}ice}$ is the convective heat transfer coefficient at the ice/water interface in [W/m^2·K], $T_{water,j}$ is the water temperature surrounding each coil segment in [°C]. The latent heat to freeze the water around the coils $q_{lat,f,j}$ in [W] is given by,

$$q_{lat,f,j} = \frac{\Delta M_{ice,j}}{\Delta t} HF_{ice} \quad (3.19)$$

Where, $\Delta M_{ice,i}$ in [kg] is the mass of ice formed at the j^{th} segment during the daily time step Δt in [s] and HF_{ice} is the latent heat of freezing of ice in [J/kg].

The heat transfer to sub-cool the ice $q_{sc,j}$ in [W] is calculated as,

$$q_{sc,j} = \frac{\Delta M_{ice,j}}{\Delta t} C_{p,ice} (T_{ice} - T_{bulk}) + \frac{Total\Delta M_{ice,j}}{\Delta t} C_{p,ice} (T_{ice} - T_{bulk,formed\ ice}) \quad (3.20)$$

Where, $Total\Delta M_{ice,i}$ is the total mass of ice formed until the current time step, $C_{p,ice}$ is the specific heat capacity of ice in [J/kg·K], T_{bulk} is the bulk temperature for the ice formed in the current time step in [°C], and $T_{bulk,formed\ ice}$ is the bulk temperature for the ice formed till the previous time step in [°C].

Once, the ice thickness values of the heat exchanger segment is converged the heat exchanger ExFT for every segment is calculated as

$$ExFT_j = EFT_j + \frac{q_{coil,j}}{\dot{m}_{fluid} C_{p,fluid}} \quad (3.21)$$

This procedure is repeated for all the coil segments. The calculated ExFT for a tube segment is taken as the EFT for the successive tube segment. The heat transfer from each tube segment $q_{coil,j}$ is summed up to calculate the overall heat transfer of the heat exchanger coil (q_{hx}).

During the ice melting period, heat transferred from the heat exchanger fluid is used to melt the ice surrounding the heat exchanger. The thermal network during the ice melt period is shown in Figure 3-2.

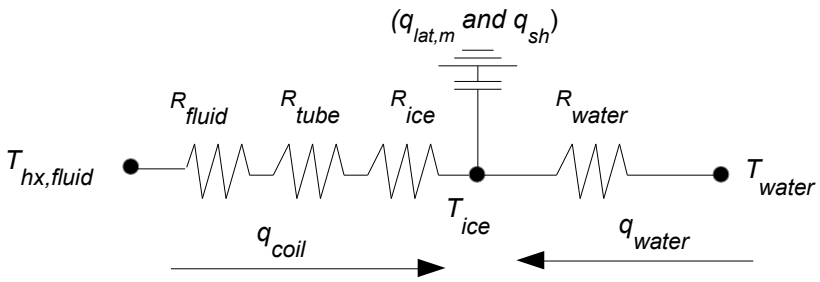

Figure 3- 2: Thermal network for ice melt period

The model assumes the ice melting to take place in one direction, and the heat from the coil is applied to the outside surface of the ice. The heat balance equation during the ice melting period can be written as,

$$q_{coil,j} + q_{water,j} = q_{lat,m,j} + q_{sh,j} \tag{3.22}$$

Where, $q_{lat,m,j}$ is the latent heat to melt the ice around the tube segments in [W] and $q_{sh,j}$ is the sensible heat to increase the water bulk temperature above the freezing point in [W].

The heat transfer between the ice/water interface and the heat exchanger fluid for every heat exchanger segment during the melting period is calculated as,

$$q_{coil,j} = UA_{m,j}(EFT_j - T_{ice}) \tag{3.23}$$

$q_{lat,m,j}$ and $q_{sh,j}$ are calculated as.

$$q_{lat,m,j} = \frac{\Delta M_{water,j}}{\Delta t} HF_{ice} \tag{3.24}$$

$$q_{sh,j} = \frac{\Delta M_{water,j}}{\Delta t} C_{p,water}(T_{bulk} - 0°C) \tag{3.25}$$

Where, $\Delta M_{water,j}$ is the mass of water in [kg] formed due to the melting of ice in the current time step Δt. The $ExFT_i$ can be calculated using Equation 65. This procedure is again repeated for all the coil segments.

3.3 SWHE model validation

Validation of the heat exchanger model is performed based on the experimental data obtained for a spiral-helical heat exchanger coil from the indoor heat extraction test performed in our test facility. In addition, the validation of the heat exchanger model when coupled with the lake model is performed based on the experimental data from a spiral-helical coil when tested in the research pond maintained by the OSU. The heat extraction tests are performed on a spiral-helical coil placed in an indoor test pool and subjected to a controlled environment. The test pool is of 4.3m (14 ft) in diameter and around 1.2m (4 ft) deep. The heat exchanger coil is suspended on a set of load cells to measure the buoyant force exerted during the ice formation around the coil.

The spiral-helical coil used in the validation both in the test facility, and in the OSU pond is made of high-density polyethylene plastic, and is 152.4 m (500 ft) long with a nominal diameter of ¾ inches (19.05 mm). The coil has an outside diameter of 2.4 m (7.9 ft) and inside diameter of 1.2 m (3.9 ft). The vertical and horizontal spacing set between adjacent coils are 2.63 inches (0.066 m) and 4.13 inches (0.0104 m). The supply and return temperatures were measured by thermistors embedded in the coil. The coil temperatures, heat exchanger loads and fluid flow rates were recorded at every 5 minutes.

3.3.1 Validation of the SWHE model

The heat exchanger model is validated using the experimental results performed on a spiral-helical coil heat exchanger placed in an indoor test pool. The validation of the ExFT predicted by the model with the experimental data is shown in Figure 3-3 and the buoyancy force validation is shown in Figure 3-4. Unlike a lake, the temperature of the test pool varies greatly in response to the heat exchanger loads. With continuous heat extraction and with low pool temperatures ice formation occurs on the surface of the coil. As this condition prevails, the coil ice thickness increases, which increase the coil buoyancy force (phase I in Figure 3-4). With further increase in coil ice thickness, overlapping of ice between adjacent coil segments occurs. This overlapping

increases the convective resistance, further reducing the coil heat transfer, which results in increased ice formation (phase II in Figure 3-4). The heating mode in the coil is reversed to melt the ice around the coils (phase III in Figure 3-4).

The heat exchanger model takes in the hourly averaged heat exchanger loads and pool temperature data as inputs to calculate the heat exchanger EFT, ExFT and coil ice thickness. The heat exchanger coil is divided into number of segments of equal length. For the calculation of the overlapping angle, the model assumes each coil turn as a separate segment. Since, the overlapping of ice around the adjacent coil segments reduces the convective heat transfer; the external convective heat transfer coefficient calculated using Hansen (2011) correlation is reduced by introducing a penalty function. The penalty to the heat transfer coefficient is given by

$$h_{o,effective,j} = h_{o,j} * (1 - Coeff_{penalty}) \quad (3.26)$$

Where, $h_{o,effective,j}$ is the exterior convective heat transfer coefficient for the j'th coil segment during the overlapping of ice [W/m^2], $h_{o,j}$ is the exterior convective heat transfer coefficient for the j'th segment obtained from Hansen (2011) and $Coeff_{penalty}$ is the penalty coefficient for the segment which depends on the number of overlapping ice segments.

The equation to calculate the penalty coefficient is obtained based on the sensitivity analysis,

$$Coeff_{penalty} = 0.187 * no\ of\ overlapping\ segments \quad (3.27)$$

With the above assumptions, the model predicted ExFT closely matches the experimental temperature values as shown in Figure 3-3. The model slightly over predicts buoyancy force and predicts formation and complete melting of ice around the coils several hours before (18 hours before the initial ice formation and 9 hours before for the actual complete ice melt) than what is observed in the experiment, as shown in Figure 3-4. Overall, it follows a similar profile and exhibits the three phases approximately in the same time.

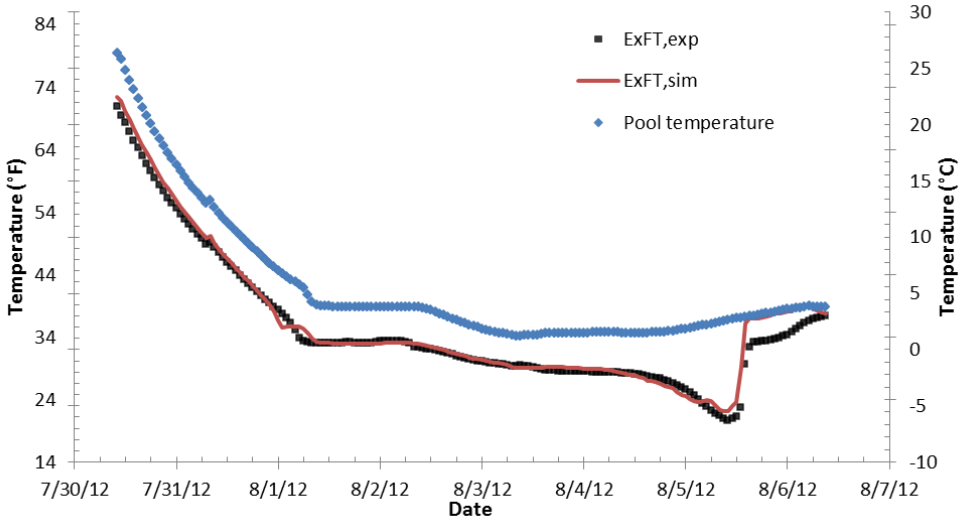

Figure 3- 3: Comparison of the model and experimental ExFT for the spiral-helical coil heat exchanger placed in a test pool

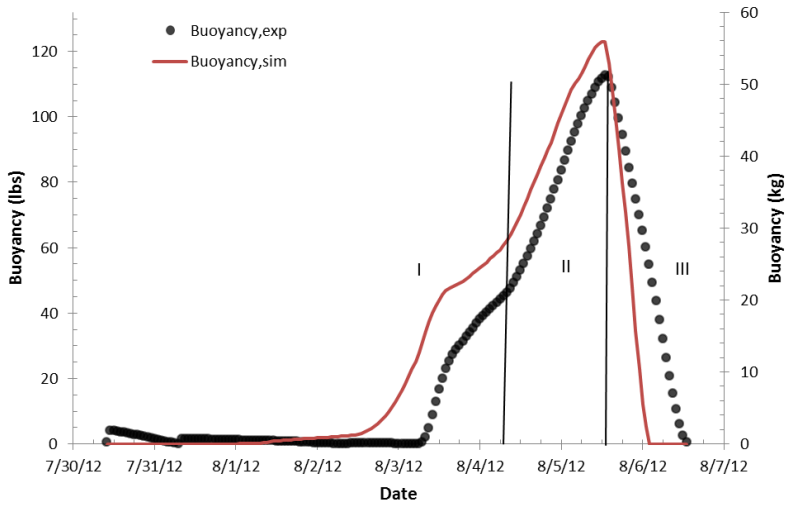

Figure 3- 4: Experimental and model predicted buoyancy comparison

3.3.2 Validation of the SWHE model when coupled with the lake model

The validation of the SWHE model with the lake model is performed for the experimental results obtained with the spiral-helical coil tested in the research pond maintained by OSU. The comparison between the model predicted and experimental ExFT is shown in Figure 3-5. The

lake model runs on a daily time step while the heat exchanger model is modified to run on an hourly time step. The steep rise and fall of the ExFT predicted by the model is in response to the availability of the heat exchanger loads and change in the available daily averaged pond simulation temperatures. The ExFT predicted by the model closely matches with that of the experimental results. The slight under prediction between the model and the experimental ExFT is due to the slight difference between the simulated and actual pond temperature values.

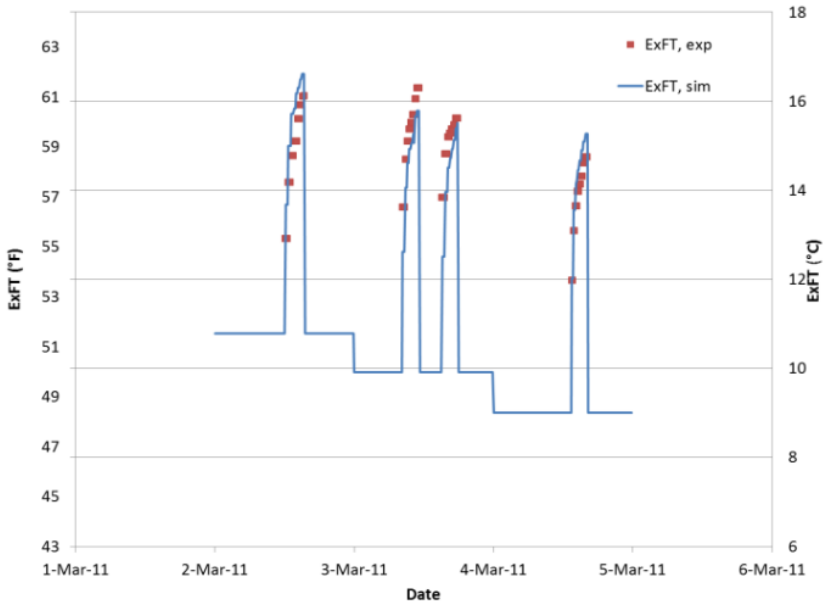

Figure 3- 5: Comparison of the model and experimental ExFT for a spiral-helical coil heat exchanger

CHAPTER 4

SURFACE CONVECTION, SURFACE EVAPORATION AND EDDY DIFFUSION SUB-MODEL SENSITIVITY STUDY

Surface evaporation and to some extent surface convection accounts for majority of heat loss from the surface of a water body and a proper estimation of these mechanisms is essential to accurately determine the surface heat balance. Similarly, a reasonable estimation of the turbulent transport mechanism, which varies with water body, is also required to predict reasonable temperature characteristics of a surface water body. Several models were developed to predict the surface convection, surface evaporation over free water surfaces and turbulent diffusion for different surface water bodies. A literature of seven surface convection/surface evaporation models and eleven eddy diffusion models were obtained and their effects on predicting water body temperatures are analyzed by comparing the water temperature simulations to the measured water temperatures obtained from fourteen lakes located across the United States.

4.1 Models for eddy diffusion coefficient

The transport of mass, energy and momentum in a surface water body is predominantly governed by the turbulent diffusion process. Turbulent diffusion is characterized by irregular, random fluctuations due to turbulent eddies in the water column and hence can be referred as eddy diffusion. The intensity of turbulence in a surface water body depends on the magnitude of several mixing mechanisms, which includes surface wind stress, internal waves, inflows, outflows, and various other mixing mechanisms (Imberger 1985). The turbulent/eddy diffusion in a lake is generally quantified by the eddy diffusion coefficient. The correlations, which predict the eddy diffusion coefficient, are derived based on water temperature measurements or concentrations of natural tracers present in the water body. The eddy diffusion coefficient is generally expressed as a form which can be written as (McCormick and Scavia 1981),

$$k_z = k_{zmax} f(s) \tag{4.1}$$

Where, k_z is the vertical eddy diffusion coefficient in [m^2/day], k_{zmax} is the maximum eddy diffusion coefficient or the eddy diffusion coefficient in the absence of stratification [m^2/day] and s is the stability parameter [-]. The stability parameter is a measure of stability of an oscillating water particle, which oscillates due to the presence of temperature-density gradient and buoyancy fluxes inside the water column and is usually represented by stability frequency or Brunt-Vaisala frequency (N) or by the Richardson number (R_i).

The thermal stratification observed in large lakes due to the formation of temperature-density gradients, which generally partitions the water column into three distinct regions namely, epilimnion or upper mixed region, metalimnion or thermocline region and hypolimnion or lower mixed region. Epilimnion region is always subjected by strong wind shear. The localized wind stress in the epilimnion, results in vigorous and large turbulent currents resulting in high eddy diffusion coefficients. The metalimnion region separates the two mixed regions (epilimnion and hypolimnion) and limits the vertical mixing of the water column due to surface wind stress.

Though the metalimnion and hypolimnion layers are isolated from the effect of wind stress on the surface, these regions are subjected to local mixing which are derived from the energy from internal waves and other mixing phenomenon (Jassby and Powell 1975 ;Imberger 1985 ;Hondzo and Stefan 1993a). The eddy diffusion coefficient in the epilimnion region is calculated using the Stefan, et al. (1982) model and in the metalimnion and hypolimnion regions eddy diffusion coefficient can be estimated from a eleven different models as discussed in the next section.

Epilimnion eddy diffusivity model

Stefan, et al. (1982) estimated the vertical eddy diffusivity coefficient based on the seasonal mean values of eddy diffusion coefficients, calculated from the temperature measurements from Lake Chicot, a large oxbow lake in Arkansas characterized by high turbidity content. Their eddy diffusivity formulation depends only on the wind speed (W).

$$k_z = 28 * (W)^{1.3} \tag{4.2}$$

Where, k_z is the eddy diffusivity coefficient and W is the wind speed.

Metalimnion and Hypolimnion eddy diffusivity models

1. ***Stefan, et al. (1982)***

Stefan, et al. (1982) formulated the eddy diffusivity coefficient for the layers below the mixed layer (thermocline and the hypolimnion) based on their experimental observations from Lake Chicot.

$$k_z = 0.1 * (W)^{1.3} \tag{4.3}$$

2. ***Hondzo and Stefan (1993a)***

Hondzo and Stefan (1993a) formulated a correlation to predict the eddy diffusivity coefficients based on their temperature results from four different lakes in northern Minnesota whose areas range from 15 acres to 1830 acres. They expressed their correlation based on the surface area of the lake and the Brunt- Vaisala frequency.

$$k_z = 8.17 * 10^{-4} \, A_s^{0.56} \, (N^2)^{-0.43} * 8.64 \tag{4.4}$$

Where, N is the stability frequency or Brunt-Vaisala frequency in [1/s] and A_s is the lake surface area in [Km^2].The stability frequency can be calculated as,

$$N^2 = \frac{g}{\rho_{water}} \frac{d\rho}{dz} \quad (4.5)$$

Where, g is the acceleration due to gravity in [m^2/s], ρ_{water} is the density of water in [kg/m3] and z is the depth of the water column in [m].

3. Gu and Stefan (1995)

Gu and Stefan (1995) studied the temperature dynamics of extremely shallow wastewater stabilization ponds. They performed their study in three wastewater stabilization ponds in Minnesota each with a surface area of 1.8 acres and a maximum depth of 1.8 m. The influence of surface wind stress in the temperature profiles of shallow ponds was clearly observed in their study. The shallow ponds, stratified, and de stratified many times in a day with respect to varying wind speeds. The vertical eddy diffusivity model by Gu and Stefan (1995) for small shallow ponds can be expressed as,

$$k_z = \min[k_{zmax}, k_{zmax} C N^{-1}] \quad (4.6)$$

Where, k_{zmax} is the maximum hypolimnion eddy diffusion coefficient and C is a constant taken as 8.66 * 10^{-3} (s^{-1})(Jassby and Powell 1975).

The maximum eddy diffusion coefficient can be observed in a lake during weakly stratified conditions because of extensive turbulent mixing of water layers due to strong wind action. k_{zmax} is dependent on the physical and physiological characteristics of the lake. Hondzo and Stefan (1993a) derived the relationship between k_{zmax} and the surface area of the lake as,

$$k_{zmax} = 0.048(A_s)^{0.56} \quad (4.7)$$

The expression for k_{zmax} holds good for large ponds and lakes. In case of shallow ponds, which tend to stratify and de-stratify many times in a day, there does not appear to be a standard procedure to estimate the value of k_{zmax}. Gu and Stefan (1995) estimated the k_{zmax} value of 0.1m^2/day for their 1.8 acre rectangular waste water pond in Minnesota subjected to inflows to match the experimental temperature profiles.

(McCormick and Scavia 1981) and Henderson-Sellers (1985) expressed the vertical eddy diffusivity coefficient as a non- linear function of wind strength with depth and stratification stability.

4. McCormick and Scavia (1981)

McCormick and Scavia (1981) obtained a correlation of eddy diffusivity coefficient to match the eddy diffusion calculated based on the temperature observations in Lake Ontario (surface area 4,685,118 acres) and Lake Washington (surface area 21,745 acres). The model can be given as,

$$k_z = \frac{u^*}{\beta R_i} \tag{4.8}$$

Where, u^* is the surface wind friction velocity caused by the wind stress on the lake surface in [m/s], β is a constant, and it varies proportional to lake size. McCormick and Scavia (1981) estimated the value of $\beta = 3.5*10^{-4}$ for Lake Ontario and $1.6*10^{-3}$ for Lake Washington to match with the experimental eddy diffusion.

Richardson number is a measure of stratification stability and is calculated based on the following equation

$$R_i = \frac{N^2}{\left(\frac{u^*}{V_k\, z}\right)^2} \tag{4.9}$$

Where, V_k is the Von Karmon constant = 0.4.

5. Henderson-Sellers (1985)

Henderson-Sellers (1985) formulated an analytical expression for eddy diffusion coefficient by also including the Coriolis effect for the lake by considering the latitude of the position of the lake. This Coriolis force can be effective for water bodies with huge surface area.

$$k_z = V_k u^* z \exp(-k^* z)\, f(R_i) \tag{4.10}$$

Where, $k*$ is a non-linear function of wind speed expressed in Equation 4.11 and R_i is the Richardson number

$$k^* = 6.6(sin\theta)^{1/2} W^{-1.84} \quad (4.11)$$

Where, θ is the latitude of the lake in [radians] and W is the wind velocity over the lake surface in [m/s].

The Richardson number is given by the expression,

$$R_i = \frac{1}{20}\left(-1 + \sqrt{1 + \frac{40N^2{V_k}^2 z^2}{u^* \exp(-k^* z)}}\right) \quad (4.12)$$

6. Banks (1975)

Banks (1975) obtained an eddy diffusivity correlation which depends mainly on the wind stress. The correlation calculates the eddy diffusivity based on the amount of wind shear experienced on the lake at every depth. Banks (1975) correlation can be expressed as,

$$k_z = \frac{1}{4\beta}\left(\frac{\rho_{air}}{\rho_{water}}\right) C_d^{\frac{1}{2}} z\, W * 86400 \quad (4.13)$$

Where, β is a constant = 0.55, C_d is the drag coefficient [-], ρ_{air} is the density of air [kg/m^3] and ρ_{water} is the density of the surface water body in [kg/m^3] at the depth z.

7. Tucker and Green (1977)

Tucker and Green (1977) developed their eddy diffusion coefficient correlation as a function of wind speed and stratification strength. Their eddy diffusion coefficient correlation is given by (Kullenberg 1971)

$$k_z = cW^2 N^{-2}\left(\frac{\partial u}{\partial z}\right) \quad (4.14)$$

Where, c is an empirical constant = 0.1, W is the wind speed over the surface of the water body in [m/s], $\left(\frac{\partial u}{\partial z}\right)$ = vertical shear caused by the horizontal wind action.

Tucker and Green (1977) approximated the value for vertical shear which is a function of Richardson number. It is given by the following equation,

$$\left(\frac{\partial u}{\partial z}\right) = \frac{u^*}{V_k\, z}(1 + 10Ri)^{1/2} \quad (4.15)$$

The Richardson number is obtained using an empirical relationship and is given by,

$$R_i = -5 + \left(25 + \frac{N^2 {V_k}^2 z^2}{u^{*2}}\right) \quad (4.16)$$

8. Rohden, et al. (2007)

Rohden, et al. (2007) analyzed the vertical diffusion in small lake of surface area 49 acres. The lake is characterized by strong stratification. They observed very low eddy diffusivity values near the stratified regions and the eddy diffusion coefficient value increased as they approached the lake bottom due to the exchange of heat with the sediment layer. This suggested a relation between eddy diffusion coefficients with the molecular diffusion of heat. The equation formulated is given as,

$$k_z = \frac{c}{Ri} + K_b \quad (4.17)$$

Where, c = molecular diffusion coefficient = $6*10^{-6}$ [m^2/s] and K_b is the molecular diffusivity of heat.

9. Sengupta, et al. (1981)

Sengupta, et al. (1981) considered the effects of area, wind generated turbulence, heat transfer by radiation, and the effect of thermal discharges due to inflow in the hypolimnion layer in their correlation. The effect of this correlation was tested on Lake Keowee a large reservoir with surface area of 18,372 acres. The correlation is given by,

$$k_z = k_{zo}(1 + \sigma R_i)^{-1} \quad (4.18)$$

Where, K_{zo} is the eddy diffusivity under stable conditions expressed in Equation (19) and σ is a semi empirical constant = 0.1 which is obtained from the study in Lake Keowee.

The eddy diffusivity under stable conditions can be expressed as,

$$K_{zo} = 0.21 + 0.052 \sin\left(\frac{2\pi}{365} t + 2.61\right) * 8.64 \quad (4.19)$$

Where, t – 86400 s (1 day).

The Richardson number is calculated empirically,

$$R_i = \frac{\alpha_v g z^2}{u^{*2}} \frac{\partial T}{\partial z} \quad (4.20)$$

Where, α_v is the volumetric coefficient of expansion of water which is a function of temperature [-].

10. Imberger, et al. (1978)

Imberger, et al. (1978) made a field study on Wellington reservoir a medium sized reservoir with an area of 2470 acres and has a maximum depth of 30 m. The reservoir has a major inflow from the Coolie River and an outflow for irrigation purposes. The field data from the Wellington reservoir showed that the mixing in the hypolimnion is not as vigorous as in the surface layers. Imberger, et al. (1978) considers both the effect of wind stresses and the energy from the river to formulate the eddy diffusion coefficients.

$$k_z = \frac{R_c z^2}{t_m s} \tag{4.21}$$

Where, R_c is a reservoir constant a function of reservoir geometry. R_c was calculated to be 0.048 for the Wellington Reservoir. z is the depth of the reservoir, t_m is the time taken for mixing in the hypolimnion at a particular depth in [s] as given in Equation 4.22 and s is the stability of the hypolimnion layer.

$$t_m = \frac{PE}{KE_{inflow} + KE_{wind}} \tag{4.22}$$

Where, PE is the potential energy of the water column at a particular depth in [J], KE_{inflow} is the kinetic energy from the inflowing streams [W] and KE_{wind} is the kinetic energy from the wind on the reservoir in [W].

The stability of the particular layer is given by the equation

$$s = \frac{d\rho}{dz}\left(\frac{z}{\rho(0) - \rho(z)}\right) \tag{4.23}$$

This model was validated with the experimental data from the Wellington reservoir and good temperature results were obtained which is largely due to the consideration of the kinetic energy from the river inflow.

11. Ellis, et al. (1991)

Ellis, et al. (1991) used measured temperature results from Ryan Lake in Minnesota to estimate the eddy diffusion process in a lake when covered with ice. They found that the wind has little or no impact on the eddy diffusion in lakes when covered with ice. Turbulence is caused mainly due to internal seiche waves, ground water infusion and the convective transfer from the sediments. The correlation to predict the eddy diffusion based on the temperature measurements during the ice cover period in Ryan Lake can be expressed as, (Fang and Stefan 1996)

$$k_z = 8.98 * 10^{-4} \, (N^2)^{-0.43} \tag{4.24}$$

The summary of the different eddy diffusion models is given in Table 4- 1.

Table 4- 1: Literature review table on eddy diffusion models

No	Author, Year	Applicability of eddy diffusion model	Surface area of the lakes where the correlation is tested and or obtained (acres)
1	Stefan, et al. (1982)	Epilimnion	4250
2	Stefan, et al. (1982)	Hypolimnion	4250
3	Hondzo and Stefan (1993)	Hypolimnion	(14.8-1828.5) 4 lakes
4	Gu and Stefan (1995)	Hypolimnion	17.3
5	McCormick and Scavia (1981)	Hypolimnion	21745 and 4685118
6	Henderson-Sellers (1985)	Hypolimnion	Theoretical
7	Banks (1975)	Hypolimnion	281700
8	Tucker and Green (1977)	Hypolimnion	247 and 4447897
9	Rohden, et al. (2007)	Hypolimnion	49.4
10	Sengupta, et al. (1981)	Hypolimnion	18372
11	Imberger, et al. (1978)	Hypolimnion	2471
12	Ellis, et al. (1991)	Epilimnion/Hypolimnion	14.8

4.2 Models for surface convection and surface evaporation

The rate of free and forced convection on the lake surface affects the rate of evaporation at the air-water interface. Several empirical correlations exist to determine both the surface

convective and evaporative heat transfer at the lake surface. These correlations are obtained from the experimental data from flat plates, swimming pools, shallow ponds and sea surfaces.

1. *Friehe and Schmitt (1976)*

Friehe and Schmitt (1976), derived the correlations for the convective and evaporative heat fluxes based on the experimental measurements of fluxes at the air-sea interface. The data is collected from different large scale experiments conducted on the surface of the Pacific Ocean at several locations. They measured the parameters such as wind speed, air temperature, sea surface temperature, atmospheric vapor density and vapor density at the sea surface at every location and consequently derived correlations to calculate convective ($q"_c$) and evaporative ($q"_e$) heat fluxes based on these parameters.

$$q"_c = \rho_{air} c_{p,air} (C_1 + C_h W (T_{surface} - T_{air})) \quad (4.25)$$

$$q"_e = h_{fg} C_e W (w_{surface} - w_{air}) \quad (4.26)$$

$$C_e = 1.36 C_h \quad (4.27)$$

Where,

$q"_c$ is the convective heat flux in [W/m^2], $q"_e$ is the evaporative heat flux in [W/m^2], ρ_{air} is the density of air in [kg/m^3], $C_{p.air}$ is the specific heat capacity for air [J/kg °C], $T_{surface}$ is the surface water body temperature [°C], T_{air} is the air temperature [°C], h_{fg} is the latent heat of vaporization in [J/kg], W is the wind speed above the water body surface [m/s] and

C_1 and C_h are constants, which depends on $W (T_{surface} - T_{air})$

$C_1 = 0.0026$; $C_h = 0.86 \times 10^{-3}$ when $W (T_{surface} - T_{air}) < 0$

$C_1 = 0.002$; $C_h = 0.97 \times 10^{-3}$ when $0 \leq W (T_{surface} - T_{air}) \leq 25$, and

$C_1 = 0.0$; $C_h = 1.46 \times 10^{-3}$ when $W (T_{surface} - T_{air}) > 25$

2. *Molineaux, et al. (1994)*

Molineaux, et al. (1994) obtained the correlation for convective heat transfer coefficient based on experimental analysis from five outdoor swimming pools. The surface area of those

swimming pools varies between 1250 m^2 to 3140 m^2. They calculated the heat losses due to convection and evaporation from the swimming pools based on the variation in pool internal energy. The internal energy variations of the swimming pools are directly related to the change in pool temperature. The convective heat transfer coefficient is computed to match with the experimental convection and evaporation losses.

$$h_c = 3.1 + 2.1W \tag{4.28}$$

The evaporative heat flux is calculated from the convective heat transfer coefficient.

$$q"_e = \frac{h_{fg} h_c}{c_{p,air}} (w_{surface} - w_{air}) \tag{4.29}$$

Where, W is the wind speed over the swimming pool surface in [m/s], h_c is the convective heat transfer coefficient in [W/$m^{2.}$ °C], w_{air} and $w_{surface}$ are the humidity ratio of the ambient air and the humidity ratio of saturated air at the swimming pool surface respectively in [kg water/kg dry air], h_{fg} is the latent heat of vaporization in [J/kg] and $q"_e$ is the evaporative heat flux in [W/m^2].

3. Czarnecki (1978)

Czarnecki (1978) citing Sheridan (1972) developed the correlation for convective coefficient for heated swimming pools. The evaporative heat flux ($q"_e$)is calculated based on Czarnecki (1963).

$$h_c = 3.1 + 4.1W \tag{4.30}$$

$$q"_e = 0.0163 h_c (v_{p,surface} - v_{p,air}) \tag{4.31}$$

Where, $v_{p,air}$and $v_{p,surface}$ are the vapor pressure at air temperature and water surface temperature in [Pa] respectively.

4. Crocker and Wadhams (1989)

Crocker and Wadhams (1989) used the surface convection coefficient correlation given by Overland (1985) in their model to predict ice growth in the Antarctic ocean. Overland (1985)

developed the convective heat transfer coefficient correlation based on the experimental temperature observations in the Arctic sea.

$$h_c = 0.00175\rho_{air}c_{p,air}W \quad (4.32)$$

$$q"_e = 0.00175h_{fg}\rho_{air}W(w_{surface} - w_{air}) \quad (4.33)$$

5. *Chiasson, et al. (2000)*

Chiasson, et al. (2000) calculated the convective heat transfer coefficient (h_c), based on the flow over horizontal flat plates. Their correlation is given as,

$$h_c = \frac{Nu\, K_{air}}{L} \quad (4.34)$$

Where, Nu is the Nusselt number [-], k_{air} is the thermal conductivity of air evaluated at the lake-air film temperature [W/m·K] and L is the characteristic length of the lake in [m]. The Nusselt number for free and forced convection over horizontal flat plates are obtained from the correlations described in Incropera and DeWitt (1996).

From the convective heat transfer coefficient, they calculated the evaporative heat flux using Chilton and Colburn analogy. Calculation of evaporative heat flux using Chilton and Colburn analogy is given as follows. Initially the mass flux ($\dot{m}"_{water}$) in [kg/s· m^2], of evaporating water is calculated.

$$\dot{m}"_{water} = h_d\,(w_{air} - w_{surface}) \quad (4.35)$$

Where, h_d is the mass transfer coefficient in [W/m^2· °C]. The mass transfer coefficient (h_d) is calculated as,

$$h_d = \frac{h_c}{c_{p,air}Le^{2/3}} \quad (4.36)$$

Where, $c_{p,air}$ is the specific heat capacity of air evaluated at the lake-air film temperature and Le is the Lewis number [-].

Finally, from calculated mass flux the evaporative heat flux ($q"_e$) in [W/m^2] is calculated as,

$$q"_e = h_{fg}\dot{m}"_{water} \quad (4.37)$$

6. *Losordo and Piedrahita (1991)*

Losordo and Piedrahita (1991) developed a shallow pond model to measure temperature and thermal stratification for shallow aquaculture ponds. In their model they adopted the convection heat transfer coefficient correlation from Argonne National and Asbury (1970). The correlation is given as,

$$h_c = 1.5702\ W \tag{4.38}$$

From the convective heat transfer coefficient the lake model calculates the evaporative heat flux using Chilton and Colburn analogy as described in Equations 4.35 to 4.37. They successfully applied and validated their temperature results from the model implemented with this surface convection correlation, with the experimental data from five shallow ponds whose surface area varied from 0.82 Ha to 4 Ha.

7. *Branco and Torgersen (2009)*

Branco and Torgersen (2009) developed a model for predicting the onset of thermal stratification in shallow lakes and ponds. They used the surface convection model adopted from Argonne National and Asbury (1970) (equation 38) and evaporation model adopted from Adams, et al. (1990).

$$q"_e = \left\{\left(0.0272\left(T_{surface,V} - T_{air,v}\right)^{\frac{1}{3}}\right)^2 + \left(0.051{A_s}^{-0.05}W\right)^2\right\}^{\frac{1}{2}} .\left(v_{p,surface} - v_{p,air}\right) \tag{4.39}$$

$$T_{surface,v} = \frac{T_{surface}}{1 - \frac{0.378\ v_{p,surface}}{P}} \tag{4.40}$$

$$T_{air,v} = \frac{T_{air}}{1 - \frac{0.378\ v_{p,air}}{P}} \tag{4.41}$$

Where, $T_{surface,\ v}$ and $T_{air,\ v}$ are the virtual water surface temperature and air temperature in [K] respectively, P is the atmospheric pressure in [Pa].

4.3 Experimental site description and data collection

A set of 14 lakes characterized by reasonable quantities of temperature profile measurements (includes both daily data measurements and measurements made on a monthly basis), well characterized bathymetry and reasonable diverse locations across the United States have been selected for validation. This set of lakes is summarized in Table 4- 2.

Table 4- 2: List of lakes used in the validation of the pond model

No	Lake	Location	Latitude/Longitude (Decimal Degrees)	Surface area Ha (Acres)	Max depth m (Ft)	Volume m^3 (acre Ft)
1	OSU research pond	Oklahoma	36.135 /- 97.08	1.2 (3)	3.8 (12)	1.73E+04 (14.1)
2	Bradley	Oregon	43.065 /- 124.426	9.3 (23)	10.2 (33.5)	6.56E+05 (5.32E+02)
3	Ice Lake	Minnesota	45.315 / - 92.768	16.6 (41)	16.1 (53)	1.16E+06 (9.40E+02)
4	Wingra	Wisconsin	43.054 /- 89.415	136 (336)	6.3 (20.7)	6.0E+06 (4.86E+03)
5	Dunlap	Texas	29.670 /- 98.068	150 (371)	12 (39.4)	6.33E+06 (5.13E+03)
6	EA Patterson	North Dakota	46.869 /- 102.826	331.4 (819)	10 (33)	1.00E+07 (8.12E+03)
7	Otisco	New York	43.865 /- 76.288	760 (1878)	20.1 (66)	7.78E+07 (6.30E+04)
8	Monona	Wisconsin	43.068 /- 89.358	1326 (3276)	22.6 (74)	1.1E+08 (8.92E+04)
9	Sunapee	New Hampshire	43.436 /- 72.055	1674 (4136)	43.3 (142)	1.85E+08 (1.50E+05)
10	South Holston	Tennessee	36.531 /- 82.063	1853.5 (4580)	74.7 (245)	2.33E+08 (1.89E+05)
11	Sammamish	Washington	47.593 /- 122.096	1982 (4897)	32 (105)	3.5 E+09 (2.84E+06)
12	Maumelle	Arkansas	34.884/- 92.584	3600 (8895)	14 (46)	2.70E+08 (2.19E+05)
13	Mendota	Wisconsin	43.105 /- 89.420	3938 (9731)	25.3 (83)	5.05E+08 (4.09E+05)
14	Washington	Washington	47.609 /- 122.259	8700 (21500)	65.2 (214)	2.9E+09 (2.35E+06)

Of the 14 lakes, only five had near daily annual temperature data. They are OSU research pond OK, Ice Lake MN, Lake Otisco NY, Lake Sammamish WA and Lake Washington WA. The distribution of lakes across the continental United States is shown in Figure 4-1.

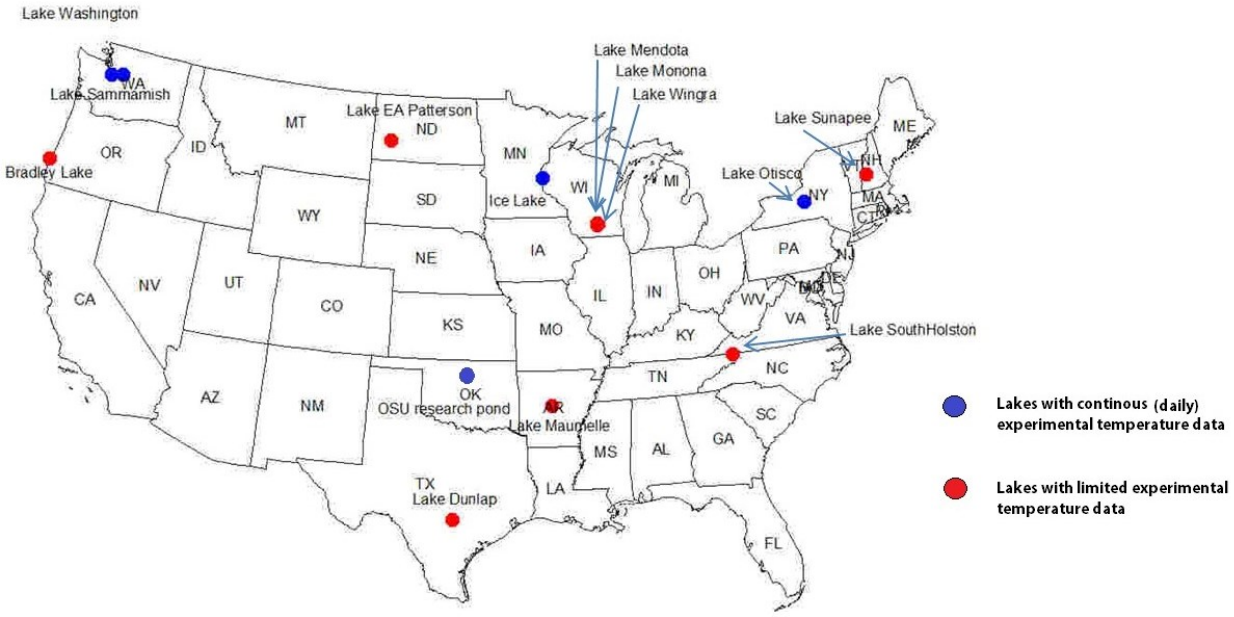

Figure 4- 1: Distribution of lakes used for validation

4.4 Model sensitivity analysis

The sensitivity of the different eddy diffusion and surface convection/surface evaporation models on lake temperatures is analyzed using the metrics such as root mean squared error (RMSE), mean biased error (MBE) and maximum temperature error. For lakes with very limited experimental temperature data, RMSE and MBE analysis are performed based on few days of experimental temperature measurements. The epilimnion, metalimnion and the hypolimnion regions are identified based on the experimental temperature profiles. Tables showing RMSE and MBE in (°C) for every model combination are listed in Appendix A. The surface convection, surface evaporation and the eddy diffusion model and their corresponding model number is given in Table 4- 3.

Table 4- 3: Eddy diffusion, surface convection/surface evaporation models with their corresponding model option numbers

Model option no.	Eddy diffusion model	Model option no.	Surface convection/surface evaporation model
1	Gu and Stefan (1990)	1	Molineaux, et al. (1994)
2	Banks (1975)	2	Losordo and Piedrahita (1991)
3	Hondzo and Stefan (1993)	3	Friehe and Schmitt (1976)
4	Henderson-Sellers (1982)	4	Czarnecki (1978)
5	Senugupta, et al. (1981)	5	Chiasson, et al. (2000)
6	Imberger, et al. (1978)	6	Crocker and Wadhams (1989)
7	McCormick and Scavia (1981)	7	Brett and Thomas (2009)
8	Stefan, et al. (1981)		
9	Tucker and Green (1977)		
10	Ellis, et al. (1991)		
11	Rohden, et al. (2007)		

For the five lakes with multiyear near daily experimental temperature measurements, separate RMSE and MBE analysis are performed for the mixed layer regions (epilimnion and hypolimnion) and the thermocline (metalimnion) region. Since, the epilimnion or the mixed layer depth varies with time, it is almost impossible to manually identify and classify the stratification regions, hence a different methodology is used separate the mixed layer region (epilimnion and hypolimnion) from the metalimnion region experimental temperatures. Epilimnion and hypolimnion regions are usually characterized by low temperature gradients, while the thermocline region in a lake is usually characterized by high temperature gradients. Based on the observations of several experimental temperature profiles, the epilimnion and the hypolimnion regions are classified as regions with temperature gradient ($dt/dz \leq 0.5°C/m$). Similarly, the metalimnion is identified with the temperature gradient $dt/dz > 0.5°C/m$.

The observed temperature gradient in a typically stratified temperature profile of a lake is shown in Figure 4-2.

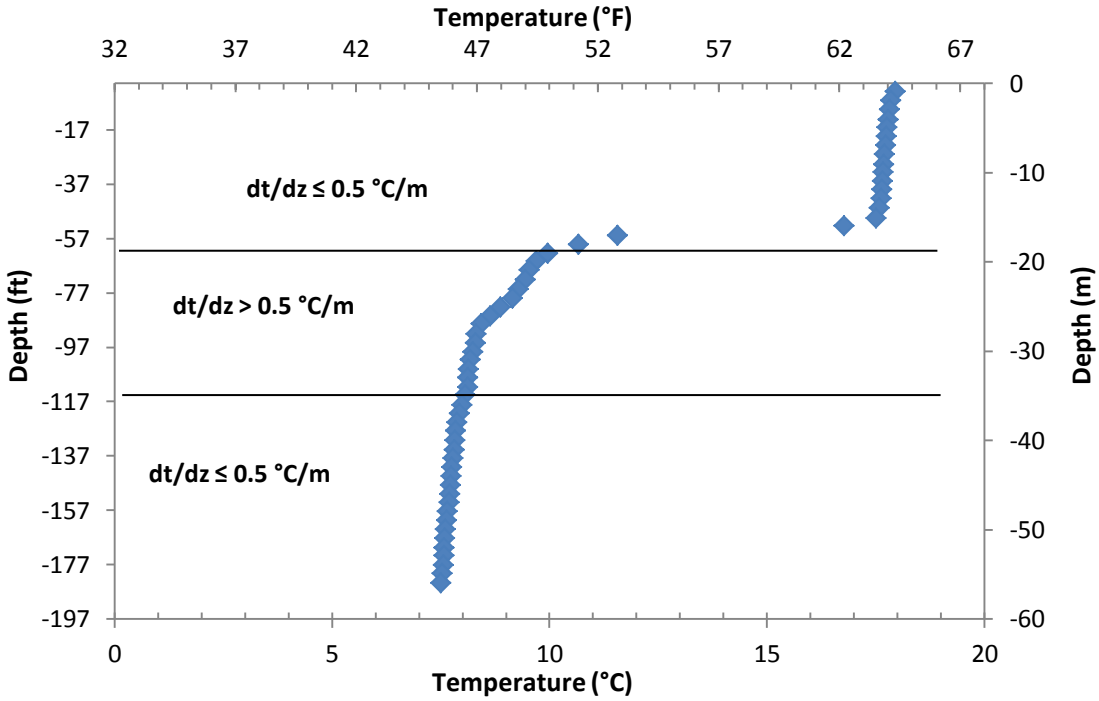

Figure 4- 2: Stratified temperature profile for Lake Washington with observed temperature gradients

The temperature gradient (*dt/dz*) between two consecutive depths '*i*' and '*i-1*' is calculated as,

$$\frac{dT}{dz}_i = \frac{T_{exp,i} - T_{exp,i-1}}{z_i - z_{i-1}} \tag{4.42}$$

Where, $T_{exp,i}$ is the experimental temperature data at a depth *i* [°C].

Using the temperature gradient, RMSE and MBE for the five lakes in the epilimnion/hypolimnion and the metalimnion regions are calculated. Table 4- 4 displays the RMSE and MBE for the best model combination for the lake. In the case for Lake Washington WA both the best and the recommended model combinations are displayed.

Table 4- 4: RMSE and MBE for the best eddy diffusion, surface convection/surface evaporation model combination for the lake

Lake	Surface area Ha (acres)	Max depth m (ft)	Eddy diffusion model no	Surface convection/surface evaporation model option no.	No of years of experimental data	Epilimnion/Hypolimnion		Metalimnion	
						RMSE (°C)	MBE (°C)	RMSE (°C)	MBE (°C)
OSU pond OK	1.2 (3)	4 (13)	1	1	2	1.28	0.37	2.37	-0.80
Ice Lake MN	16.6 (41)	16.1 (53)	6	1	6	1.42	1.01	1.45	0.67
Lake Otisco NY	760 (1878)	20.1 (66)	11	1	3	1.57	0.26	2.16	-0.43
Lake Sammamish WA	1982 (4897)	32 (105)	7	1	4	0.95	0.57	1.39	-0.62
Lake Washington WA	8700 (21500)	65.2 (214)	11	1	4	1.06	0.57	1.37	0.56
			7	1		1.25	0.79	1.58	0.88

4.5 Results and discussion

The best surface convection/ surface evaporation and eddy diffusion model combination for each lake is obtained based on the RMSE, MBE metrics. However, a more general model combination, which performs well for most lake types, is sought. Since, the collection of fourteen lakes vary greatly with the surface area, it is not possible to obtain a single model combination, which could predict reasonable temperature profiles for all lake types. Hence, the available fourteen lakes are divided into four different categories based on the surface area, and the model combination, which could reasonably predict the temperatures for each lake category, is obtained. These model combinations are referred as "Recommended sub-models". The recommended sub-models for each lake categories are identified, as shown in Table 4- 5. The RMSE, MBE and maximum error for each lake with their respective best sub-model combinations and the recommended sub-model combinations are shown in sections below.

Table 4- 5: Recommended sub- models for based on lake size

Lake category	Surface area Ha(acres)	Number of lake validated under this category	Recommended models	
			Surface convection/evaporation	Eddy diffusion
Small shallow ponds	≤ 5 (12)	1	Molineaux, et al. (1994)	Gu and Stefan (1995)
Small lakes	5(12) - 100 (250)	2	Molineaux, et al. (1994)	Imberger et al. (1978)
Medium sized lakes	100(250) - 1000(2500)	4	Molineaux, et al. (1994)	Rohden et al. (2007)
Large lakes	>1000(2500)	7	Molineaux, et al. (1994)	McCormick and Scavia (1981)

It could be noted that Molineaux, et al. (1994) developed the surface convection model based on the tests from heated swimming pools. Even though the scale of convection between the swimming pools and large lakes is not comparable, we analyzed and found that this surface convection model can be used to predict reasonable temperatures for all lakes categories. Our statement can be backed by a similar study from Rasmussen, et al. (1995), where they concluded that the surface convection/evaporation equation developed for a small heated water bodies can be successfully applied to lakes.

Table 4- 6 to 4-8 show the RMSE, MBE and maximum error for the nine lakes with limited experimental data when simulated with the best and the recommended sub-model combinations. The maximum error corresponds to the maximum temperature difference that can be observed between the model and the experimental data for the particular set of observations.

Table 4- 6: RMSE, MBE and maximum error observed in the experimental data points in the epilimnion region

						Epilimnion		
Lake	Surface area Ha(acres)	Max depth m(Ft)	Model category	Convection	Eddy diffusion	RMSE (°C)	MBE(°C)	Max Error(°C)
Lake Bradley OR	9.3 (23)	10.2 (33.5)	Best model combination	Czarnecki(1978)	Henderson-Sellers(1987)	2.4	2.3	3.6
			Recommended model combination	Molineaux, et al.(1994)	Imberger, et al.(1978)	0.8	0.8	1.5
Lake Wingra WI	136 (336)	6.3 (20.7)	Best/Recommended model combination	Molineaux, et al.(1994)	Rohden, et al.(2007)	1.2	1.1	-1.9
Lake Dunlap TX	150 (371)	12 (39.4)	Best/Recommended model combination	Molineaux, et al.(1994)	Rohden, et al.(2007)	-	-	-
Lake EA Patterson ND	331.4 (819)	10 (33)	Best/Recommended model combination	Molineaux, et al.(1994)	Rohden, et al.(2007)	0.8	0.7	-1.9
Lake Monona WI	1326 (3276)	22.6 (74)	Best model combination	Czarnecki(1978)	Imberger, et al.(1978)	1.4	1.3	2.3
			Recommended model combination	Molineaux, et al.(1994)	McCormick and Scavia (1981)	1.2	1.0	-2.0
Lake Sunapee NH	1674 (4136)	43.3 (142)	Best model combination	Czarnecki(1978)	Henderson-Sellers(1987)	1.4	1.0	5.7
			Recommended model combination	Molineaux, et al.(1994)	McCormick and Scavia (1981)	4.5	4.4	-5.9
Lake SouthHolston TN	1853.5 (4580)	74.7 (245)	Best model combination	Czarnecki(1978)	Rohden, et al.(2007)	1.0	0.8	2.0
			Recommended model combination	Molineaux, et al.(1994)	McCormick and Scavia (1981)	1.5	-1.5	-2.0
Lake Maumelle AR	3600 (8895)	14 (46)	Best model combination	Czarnecki(1978)	Henderson-Sellers(1987)	2.0	1.9	2.8
			Recommended model combination	Molineaux, et al.(1994)	McCormick and Scavia (1981)	0.6	0.4	-1.5
Lake Mendota WI	3938 (9731)	25.3 (83)	Best model combination	Czarnecki(1978)	McCormick and Scavia (1981)	0.9	0.9	4.2
			Recommended model combination	Molineaux, et al.(1994)	McCormick and Scavia (1981)	1.0	0.8	4.6

Table 4- 7: RMSE, MBE and maximum error observed in the experimental data points in the metalimnion region

						Metalimnion		
Lake	Surface area Ha(acres)	Max depth m(Ft)	Model category	Convection	Eddy diffusion	RMSE (°C)	MBE(°C)	Max Error(°C)
Lake Bradley OR	9.3 (23)	10.2 (33.5)	Best model combination	Czarnecki(1978)	Henderson-Sellers(1987)	0.8	0.7	2.3
			Recommended model combination	Molineaux, et al.(1994)	Imberger, et al.(1978)	2.4	2.1	-5.0
Lake Wingra WI	136 (336)	6.3 (20.7)	Best/Recommended model combination	Molineaux, et al.(1994)	Rohden, et al.(2007)	-	-	-
Lake Dunlap TX	150 (371)	12 (39.4)	Best/Recommended model combination	Molineaux, et al.(1994)	Rohden, et al.(2007)	1.2	1.1	-2.1
Lake EA Patterson ND	331.4 (819)	10 (33)	Best/Recommended model combination	Molineaux, et al.(1994)	Rohden, et al.(2007)	-	-	-
Lake Monona WI	1326 (3276)	22.6 (74)	Best model combination	Czarnecki(1978)	Imberger et al.(1978)	0.7	0.5	-3.9
			Recommended model combination	Molineaux, et al.(1994)	McCormick and Scavia (1981)	0.8	0.8	-4.1
Lake Sunapee NH	1674 (4136)	43.3 (142)	Best model combination	Czarnecki(1978)	Henderson-Sellers(1987)	0.9	0.7	5.2
			Recommended model combination	Molineaux, et al.(1994)	McCormick and Scavia (1981)	3.4	3.4	-5.5
Lake SouthHolston TN	1853.5 (4580)	74.7 (245)	Best model combination	Czarnecki(1978)	Rohden, et al.(2007)	1.4	1.2	2.9
			Recommended model combination	Molineaux, et al.(1994)	McCormick and Scavia (1981)	2.2	1.8	6.0
Lake Maumelle AR	3600 (8895)	14 (46)	Best model combination	Czarnecki(1978)	Henderson-Sellers(1987)	1.4	1.2	-4.1
			Recommended model combination	Molineaux, et al.(1994)	McCormick and Scavia (1981)	4.0	3.9	-7.6
Lake Mendota WI	3938 (9731)	25.3 (83)	Best model combination	Czarnecki(1978)	McCormick and Scavia (1981)	1.9	1.7	4.3
			Recommended model combination	Molineaux, et al.(1994)	McCormick and Scavia (1981)	2.1	1.9	4.5

Table 4- 8: RMSE, MBE and maximum error observed in the experimental data points in the hypolimnion region

						Hypolimnion		
Lake	Surface area Ha(acres)	Max depth m(Ft)	Model category	Convection	Eddy diffusion	RMSE (°C)	MBE(°C)	Max Error(°C)
Lake Bradley OR	9.3 (23)	10.2 (33.5)	Best model combination	Czarnecki(1978)	Henderson-Sellers(1987)	1.1	0.9	1.7
			Recommended model combination	Molineaux, et al.(1994)	Imberger, et al.(1978)	0.8	0.7	1.2
Lake Wingra WI	136 (336)	6.3 (20.7)	Best/Recommended model combination	Molineaux, et al.(1994)	Rohden, et al.(2007)	-	-	-
Lake Dunlap TX	150 (371)	12 (39.4)	Best/Recommended model combination	Molineaux, et al.(1994)	Rohden, et al.(2007)	-	-	-
Lake EA Patterson ND	331.4 (819)	10 (33)	Best/Recommended model combination	Molineaux, et al.(1994)	Rohden, et al.(2007)	-	-	-
Lake Monona WI	1326 (3276)	22.6 (74)	Best model combination	Czarnecki(1978)	Imberger, et al.(1978)	1.2	1.0	-2.1
			Recommended model combination	Molineaux, et al.(1994)	McCormick and Scavia (1981)	3.2	2.5	-4.5
Lake Sunapee NH	1674 (4136)	43.3 (142)	Best model combination	Czarnecki(1978)	Henderson-Sellers(1987)	1.3	0.7	2.5
			Recommended model combination	Molineaux, et al.(1994)	McCormick and Scavia (1981)	2.0	1.8	-3.4
Lake SouthHolston TN	1853.5 (4580)	74.7 (245)	Best model combination	Czarnecki(1978)	Rohden,, et al.(2007)	-	-	-
			Recommended model combination	Molineaux, et al.(1994)	McCormick and Scavia (1981)	-	-	-
Lake Maumelle AR	3600 (8895)	14 (46)	Best model combination	Czarnecki(1978)	Henderson-Sellers(1987)	2.4	2.3	-4.3
			Recommended model combination	Molineaux, et al.(1994)	McCormick and Scavia (1981)	6.7	6.4	-9.1
Lake Mendota WI	3938 (9731)	25.3 (83)	Best model combination	Czarnecki(1978)	McCormick and Scavia (1981)	2.2	2.2	3.4
			Recommended model combination	Molineaux, et al.(1994)	McCormick and Scavia (1981)	2.3	2.3	3.3

4.6 Validation of design temperatures

For the five lakes with multi-year near daily temperature data (OSU research pond OK, Ice Lake MN, Lake Otisco NY and Lake Sammamish WA and Lake Washington WA), the maximum of the multi-year experimental temperature data at every depth is compared with the corresponding multi-year maximum model simulated temperature results. This method of validation of comparing maximum temperatures is more useful in terms of a design engineer perspective. A design engineer could approximately size a SWHP system using the maximum surface water body temperatures (maximum water body design temperatures) and the building peak cooling loads as inputs. However, this method might result in a slightly oversized SWHP design as the occurrence of peak building cooling loads generally do not coincide maximum water body design temperatures. Based on the available experimental data, the maximum water body temperatures are generally observed during the months of September and October.

Figure 4- 3 to Figure 4- 7 show the comparison between the multi-year maximum experimental temperature data and the maximum model temperatures at every depth when simulated with the best and recommended sub-model combination for multiple years for the five lakes. In the case of OSU research pond OK, Ice Lake MN, Lake Otisco NY and Lake Sammamish WA, both the recommended and the best sub-model combinations are the same.

Figure 4- 3 shows the maximum temperature comparison for OSU research pond based on two years of experimental data. For a shallow OSU pond very little stratification is observed. The simulation slightly over predicts the design temperatures and a maximum error of 1.6 °C (5.8°F) is observed at a depth of 1m (3.2 ft). In the case of the temperature comparison for Ice Lake (Figure 4- 4), the model closely matches with the experimental design temperatures in the epilimnion and generally underpredicts in the metalimnion region. This might be due to the underprediction of the epilimnion layer thickness by the model.

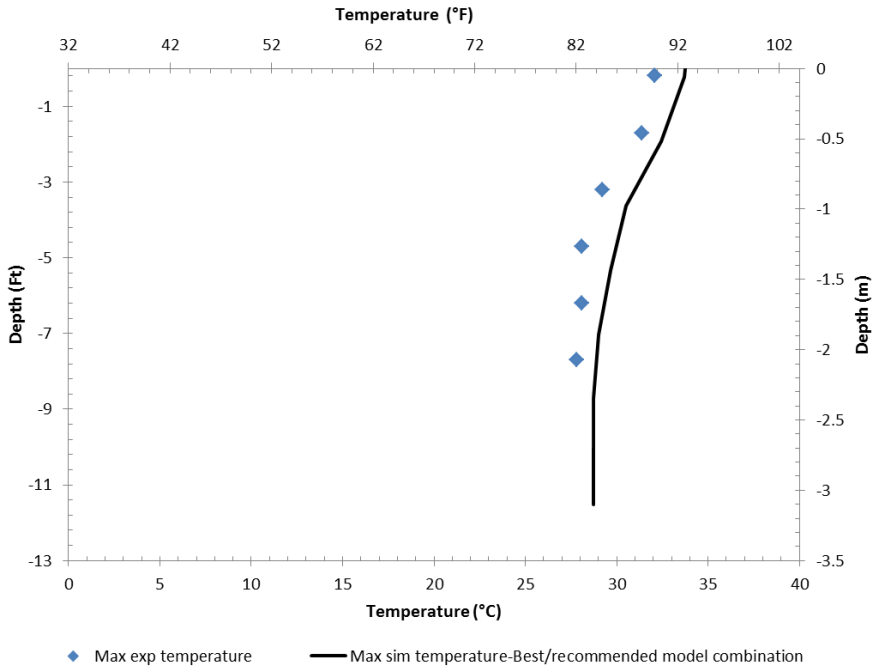

Figure 4- 3: Comparison between the maximum experimental and simulation temperatures obtained from a 2 year data between the years 2011 and 2012 for OSU research pond OK

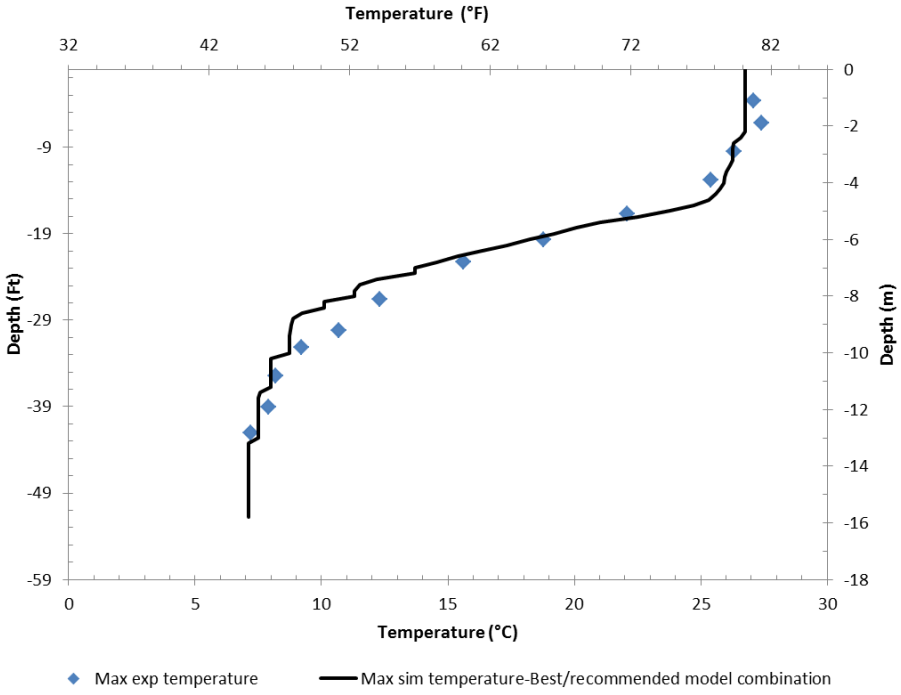

Figure 4- 4: Comparison between the maximum experimental and simulation temperatures obtained from a 6 year data between the years 1998-2003 for Ice Lake MN

The maximum temperature comparison for Lake Otisco is shown in Figure 4- 5. The model generally underpredicts the design temepratures, with higer temperature error in the metalimnion region. After the depth of 15m (49 ft) the model overpredicts the experimental design temperatures, also a near constant temperature profile is observed. This is due to the model predicting a compelte mixing in a lake on a particular day. Also, the lack of continuous experimental data set adds more uncertainity to the validation.

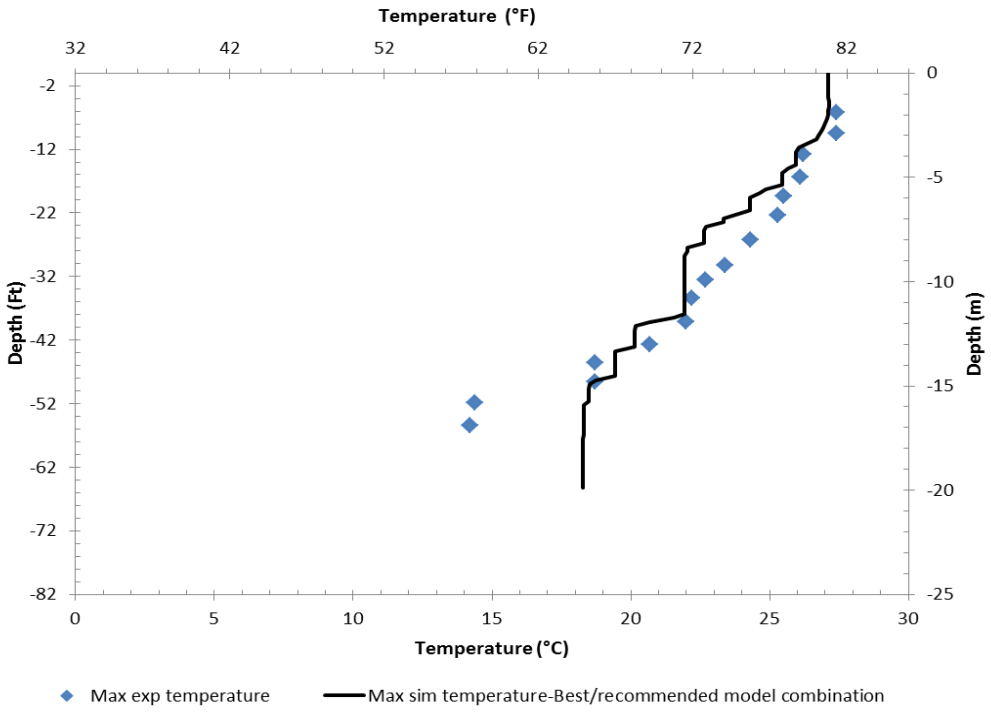

Figure 4- 5: Comparison between the maximum experimental and simulation temperatures obtained from a 3 year data between the years 2002-2004 for Lake Otisco NY

The model predicted design temperature closely matches with the experimental temperatures for Lake Sammamish (Figure 4- 6) except in the hypolimnion where the model slightly under predicts by 1.4°C (2.3 °F). For Lake Washington (Figure 4- 7) the design temperature comparison is performed with the best and the recommended sub-model combination. Both the model combinations underpredicts the design temperatures. Higher errors are observed in the recommended model combination especially in the metalimnion region.

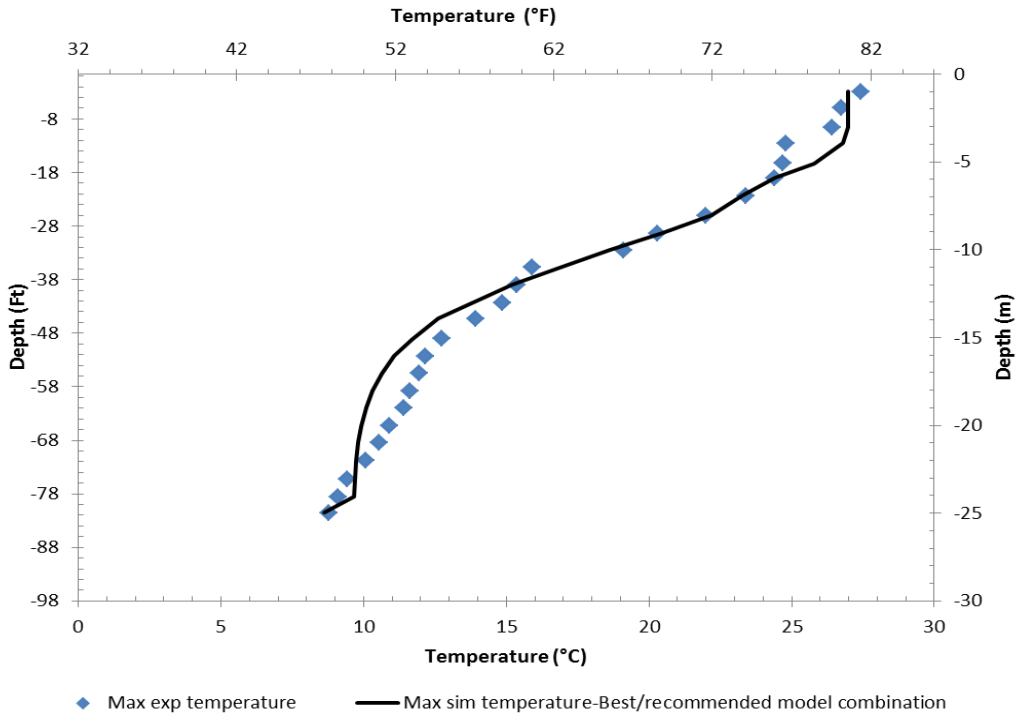

Figure 4- 6: Comparison between the maximum experimental and simulation temperatures obtained from a 4 year data between the years 2005- 2009 for Lake Sammamish WA

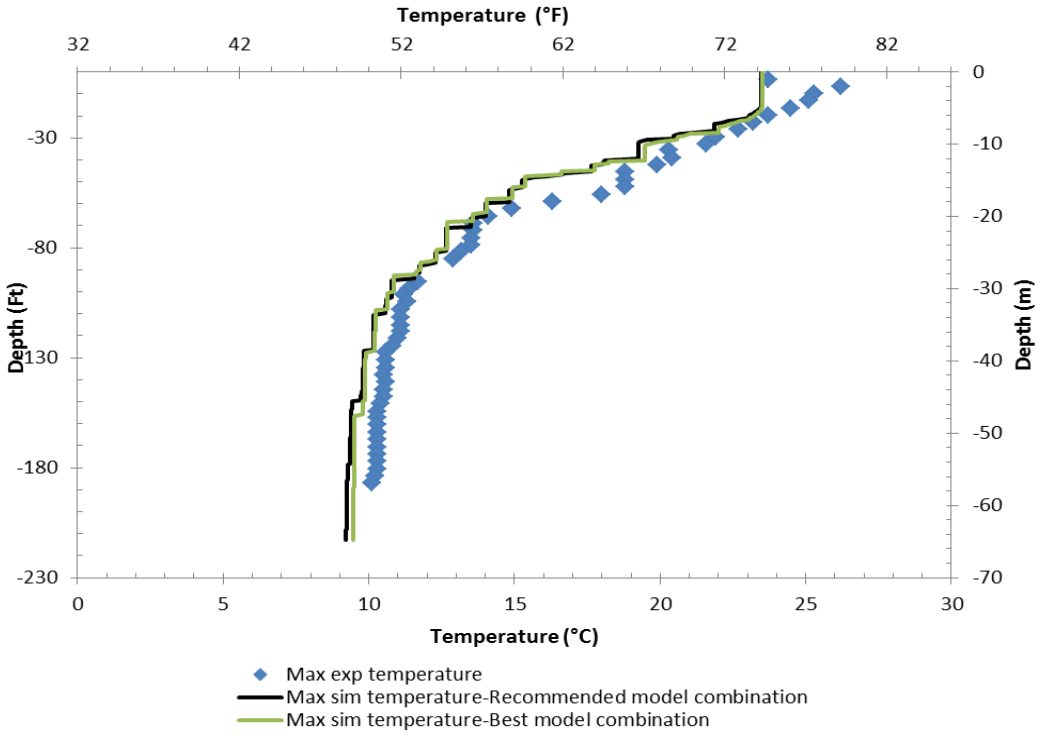

Figure 4- 7: Comparison between the maximum experimental and simulation temperatures obtained from a 4 year data between the years 2009- 2012 for Lake Washington WA

The maximum error between the maximum obtained experimental and simulation temperatures for the multi-years in the epilimnion, metalimnion and the hypolimnion regions when the model is simulated using the best surface convection/eddy diffusion sub-models and the recommended sub models as mentioned in Table 4- 9 to Table 4- 11. The depth range for every region (epilimnion, metalimnion and hypolimnion) is the approximate depth for the regions based on the multi-year maximum experimental data for all lakes except OSU research pond. Since, OSU research pond showed very little stratification, the maximum error for the entire depth is obtained and tabulated in Table 4-9 in the epilimnion region. A negative maximum error indicates that the model over predicts the experiment by the magnitude and vice versa.

Table 4- 9: Maximum error of the maximum temperature difference in the epilimnion region using the best and the recommended surface convection/eddy diffusion models.

						Epilimnion	
Lake	Surface area Ha(acres)	Max depth m(ft)	Model category	Convection	Eddy diffusion	Depth range m(Ft)	Max error of maximum(°C)
OSU research pond OK	1.2 (3)	4 (13)	Best/Recommended model combination	Molineaux, et al.(1994)	Gu and Stefan (1995)	0-4 (0-13)	-1.6
Ice Lake MN	16.6 (41)	16.1 (53)	Best/Recommended model combination	Molineaux, et al.(1994)	Imberger, et al.(1978)	0-4 (0-13)	0.64
Lake Otisco NY	760 (1878)	20.1 (66)	Best/Recommended model combination	Molineaux, et al.(1994)	Rohden, et al.(2007)	0-5 (0-16.4)	-0.34
Lake Sammamish WA	1982 (4897)	32 (105)	Best/Recommended model combination	Molineaux, et al.(1994)	McCormick and Scavia (1981)	0-5(0-16.4)	2
Lake Washington WA	8700 (21500)	65.2 (214)	Best model combination	Molineaux, et al.(1994)	Rohden, et al.(2007)	0-7(0-23)	2.7
			Recommended model combination	Molineaux, et al.(1994)	McCormick and Scavia (1981)		2.7

Table 4- 10: Maximum error of the maximum temperature difference in the metalimnion region using the best and the recommended surface convection/eddy diffusion models.

						Metalimnion	
Lake	Surface area Ha(acres)	Max depth m(ft)	Model category	Convection	Eddy diffusion	Depth range m(Ft)	Max error of maximum(°C)
OSU research pond OK	1.2 (3)	4 (13)	Best/Recommended model combination	Molineaux, et al.(1994)	Gu and Stefan (1995)	-	-
Ice Lake MN	16.6 (41)	16.1 (53)	Best/Recommended model combination	Molineaux, et al.(1994)	Imberger, et al.(1978)	5-10 (16.4-33)	4.1
Lake Otisco NY	760 (1878)	20.1 (66)	Best/Recommended model combination	Molineaux, et al.(1994)	Rohden, et al.(2007)	6-13(20-43)	3.4
Lake Sammamish WA	1982 (4897)	32 (105)	Best/Recommended model combination	Molineaux, et al.(1994)	McCormick and Scavia (1981)	6-18(20-59)	0.9
Lake Washington WA	8700 (21500)	65.2 (214)	Best model combination	Molineaux, et al.(1994)	Rohden, et al.(2007)	8-30(26-99)	3.4
			Recommended model combination	Molineaux, et al.(1994)	McCormick and Scavia (1981)		3.5

Table 4- 11: Maximum error of the maximum temperature difference in the hypolimnion region using the best and the recommended surface convection/eddy diffusion models.

						Hypolimnion	
Lake	Surface area Ha(acres)	Max depth m(ft)	Model category	Convection	Eddy diffusion	Depth range m(Ft)	Max error of maximum(°C)
OSU research pond OK	1.2 (3)	4 (13)	Best/Recommended model combination	Molineaux, et al.(1994)	Gu and Stefan (1995)	-	-
Ice Lake MN	16.6 (41)	16.1 (53)	Best/Recommended model combination	Molineaux, et al.(1994)	Imberger, et al.(1978)	11-13 (36-43)	0.4
Lake Otisco NY	760 (1878)	20.1 (66)	Best/Recommended model combination	Molineaux, et al.(1994)	Rohden, et al.(2007)	14-17(46-56)	-4.0
Lake Sammamish WA	1982 (4897)	32 (105)	Best/Recommended model combination	Molineaux, et al.(1994)	McCormick and Scavia (1981)	19-25(62-82)	-0.6
Lake Washington WA	8700 (21500)	65.2 (214)	Best model combination	Molineaux, et al.(1994)	Rohden, et al.(2007)	31-57(102-187)	0.6
			Recommended model combination	Molineaux, et al.(1994)	McCormick and Scavia (1981)		0.8

CHAPTER 5

MODEL LIMITATIONS

This chapter provides some of the important limitations of both the lake model and the SWHE model.

5.1 Lake model limitations

The limitations of this lake model includes,

a. One-dimensional nature of the model:

The surface water body temperatures predicted by the model is assumed to vary with time only in the vertical direction (i.e.) the model considers change in temperatures only along the depth and assumes uniform horizontal lake temperatures. Though, the horizontal variation in lake temperatures are generally minimal (Yeates and Imberger 2003) the presence of local mixing (inflows, outflows) or other mechanisms might cause variations in the lake temperatures.

The extent of horizontal variation in temperatures is observed based on the temperature data from South Holston reservoir in Tennessee and Lake Maumelle in Arkansas. The temperature data in both the lakes show little variation in horizontal temperatures. South Holston reservoir in Tennessee is a large reservoir with a surface area 1853.5 Ha (4580 acres) and a maximum depth 75m (245 ft). The reservoir water quality is monitored by the Tennessee Valley Authority. Figure 5- 1**Error! Reference source not found.** shows the map of the South Holston reservoir with the approximate location of the temperature measuring sites (in red dots).

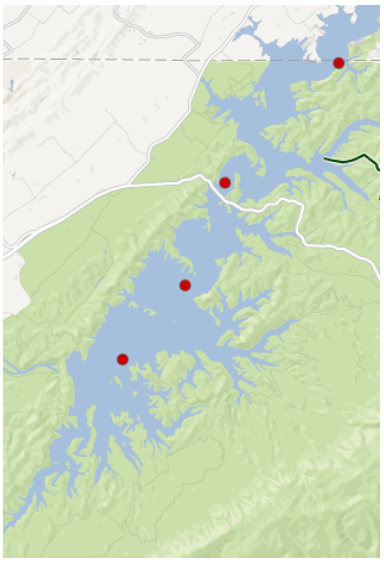

Figure 5- 1: Google map image view of the South Holston reservoir in Tennessee © Google 2013 with the location of the temperature measuring sites (red dots).

The measured temperature values obtained from different sites for a particular day during the months of August and September 2008 is shown in Figure 5- 2 and Figure 5- 3. Both experimental temperature measurements show almost no horizontal variations in lake temperatures.

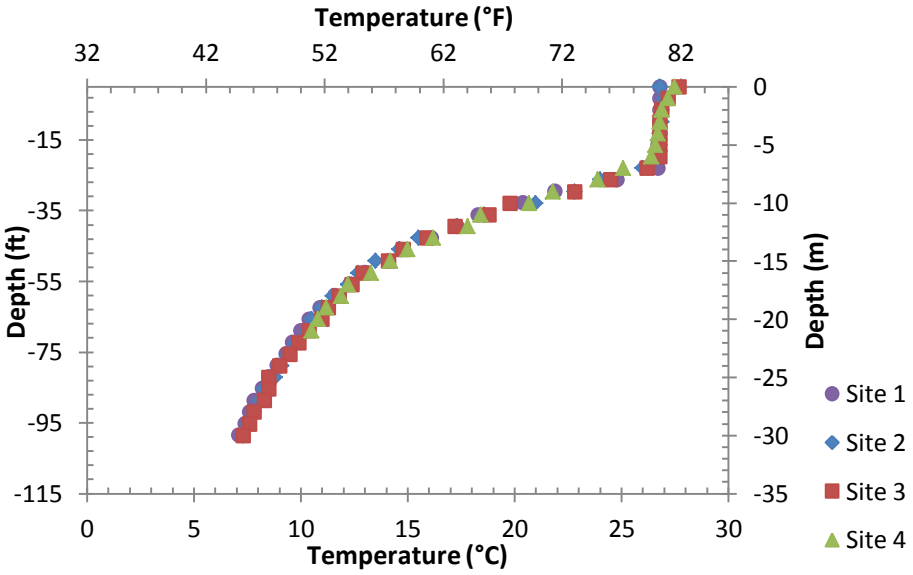

Figure 5- 2: Experimental temperature measurements for South Holston reservoir on August 4, 2008

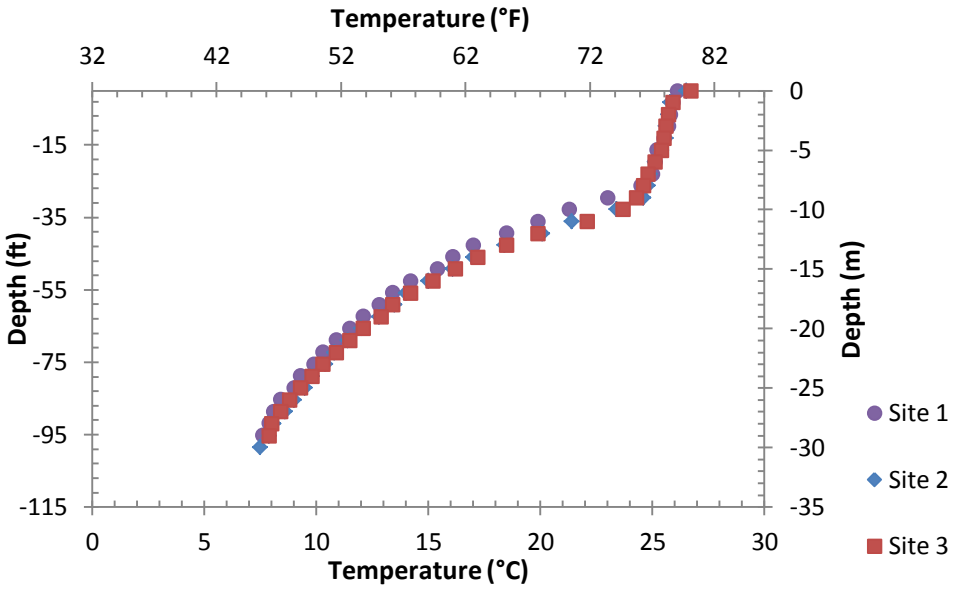

Figure 5- 3: Experimental temperature measurements for South Holston reservoir on September 2, 2008

Lake Maumelle in Arkansas is also a relatively large lake with a surface area 3600 Ha (8895 acres) and a maximum depth of 14 m (46 ft). The water temperature data for three different locations along the lake for month of August and September 2007 is obtained from USGS (2013). Figure 5- 4 shows the map for Lake Maumelle along with the temperature measuring stations.

Figure 5- 4: Google map image view of Lake Maumelle in Arkansas © Google 2013 with the location of the temperature measuring stations

Figure 5- 5 and Figure 5-6 show the experimental temperature measurements obtained from the three measuring stations measured on August 16 and September 12, 2007 respectively. The

observed temperature measurements show only slight variation in lake temperatures though the lake depth observed in the three measuring stations varies significantly.

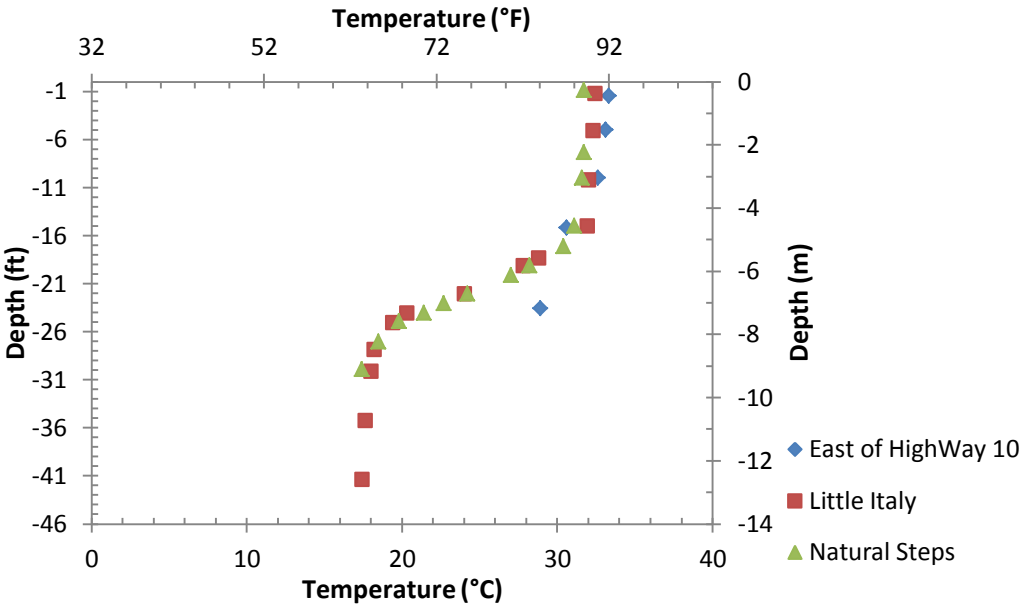

Figure 5- 5: Experimental temperature measurements for Lake Maumelle on August 16, 2007

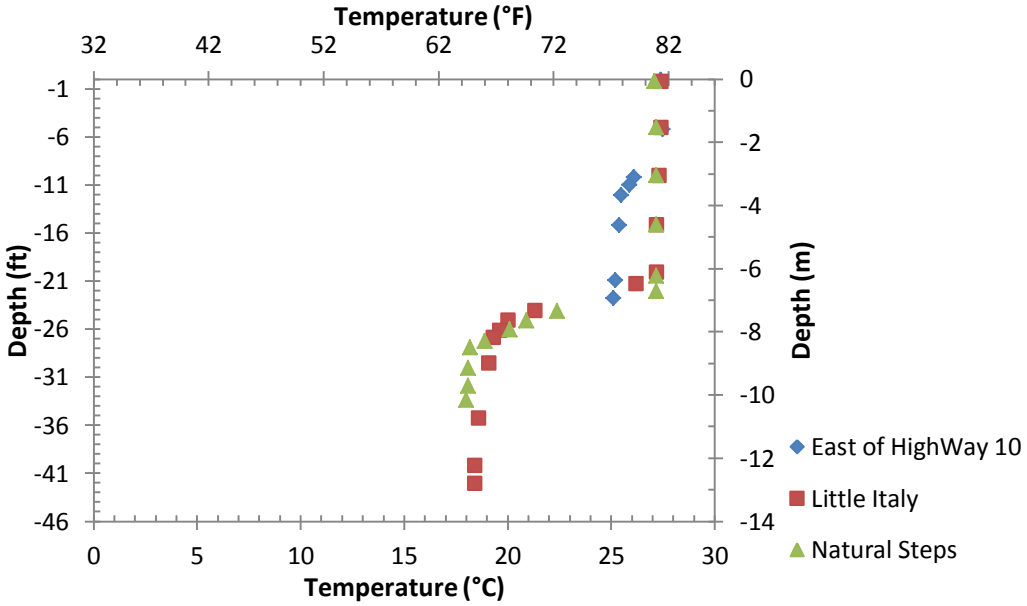

Figure 5- 6: Experimental temperature measurements for Lake Maumelle on September 12, 2007

Temperature data from multiple sites in Lake South Holston TN and Lake Maumelle AR, show a minimal variation in horizontal temperatures. This suggests that a one-dimensional model is sufficient to provide reasonable temperature results for lakes; however, a more detailed analysis is required to completely understand the horizontal temperature variation.

b. Sub-daily variation in lake temperatures

Of all the physical parameters, which control the water temperatures, the effect of wind speed can be quite significant. The effect of wind speed on the variations in water temperatures and the comparison with the daily simulation lake model is presented with the following example. Lake Sammamish is a large lake (surface area 4987 acres (1982 Ha); maximum depth 33 m (105 ft)) located in Seattle, Washington. The lake is subjected to alternative calm and windy conditions from 6th through 8th of October 2008. The hourly and daily average wind speeds are shown in Figure 5-7.

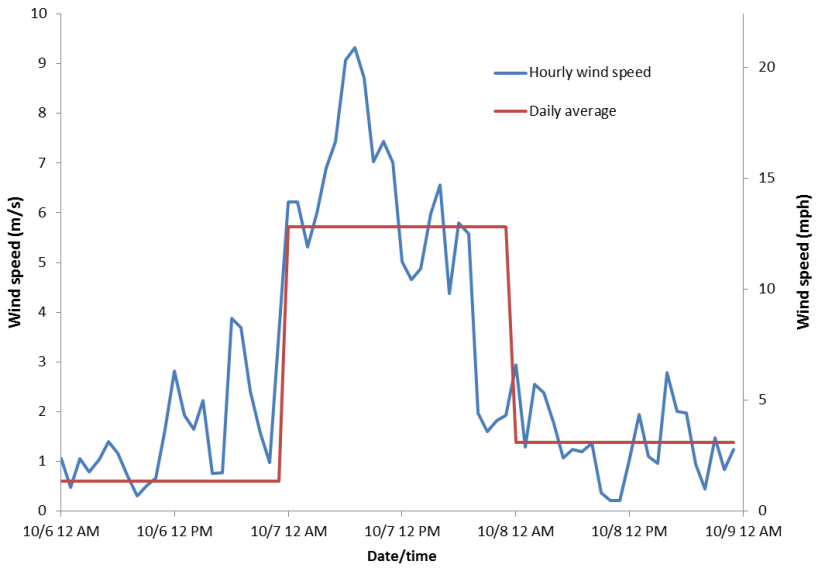

Figure 5- 7: Hourly and daily averaged wind speeds for Lake Sammamish, Oct 6-8, 2008

Temperatures were measured from a single measuring station at four-hour period intervals everyday as shown in Figures 5-8 to 5-10. Even on a relatively calm day (October 6, Figure 5-8),

the hourly measurements showed some variation. The daily temperature simulation comes closest to matching the 8 PM temperature profile.

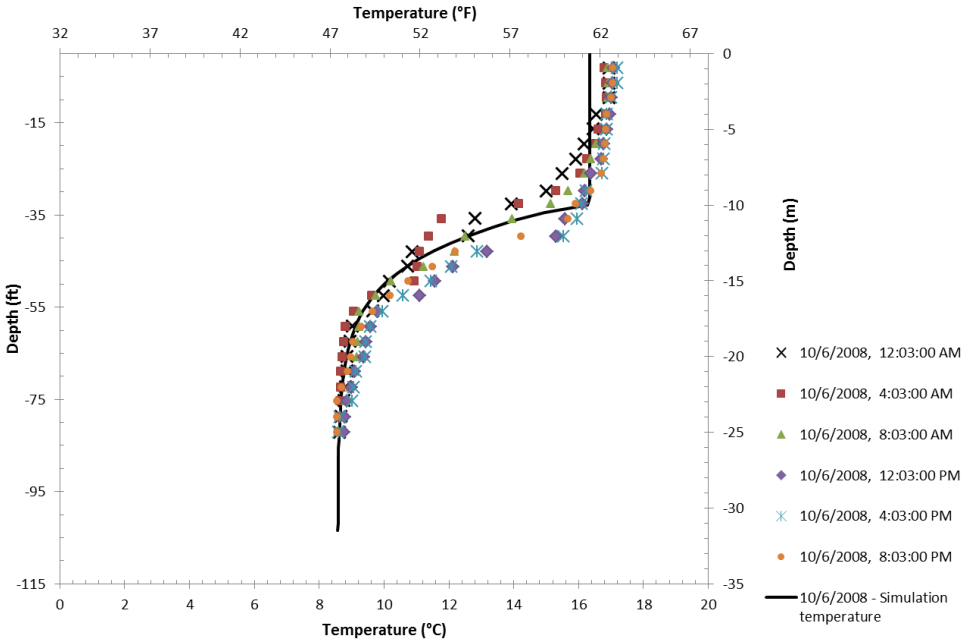

Figure 5- 8: Temperature profiles for Lake Sammamish, October 6, 2008

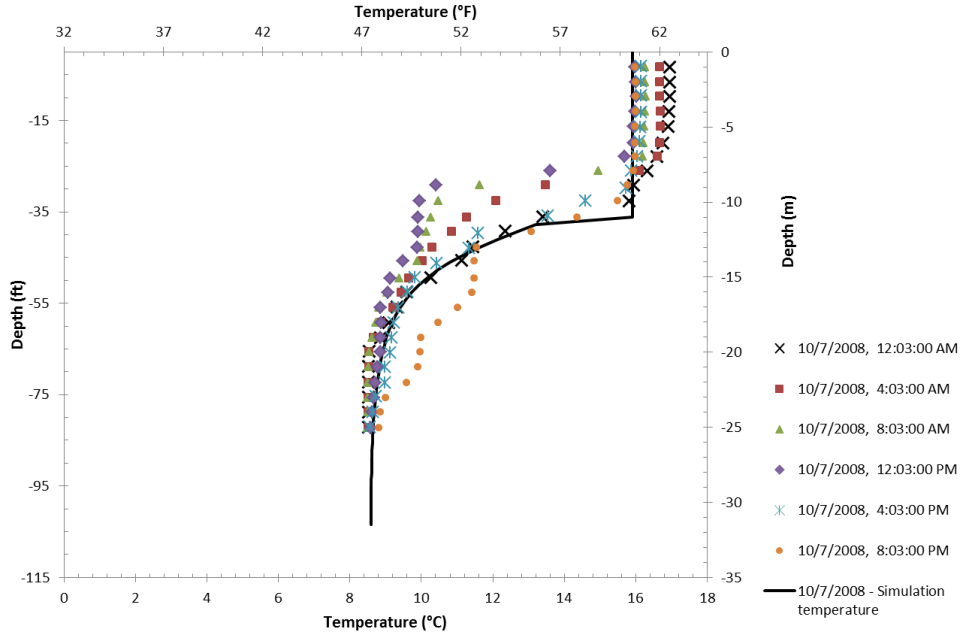

Figure 5- 9: Temperature profiles for Lake Sammamish, October 7, 2008

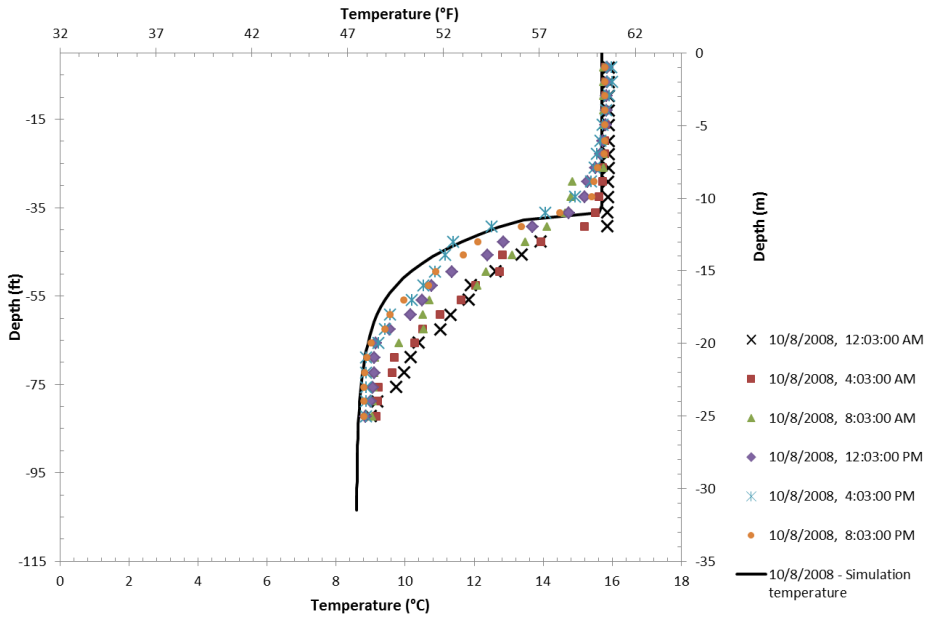

Figure 5- 10: Temperature profiles for Lake Sammamish, October 8, 2008

All the three days shows some variation in temperatures at lower depths. But, within the metalimnion (thermocline) at a depth of 20 m (66ft) on the 7th of October 2008, the temperature cools down by 6°C (10°F) during the first half of the day, and then warms by about 6°C (10°F) during the second half of the day. The proximate cause for this is the epilimnion becoming more shallow, then increasing in depth. This is apparently driven by the wind. It can be concluded that, at least, a windy day can affect temperatures down to a significant depth. The model accuracy is limited by the use of the daily averaged data.

c. Variation in the water body depth

The lake model assumes the depth of the water body to remain constant throughout the year. However, the water body depth varies with the amount of inflow, outflow, evaporation and precipitation. Though the lake model predicted the temperatures reasonably for the fourteen lakes (which also exhibits depth variation), the model could not be reasonably validated with the temperature results from reservoirs, which especially exhibit very high water level fluctuations in a year. This limitation is explained with the validation of the lake model with the experimental

temperature measurements from Henry Hagg reservoir in Oregon. Henry Hagg reservoir is a medium sized reservoir with a surface area of 467 Ha (1153 acres) and has a maximum depth of 33.5 m (110 ft).

The Henry Hagg reservoir is characterized by high inflows and outflows, which make the maximum depth of the reservoir to vary between 15-33 m (49-108 ft) every year. Figure 5- 11 compares the model predicted temperature values with the experimental observations from Henry Hagg Lake. The lake depth is observed to vary from 15.5m (51 ft) in July to approximately 30 m (98 ft) in October. Such high variations in lake depth coupled with the high inflow conditions result in a different surface heat balance and mixing dynamics, which could not be predicted by the lake model. Hence, high temperature difference between the model and the experiment in the order of 8°C (15°F) is observed as shown in Figure 5- 11.

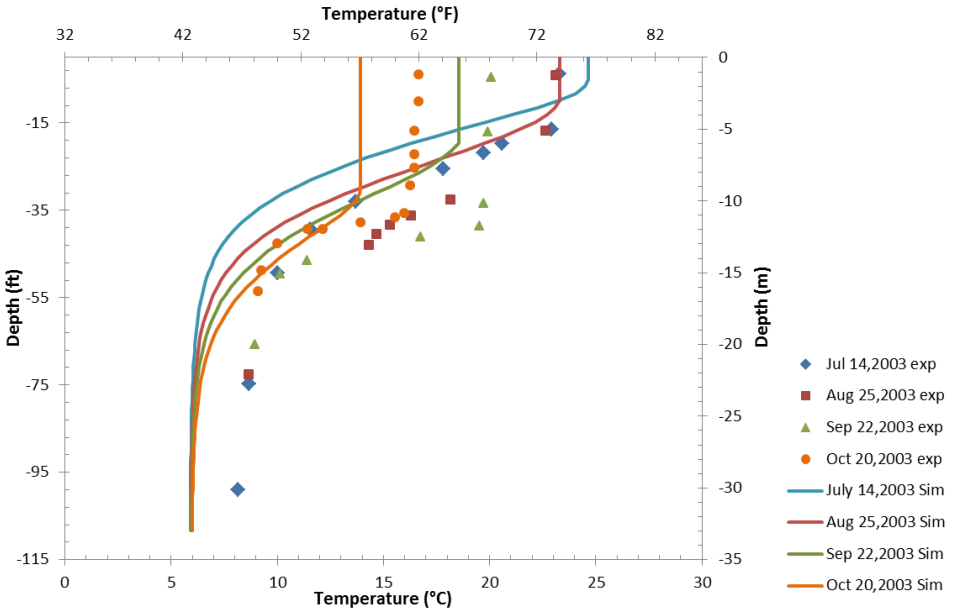

Figure 5- 11: Comparison between experimental and simulated temperatures for Henry Hagg Lake OR

The model also assumes the heat exchanger is placed in an absolute depth inside the water column, but as the relative depth of the heat exchanger varies with the water depth, it might also result in poor heat exchanger heat transfer prediction by the model.

d. Effect of saline intrusion and other limnological factors

The lake model considers the density variation in the water column as a function of temperature alone. It does not consider the effects of salinity or saturation of other minerals on water density. In addition, certain limnological factors unique to certain lakes as in the case of Lake Seneca in New York could also add to the poor prediction by the lake model.

Lake Seneca with the surface area of 17500 Ha (43243 acres) and a maximum depth of 200m (656 ft) is one of the largest, and the deepest of the "Finger Lakes". Lake Seneca sits on top of a shale/rock salt bed and is often subjected to very large and sudden internal waves, and internal saline surges. Hunkins and Fliegel (1973) observed and recorded the sudden temperature changes in a short span of time of time in Lake Seneca and attributed the cause as due to very large internal waves. Wing, et al. (1995) analyzed the morphology of Lake Seneca and postulated the reason for the sudden temperature change due to seepage of saline water from the bed rock caused by the action of large internal waves. Figure 5- 12, shows the buoy measured 12 hour temperature values for Lake Seneca for October 21-23, 2010. Temperature values on October 23, 2010 shows a sudden deepening of the epilimnion and a maximum temperature difference of 6.2°C (12°F) is observed at a depth of 20m (67 ft) within 12 hours. In this case, the epilimnion deepening is not only caused by the wind action, but might also due to the sudden saline intrusion. The lake model could not track such changes in lake temperatures.

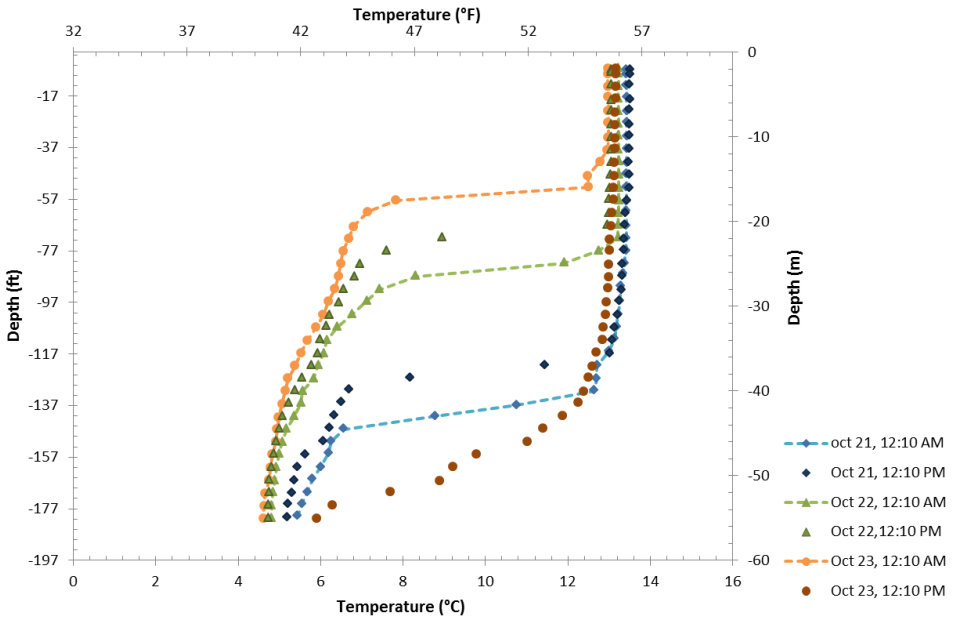

Figure 5- 12: Buoy measured temperature values for Lake Seneca for October 21-23, 2010.

e. Distribution of the heat exchanger energy in the lake

The energy supplied to the lake by the SWHE is generally dissipated by means of a buoyant plume. The direction of the motion of the plume (upwards to the surface or downwards to the lake bottom) depends on the density difference between the plume and the surrounding water. The lake model currently determines the direction of the buoyant plume and distributes the energy from the SWHE uniformly (proportionally to the volume) to each water layer between the heat exchanger and the surface (for upward plumes) or in the layers between the heat exchanger and the bottom (for downward plumes). Though the methodology is reasonable an actual buoyant plume model is necessary for an accurate energy analysis of a SWHP system.

5.2. SWHE model limitations

1. The SWHE model includes a simple algorithm to calculate the overlapping angle of ice layers between adjacent coil segments for only the spiral-helical coil heat exchanger configuration. The algorithm for calculating the overlapping angle for

other coil type heat exchanger configurations are not included owing to the combination of both complicated geometry of the heat exchanger and due to lack of experimental data.

2. The SWHE model considers the undisturbed lake temperature as its boundary condition in the heat transfer calculations. It does not consider the heat interactions with the neighboring heat exchanger coils/plates.

CHAPTER 6

DESIGN TOOL DEVELOPMENT

6.1 Introduction

The design tool for surface water heat pump systems can be used as an aid in the sizing of the SWHE used in a closed loop SWHP system. The procedure utilized by the design tool can be divided into three tasks:

a. First, based on user input regarding the physical characteristics and location of the water body, the design tool simulates the lake and finds the daily water body temperatures[2] at the depth of the heat exchanger.

b. Second, based on the water body temperatures at the depth where the heat exchanger is placed, the design tool calculates the heat transfer performance and determines the required size of the SWHE. The design tool can do this for four different SWHE configurations - spiral-helical, flat spiral, horizontal/vertical slinky and vertical flat plate heat exchangers. The design tool also determines the buoyancy force exerted on each heat exchanger if/when ice forms on the SWHE.

c. Third, as a final check, the design tool simulates the lake considering the heat input and heat extraction of the SWHP system. Although, for most systems, the effect of the SWHP system on the lake will be negligible

[2] These temperatures are the undisturbed temperatures; only in the last step is the effect of the heat exchangers on the lake temperature analyzed.

6.2 Overview

The design tool is comprised of a Microsoft Excel spreadsheet and two executable files (LakeModel.exe) that contains the lake simulation and (SWHEmodel.exe) that contains the heat exchanger simulation model; originally written in Fortran 90. Figure 6-1 is a flowchart, which shows a general overview on the operational structure of the design tool.

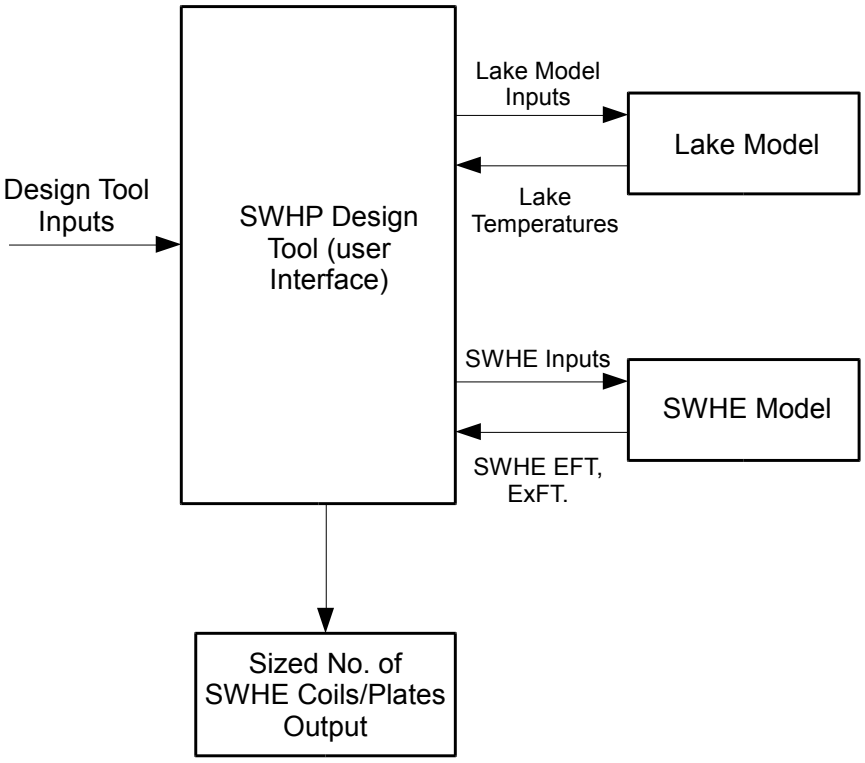

Figure 6- 1: Flow chart of the operation of SWHP design tool

The design tool requires eight sets of user inputs. The inputs can be classified into two major categories.

1. Lake model inputs:

The lake model inputs contain user information to simulate the lake temperatures. The lake model input contains,

a. Hourly weather data for the location.

b. Lake morphometry - which describes the physical characteristics of the lake that are relevant to the lake simulation, specifically the bathymetry and turbidity.

c. Undisturbed ground temperature and initial water body temperatures.

2. SWHE model inputs

The following inputs are required for the SWHE model.

a. Hourly or monthly and monthly peak total building heating and cooling loads.

b. Surface water heat exchanger information.

c. Type and percentage of concentration of antifreeze used, if any.

d. Surface water heat pump characteristics.

e. Surface water heat pump design temperatures.

All the design tool inputs are explained in detail in the design tool documentation and example of usage (Appendices B and C) respectively.

6.2.1 Simulating lake temperatures

Upon final verification of the input data by the user, the design tool creates a set of text files containing the lake model inputs and simulates the lake using the Lakemodel.exe file. Based on the lake surface area the design tool automatically utilizes the recommended eddy diffusion, surface convection/evaporation sub-model combination obtained for each lake category. The recommended sub-model combination for each lake category is discussed in detail in Chapter 4 of this thesis. For some cases, since the user provides the design tool with an assumed initial lake temperature, the design tool simulates the lake model twice or thrice until a steady state is obtained in the predicted lake temperatures. Once, the lake temperatures are simulated, the Lakemodel.exe outputs a text file containing the daily average lake temperatures between the depths where the surface water heat exchangers are placed.

6.2.2 Simulating SWHE heat transfer and fluid temperatures

The design tool uses the SWHE model inputs and the average lake temperature at the heat exchanger depth to simulate the SWHE fluid temperatures and the heat transfer using the SWHEmodel.exe file. The SWHE model uses the average lake temperatures as a boundary condition in predicting the heat transfer performance of the SWHE. The SWHE model output is a text file with the hourly heat exchanger entering, exit fluid temperatures, heat exchanger buoyancy force during icing conditions and the heat extraction and rejection rates of the SWHE.

6.2.3 Sizing the number of SWHE coils/plates

The design tool iteratively estimates the optimum number of SWHE coils/plates required to satisfy the design conditions. The design tool calculates the initial guess value on the number of SWHE coils/plates based on the maximum design conditions. That is, the peak cooling load and the maximum lake temperature is used as boundary conditions to estimate the number of coils/plates required to satisfy the design maximum heat pump entering fluid temperatures. Similarly, the peak heating load and the minimum lake temperature is used to estimate the number of coils/plates required to satisfy the design minimum heat pump entering fluid temperatures. With this initial guess, the design tool simulates the SWHE model to predict the hourly heat pump entering and exit fluid temperatures. For the consecutive iterations, the design tool estimates the number of coils using the golden section search optimization algorithm. For every sizing iteration the design tool simulates the SWHE model.

The design tool finally displays the optimum number of SWHE coils/plates among the other outputs in a separate output sheet.

6.2.4 Estimating the impact of the SWHE on lake temperatures

Although in most cases, SWHP systems have minimal to negligible impact on the water body, it is possible that excessive heat extraction or rejection by the SWHP system relative to

lake size would have an adverse impact on the lake temperatures and hence could adversely affect the capacity and heat transfer performance of the SWHP system. The design tool simulates the lake considering the heat transfer effects from the sized SWHE. The design tool outputs the change in lake temperatures at the heat exchanger depth in a separate output sheet.

Based on several test run conditions, the average time required by the design tool to perform one complete simulation is around 15-20 minutes, although the design tool "run" time may vary with the user input conditions.

6.3 Design tool limitations

Since, the design tool utilizes the both lake model and the SWHE model in its sizing calculations, the limitations of both the models applies to the design tool. Some general limitations to the design tool performance includes,

1. The application of the design tool is limited to SWHP design on relatively stagnant water bodies, as the lake model could not reasonably predict the water body temperatures, which exhibit high fluctuation in its depth in a year.
2. The design tool uses the automated procedure in the selection of the recommended sub-model combination for each lake category in the calculation of lake temperatures. Hence, the design tool might provide different lake temperatures for two lakes with almost the same surface area but which fall under different lake categories (100 acre and a 101 acre lake). Hence, the design tool might estimate different number of SWHE coils/plates for the same design conditions for such conditions.

CHAPTER 7

SUMMARY, CONCLUSIONS AND RECOMMENDATIONS

A lake model that treats both the lake and the surface water heat exchanger, to effectively predict the lake temperature and stratification dynamics, as well as the heat transfer performance of a surface water heat exchanger is developed. The following sections provide a general summary, conclusions that can be derived from this work, and a list of possible recommendations for future research.

7.1 Summary

7.1.1 Lake model

1. A one-dimensional lake model to predict the lake dynamics (temperature, stratification, ice/snow cover) has been developed. The model also considers the effect of surface water heat exchangers (SWHE) on lake temperatures.
2. Seven surface convection/surface evaporation models and eleven different eddy diffusion models were implemented in the one-dimensional lake model, and validated with the experimental temperatures obtained from fourteen lakes diversely located across the continental United States. The best sub-model combination for each lake and the recommended sub-model combination for each lake category are identified based on the RMSE and MBE metrics. The best sub-model combination for each lake is presented in tables 4-6 to 4-8 and the recommended model combination for each lake category is presented in table 4-5 respectively.

3. The surface convection/surface evaporation model by Molineaux, et al. (1994) predicted reasonable temperatures for all lake categories. Though the model was developed from the experimental measurements from heated swimming pools it can be successfully applied to large water bodies. Our statement can be backed by a similar study from Rasmussen, et al. (1995).
4. For the lakes with multi-year near daily experimental temperature data, a design temperature validation is performed by comparing the maximum multi-year experimental data with the predicted model temperatures. As expected higher errors were observed in the metalimnion region due to the uncertainty by the model in accurately predicting the mixed layer depth.

7.1.2 SWHE model

1. A SWHE model that can predict the heat transfer performance for four SWHE configurations was developed. The SWHE model includes a separate ice-on-coil model to predict the heat transfer and the buoyant force experienced on the heat exchangers during the conditions of the formation, growth and melting of ice around the SWHE's.
2. The ice-on-coil model is implemented using a segment-by-segment algorithm for coil type SWHE configurations (spiral-helical, flat spiral and slinky coil), to predict the variation in ice thickness in the direction of the refrigerant flow. In the case of vertical flat plate heat exchangers, the ice-on-coil model considers it as a single entity.
3. The algorithm to calculate the ice-overlapping angle between adjacent coil segments is estimated for only the spiral-helical coil heat exchanger configuration. The reduction in the outside heat transfer coefficient during the ice-overlapping condition is estimated by introducing a penalty coefficient in the Hansen (2011) correlation. The penalty coefficient is obtained by sensitivity analysis to match the experimental data.

4. The model validation of exit fluid temperatures (ExFt) for a spiral-helical coil during coil icing conditions closely matched with the experimental results. The model however, slightly over predicts the buoyancy force experienced by the heat exchanger. The model also predicts the onset and melting of coil ice several hours before the actual occurrence as observed from the experimental data.
5. The validation of the heat exchanger ExFT when the SWHE model is coupled with the lake model also showed reasonable agreement with the experimental results. The slight difference with the model predicted temperatures would have little effect on the heat pump performance calculations.

7.1.3 Design tool for SWHP systems

1. A design tool to aid in the sizing of SWHE used in a closed loop SWHP system has been developed. The design tool is comprised of a Microsoft Excel spreadsheet and two executable files (LakeModel.exe) that contains the lake simulation and (SWHEmodel.exe) that contains the heat exchanger simulation model; originally written in Fortran 90.
2. The design tool estimates the optimum number of SWHE coils/plates required to satisfy the user input design conditions. The design tool can also estimate the impact on the lake temperatures due to the heat input and heat extraction from the sized SWHE coils/plates.

7.2 Conclusions and recommendations for future research

While the study covered the development and validation of a lake model, which treats, both the lake as well as the surface water heat exchanger, the limitations of the models suggested that there are still some issues that need to be addressed for future research.

1. The significant variation in water temperatures with respect to wind speed is observed from the experimental results from Lake Sammamish in Seattle Washington. This suggests the development of the lake model to sub-daily or hourly time steps to accurately track the temperature variations.

2. The lake model was developed with an intention for the use of HVAC design engineers. Hence, one of the major assumptions of the model is considering the lake water level as being constant. The model also neglects the changes in lake level due to evaporation, precipitation and varying inflows and outflows. The model can be enhanced to use the weather data to at least track the lake level due to evaporation and precipitation.
3. More experimental lake temperature data is required to enhance the current list of the recommended surface convection, surface evaporation and eddy diffusion model for each lake category.
4. An improved algorithm to calculate the ice-overlapping angle between adjacent segments is required for other SWHE configurations except for the flat plate heat exchanger, which does not have the overlapping phenomenon. Experimental analysis and validation of the model for the coil icing conditions for spiral coil and vertical/horizontal slinky coil configurations needs to be performed.
5. The ice formation around the SWHE increases the resistance to the exterior convection. The SWHE model currently estimates this reduction in the exterior convective heat transfer coefficient in the case of spiral-helical coil heat exchanger by introducing a penalty coefficient to the Hansen (2011) correlation. The penalty coefficient is obtained from a sensitivity analysis to match the experimental data. Hansen (2011) correlations needs to be enhanced to also include this phenomenon.
6. The extraction and rejection of heat by the SWHE directly affects the layers, at which the heat is being extracted or rejected. The lake model currently determines the direction of the buoyant plume and distributes the energy from the SWHE uniformly (proportionally to the volume) to each water layer between the heat exchanger and the surface (for upward plumes) or in the layers between the heat exchanger and the bottom (for downward plumes). The development, validation and testing of an actual

buoyant plume model is necessary for an accurate energy analysis of a SWHP system.

7. The EnergyPlus weather (.epw) file contains a typical meteorological weather data for a location, which is obtained based on statistical analysis from a thirty year weather data obtained from the location. The actual weather files are not readily available to the user. Using the design tool to size the SWHE coils based on an EnergyPlus weather file, may not be accurate for extreme weather conditions. Development of actual weather data files for multiple locations throughout the world is highly sought after, to enable the SWHP design for extreme conditions.

REFERENCES

Adams, E. E., D. J. Cosler and K. R. Helfrich.(1990). Evaporation from heated water bodies: Predicting combined forced plus free convection. Water Resources Research 26(3): 425-435.

Ali, M. E.(2006). Natural Convection Heat Transfer from Vertical Helical Coils in Oil. Heat Transfer Engineering 27(3): 79-85.

Argonne National, L. and J. G. Asbury. (1970). Effects of thermal discharges on the mass/energy balance of Lake Michigan. Argonne, Ill.; The Laboratory.

ASHRAE. (2009). 2009 ASHRAE Fundamentals Handbook, I-P Edition, American Society of Heating, Refrigerating and Air-Conditioning Engineers, Inc., Atlanta, GA.

Banks, R. B.(1975). Some features of wind action on shallow lakes. Journal of Environmental Engineering Division 101(5): 813-827.

Blumberg, A. F. and G. L. Mellor.(1987). A Description of a Three-Dimensional Coastal Ocean Circulation Model. Coastal and Estuarine Sciences 4: 1-16.

Branco, B. and T. Torgersen.(2009). Predicting the onset of thermal stratification in shallow inland waterbodies. Aquatic Sciences - Research Across Boundaries 71(1): 65-79.

Chiasson, A. D., J. D. Spitler, S. J. Rees and M. D. Smith.(2000). A Model for Simulating the Performance of a Shallow Pond as a Supplemental Heat Rejector with Closed-Loop Ground-Source Heat Pump Systems. ASHRAE Transcations 106(2): 107-121.

Crocker, G. B. and P. Wadhams.(1989). Modelling Antarctic Fast-Ice Growth. Journal of Glaciology 35(119): 3-8.

Czarnecki, J. T.(1963). A method of heating swimming pools by solar energy. Solar Energy 7(1): 3-7.

Czarnecki, J. T. (1978). Swimming pool heating by solar energy. Highett, Victoria; CSIRO Division of Mechanical Engineering.

Dake, J. M. K. and D. R. F. Harleman.(1969). Thermal stratification in lakes: Analytical and laboratory studies. Water Resources Research 5(2): 484-495.

Ellis, C. R., H. G. Stefan and R. Gu.(1991). Water Temperature Dynamics and Heat Transfer Beneath the Ice Cover of a Lake. Limnology and Oceanography 36(2): 324-335.

Fang , X. and H. G. Stefan.(1996). Long-term lake water temperature and ice cover simulations/measurements. Cold Regions Science and Technology 24: 289-304.

Ford, D. E. and H. G. Stefan.(1980). Thermal predictions using integral energy model. Journal of the Hydraulics Division 106(1): 39-55.

Friehe, C. A. and K. F. Schmitt.(1976). Parameterization of Air-Sea Interface Fluxes of Sensible Heat and Moisture by the Bulk Aerodynamic Formulas. Journal of Physical Oceanography 6(6): 801-809.

Gu, R. and H. G. Stefan.(1990). Year-round temperature simulation of cold climate lakes. Cold Regions Science and Technology 18(2): 147-160.

Gu, R. and H. G. Stefan.(1995). Stratification dynamics in wastewater stabilization ponds. Water Research 29(8): 1909-1923.

Håkanson, L. (1981). A manual of lake morphometry. New York; Springer-Verlag.

Hamilton, D. P. and S. Schladow, G (1997). Prediction of water quality in lakes and reservoirs. Part I - Model description. Ecological Modelling 96: 91-110.

Hamrick, J. M. (1992). A three-dimensional environmental fluid dynamics computer code: Theoretical and computational aspects; Virginia Institute of Marine Science, College of William and Mary.

Hansen, G. M.2011.Experimental testing and analysis of spiral-helical surface water heat exchanger configurations. Masters thesis. Oklahoma State University, Stillwater.

Hayter, E. J., M. A. Bergs, R. Gu, S. C. McCutcheon, S. J. Smith and H. J. Whiteley. (1998). HSCTM-2D, a finite element model for depth-averaged hydrodynamics, sediment and contaminant transport. U. S. E. E. R. Laboratory. Athens, GA.

Henderson-Sellers, B.(1985). New formulation of eddy diffusion thermocline models. Applied Mathematical Modelling 9(6): 441-446.

Hondzo, M. and H. G. Stefan.(1993a). Lake Water Temperature Simulation Model. Journal of Hydraulic Engineering 119(11): 1251-1274.

Hondzo, M. and H. G. Stefan.(1993b). Regional water temperature characteristics of lakes subjected to climate change. Climatic Change 24(3): 187-211.

Hunkins, K. and M. Fliegel.(1973). Internal Undular Surges in Seneca Lake: A Natural Occurence of Solitons. Journal of Geophysical Research 78(3): 539-548.

Imberger, J.(1985). Thermal characteristics of standing waters: an illustration of dynamic processes. Hydrobiologia 125(1): 7-29.

Imberger, J., J. Patterson, B. Hebbert and I. Loh.(1978). Dynamics of Reservoir of Medium Size. Journal of Hydraulics Division 104(5): 725-743.

Incropera, F. P. and D. P. DeWitt. (1996). Introduction to heat transfer. New York; John Wiley and Sons.

Jassby, A. and T. Powell.(1975). Vertical patterns of eddy diffusion during stratification in Castle Lake, California. Limnology and Oceanography 20(4): 530-543.

Jekel, T. B., J. W. Mitchell and S. A. Klein.(1993). Modeling of Ice-Storage Tanks. ASHRAE Transcations 99(1): 1016-1024.

Ji, Z. G., M. R. Morton and J. M. Hamrick.(2001). Wetting and Drying Simulation of Estuarine Processes. Estuarine, Coastal and Shelf Science 53(5): 683-700.

Johansson, H., A. A. Brolin and L. Håkanson.(2007). New approaches to the modelling of lake basin morphometry. Environmental Modeling and Assessment 12(3): 213-228.

Johansson, I. (1983). Comparison between Soil, Rock, Ground Water and Lakes as Heat Source for Heat Pumps. 16th International Congress of Refrigeration, Paris.

Kullenberg, G.(1971). Vertical Diffusion in Shallow Waters. Tellus 23(2): 129-135.

Lepparanta, M.(1993). A review of analytical models of sea-ice growth. Atmosphere-Ocean 31: 123-138.

Losordo, T. M. and R. H. Piedrahita.(1991). Modelling temperature variation and thermal stratification in shallow aquaculture ponds. Ecological Modelling 54(3–4): 189-226.

McCormick, M. J. and D. Scavia.(1981). Calculation of vertical profiles of lake-averaged temperature and diffusivity in Lakes Ontario and Washington. Water Resources Research 17(2): 305-310.

Michaud, J. P. (1994). A citizen's guide to understanding and monitoring lakes and streams. Retrieved April 1, 2013, from http://www.ecy.wa.gov/programs/wq/plants/management/joysmanual/.

Mitchell, M. S. and J. D. Spitler.(2013). Open-loop direct surface water cooling and surface water heat pump systems—A review. HVAC&R Research 19(2): 125-140.

Molineaux, B., B. Lachal and O. Guisan.(1994). Thermal analysis of five outdoor swimming pools heated by unglazed solar collectors. Solar Energy 53(1): 21-26.

Neto, J. H. M. and M. Krarti.(1997). Deterministic model for an internal melt ice-on-coil thermal storage tank. ASHRAE Transactions 103(1): 113-124.

Omstedt, A.(1990). A coupled one-dimensional sea ice–ocean model applied to a semi-enclosed basin. Tellus A 42(5): 568-582.

Overland, J. E.(1985). Atmospheric boundary layer structure and drag coefficients over sea ice. Journal of Geophysical Research 90(C5): 515-528.

Perovich, D. K. (1996). The optical properties of sea ice / Donald K. Perovich ; prepared for Office of Naval Research. [Hanover, N.H.] :; US Army Corps of Engineers, Cold Regions Research & Engineering Laboratory ; [Springfield, Va. : Available from National Technical Information Service.

Pezent, M. C. and S. P. Kavanaugh.(1990). Development and verification of a thermal model of lakes used with water source heat pumps. ASHRAE Transactions 96(1): 574-582.

Prabhanjan, D. G., T. J. Rennie and G. S. Vijaya Raghavan.(2004). Natural convection heat transfer from helical coiled tubes. International Journal of Thermal Sciences 43(4): 359-365.

Raphael, J. M.(1962). Prediction of temperature in rivers and reservoirs. Journal of the Power Division, Procedings of the American Society of Civil Engineers 88(P02): 157-181.

Rasmussen, A. H., M. Hondzo and H. G. Stefan.(1995). A test of several evaporation equations for water temperature simulations in lakes. Journal of the American Water Resources Association 31(6): 1023-1028.

Riley, M. J. and H. G. Stefan.(1988). Minlake: A dynamic lake water quality simulation model. Ecological Modelling 43(3–4): 155-182.

Rogers, G. F. C. and Y. R. Mayhew.(1964). Heat transfer and pressure loss in helically coiled tubes with turbulent flow. International Journal of Heat and Mass Transfer 7(11): 1207-1216.

Rohden, C. v., K. Wunderle and J. Ilmberger.(2007). Parameterisation of the vertical transport in a small thermally stratified lake. Aquatic Sciences - Research Across Boundaries 69(1): 129-137.

Salimpour, M. R.(2009). Heat Transfer Coefficients of Shell and Coiled Tube Heat Exchangers. Experimental Thermal and Fluid Science 33(2): 203-207.

Saloranta, T. M.(2000). Modeling the evolution of snow, snow ice and ice in the Baltic Sea. Tellus A 52(1): 93-108.

Saloranta, T. M. and T. Andersen. (2004). Mylake (v.1.1): Technical model documentation and user's guide. NIVA-report 4838. Olso,Norway, Norwegian Institute for Water Research. 44.

Saloranta, T. M. and T. Andersen.(2007). MyLake—A multi-year lake simulation model code suitable for uncertainty and sensitivity analysis simulations. Ecological Modelling 207(1): 45-60.

Sengupta, S., E. Nwadike and S. S. Lee.(1981). Long term simulation of stratification in cooling lakes. Applied Mathematical Modelling 5(5): 313-320.

Sheridan, N. R. (1972). The Heating of Swimming Pools, Solar Research notes No. 4, University of Queensland.

Signorelli, S. and T. Kohl.(2004). Regional ground surface temperature mapping from meteorological data. Global and Planetary Change 40(3–4): 267-284.

Silver, S. C., A. F. Milbitz, J. W. Jones, J. L. Peterson and B. D. Hunn.(1989). Component models for computer simulation of ice storage systems. ASHRAE Transactions 95(1): 1214-1226.

Srinivasan, J. and A. Guha.(1987). The effect of bottom reflectivity performance of a solar pond. Solar Energy 39(4): 361-367.

Stefan, H. G., J. J. Cardoni and A. W. Fu. (1982). Resqual 2: A dynamic water quality simulation program for a stratified shallow lake or reservoir: application to Lake Chicot, Arkansas. Minneapolis, St Anthony Falls Laboratory: 154.

Svensson, T. and L.-O. Sörman (1983). Pipe heat exchangers on lake bottoms: Results of laboratory and field tests. International Conference on Subsurface Heat Storage in Theory and Practice, Stockholm, Swedish Council for Building Research.

Swinbank, W. C.(1963). Long-wave radiation from clear skies. Quarterly Journal of the Royal Meteorological Society 89(381): 339-348.

Tucker, W. A. and A. W. Green.(1977). A Time-Dependent Model of the Lake-Averaged, Vertical Temperature Distribution of Lakes. Limnology and Oceanography 22(4): 687-699.

USGS. (2013). United States Geological Survey-Water Resources of the United States. http://ar.water.usgs.gov/data-bin/maumelle/ts.pl.

Wing, M. R., A. Preston, N. Acquisto and W. F. Ahrnsbrak.(1995). Intrusion of saline groundwater into Seneca and Cayuga Lakes, New York. Limnology and oceanography: 791-801.

WOW. (2012). Water on the Web-Monitoring Minnesota lakes on the internet and training water science technicians for the future - A national on-line curriculum using advanced technologies and real-time data, University of Minnesota-Duluth, Duluth. Retrieved June 20, 2012, from http://WaterOntheWeb.org.

Yeates, P. S. and J. Imberger.(2003). Pseudo two- dimensional simulations of internal and boundary fluxes in stratified lakes and reservoirs. International Journal of River Basin Management 1(4): 297-319.

Yen, Y. C. (1981). Review of thermal properties of snow, ice and sea-ice. Hanover,NH,USA, US Army Cold Regions Research and Engineering Laboratory. CRREL Report 81-10: 34.

APPENDIX A

RMSE AND MBE TABLES FOR 14 LAKES

RMSE and MBE are in °C. The number of days mentioned in every table represents, the number of days of spot experimental measurements used in the model sensitivity analysis. The corresponding surface convection/surface evaporation and eddy diffusion model for every model option number is discussed in section 4.3 of this thesis.

Table A- 1: RMSE observed in epilimnion region for Lake Bradley OR (No. of days = 3)

Eddy diffusion model option no	Surface convection/evaporation model option no						
	1	2	3	4	5	6	7
1	0.8	1.7	3.1	2.4	3.3	1.7	1.0
2	0.7	1.5	3.1	2.5	3.2	1.6	0.8
3	0.8	1.6	3.1	2.5	3.2	1.6	0.9
4	0.8	1.9	3.2	2.4	3.5	1.9	1.1
5	0.8	1.6	3.1	2.5	3.1	1.6	0.9
6	0.8	1.8	3.1	2.4	3.5	1.9	1.0
7	0.6	1.7	3.1	2.4	3.4	1.8	0.9
8	0.7	1.5	3.1	2.5	3.2	1.6	0.8
9	0.7	1.5	3.1	2.5	3.2	1.6	0.8
10	0.8	1.8	3.1	2.4	3.5	1.9	1.1
11	0.7	1.5	3.1	2.5	3.2	1.6	0.8

Table A- 2: RMSE observed in metalimnion region for Lake Bradley OR (No. of days = 3)

Eddy diffusion model option no	Surface convection/evaporation model option no						
	1	2	3	4	5	6	7
1	1.4	1.7	2.1	1.4	2.5	1.8	1.4
2	2.9	4.1	5.2	1.2	5.8	4.2	3.2
3	2.3	3.1	3.8	1.1	4.2	3.2	2.5
4	1.8	3.1	2.4	0.9	3.9	2.7	2.6
5	2.4	3.4	4.2	1.1	4.5	3.4	2.7
6	2.4	3.7	2.7	0.8	4.5	3.4	3.1
7	3.2	4.6	5.2	1.2	6.4	4.6	3.7
8	2.9	4.1	5.2	1.2	5.8	4.2	3.2
9	2.9	4.1	5.2	1.2	5.8	4.2	3.2
10	2.5	3.9	3.0	0.8	4.9	3.5	3.2
11	2.9	4.1	5.2	1.2	5.8	4.2	3.2

Table A- 3: RMSE observed in hypolimnion region for Lake Bradley OR (No. of days = 3)

Eddy diffusion model option no	Surface convection/evaporation model option no						
	1	2	3	4	5	6	7
1	1.4	1.2	1.1	2.1	0.9	1.1	1.4
2	6.5	7.7	8.7	4.8	9.1	7.7	6.9
3	3.4	3.6	4.0	2.9	3.9	3.7	3.4
4	0.8	0.6	0.7	1.6	0.7	0.6	0.8
5	5.0	5.4	5.9	3.8	5.7	5.4	5.1
6	0.8	0.7	0.7	1.1	0.8	0.7	0.8
7	6.8	8.3	8.7	4.8	9.7	8.2	7.5
8	6.5	7.7	8.7	4.8	9.1	7.7	6.9
9	6.5	7.7	8.7	4.8	9.1	7.7	6.9
10	1.1	1.4	2.0	1.0	1.7	1.4	1.4
11	6.5	7.7	8.7	4.8	9.1	7.7	6.9

Table A- 4: MBE observed in epilimnion region for Lake Bradley OR (No. of days = 3)

Eddy diffusion model option no	Surface convection/evaporation model option no						
	1	2	3	4	5	6	7
1	0.7	1.4	2.9	2.3	3.1	1.4	1.0
2	0.5	1.4	3.0	2.4	3.1	1.4	0.8
3	0.7	1.3	2.9	2.4	3.0	1.3	0.9
4	0.8	1.6	2.9	2.3	3.3	1.6	1.0
5	0.6	1.3	2.9	2.4	3.0	1.3	0.9
6	0.8	1.5	2.9	2.3	3.3	1.6	1.0
7	0.6	1.6	3.0	2.3	3.3	1.6	0.8
8	0.5	1.4	3.0	2.4	3.1	1.4	0.8
9	0.5	1.4	3.0	2.4	3.1	1.4	0.8
10	0.8	1.5	2.9	2.3	3.3	1.6	1.0
11	0.5	1.4	3.0	2.4	3.1	1.4	0.8

Table A- 5: MBE observed in metalimnion region for Lake Bradley OR (No. of days = 3)

Eddy diffusion model option no	Surface convection/evaporation model option no						
	1	2	3	4	5	6	7
1	1.2	1.3	1.5	1.2	1.7	1.3	1.2
2	2.5	3.6	4.8	1.2	5.2	3.7	2.8
3	2.0	2.5	3.3	1.0	3.6	2.6	2.1
4	1.4	2.8	1.8	0.8	3.4	2.4	2.4
5	2.1	2.8	3.7	1.1	3.9	2.9	2.2
6	2.1	3.5	2.2	0.7	4.1	3.1	2.9
7	2.9	4.3	4.8	1.1	6.0	4.3	3.4
8	2.5	3.6	4.8	1.2	5.2	3.7	2.8
9	2.5	3.6	4.8	1.2	5.2	3.7	2.8
10	2.2	3.6	2.6	0.7	4.5	3.2	2.9
11	2.5	3.6	4.8	1.2	5.2	3.7	2.8

Table A- 6: MBE observed in hypolimnion region for Lake Bradley OR (No. of days = 3)

Eddy diffusion model option no	Surface convection/evaporation model option no						
	1	2	3	4	5	6	7
1	1.3	1.0	0.9	2.0	0.8	0.9	1.3
2	5.5	6.5	7.6	4.0	7.8	6.6	5.8
3	2.9	3.0	3.4	2.6	3.2	3.0	2.9
4	0.8	0.6	0.6	1.4	0.4	0.6	0.7
5	4.2	4.4	4.9	3.5	4.7	4.4	4.2
6	0.7	0.6	0.5	0.9	0.5	0.6	0.7
7	5.9	7.3	7.6	3.9	8.6	7.2	6.6
8	5.5	6.5	7.6	4.0	7.8	6.6	5.8
9	5.5	6.5	7.6	4.0	7.8	6.6	5.8
10	1.1	1.2	1.7	0.9	1.4	1.2	1.2
11	5.5	6.5	7.6	4.0	7.8	6.6	5.8

Table A- 7: RMSE observed for Lake Wingra WI (No. of days = 5)

Eddy diffusion model option no	Surface convection/evaporation model option no						
	1	2	3	4	5	6	7
1	1.0	1.9	3.5	2.4	4.3	2.2	1.4
2	1.2	2.5	4.2	2.0	4.8	2.8	1.8
3	1.2	2.4	4.1	2.1	4.7	2.7	1.8
4	1.1	2.1	3.8	2.2	4.5	2.4	1.6
5	1.2	2.3	4.0	2.2	4.7	2.6	1.7
6	1.2	2.3	3.9	2.2	4.7	2.6	1.7
7	1.2	2.5	4.2	2.0	4.8	2.8	1.8
8	1.1	2.3	4.2	2.1	4.6	2.6	1.7
9	1.2	2.5	4.3	2.0	4.8	2.8	1.8
10	1.2	2.3	3.8	2.2	4.7	2.6	1.7
11	1.2	2.4	4.2	2.1	4.8	2.7	1.8

Table A- 8: MBE observed for Lake Wingra WI (No. of days = 5)

Eddy diffusion model option no	Surface convection/evaporation model option no						
	1	2	3	4	5	6	7
1	0.7	1.8	3.0	2.4	4.0	2.1	1.2
2	1.2	2.5	3.7	2.0	4.8	2.8	1.8
3	1.2	2.4	3.6	2.1	4.7	2.7	1.8
4	1.0	1.9	3.4	2.1	4.2	2.2	1.4
5	1.1	2.1	3.5	2.0	4.3	2.3	1.5
6	1.1	2.1	3.4	2.0	4.3	2.3	1.5
7	1.1	2.2	3.7	1.9	4.4	3.1	1.6
8	1.0	2.0	3.7	2.0	4.2	2.3	1.5
9	1.2	2.5	3.8	2.0	4.8	2.8	1.8
10	1.2	2.3	3.4	2.2	4.7	2.6	1.7
11	1.1	2.2	3.7	1.9	4.3	2.4	1.6

Table A- 9: RMSE observed for Lake Dunlap TX (No. of days = 4)

Eddy diffusion model option no	Surface convection/evaporation model option no						
	1	2	3	4	5	6	7
1	2.7	2.5	3.1	3.5	3.3	2.6	2.6
2	2.3	3.0	4.9	1.2	5.5	3.5	2.7
3	5.2	2.6	4.4	1.8	4.9	3.1	2.4
4	2.5	2.6	4.0	2.7	4.4	3.0	2.5
5	2.2	2.2	1.7	2.1	4.7	2.9	2.3
6	2.2	2.6	1.7	2.1	4.7	2.9	2.3
7	2.3	2.8	4.7	1.2	5.6	3.5	2.8
8	2.1	2.7	4.6	1.2	5.1	3.1	2.4
9	2.1	2.8	4.7	1.2	5.3	3.2	2.5
10	2.2	2.5	1.7	2.1	4.7	2.9	2.3
11	2.2	2.6	4.2	2.1	5.4	3.4	2.7

Table A- 10: MBE observed for Lake Dunlap TX (No. of days = 4)

Eddy diffusion model option no	Surface convection/evaporation model option no						
	1	2	3	4	5	6	7
1	2.2	2.1	2.2	2.9	2.5	2.1	2.2
2	2.1	2.8	4.6	1.1	5.2	3.2	2.5
3	4.7	2.4	3.8	1.4	4.4	2.7	2.3
4	2.3	2.5	3.5	1.7	3.8	2.8	2.3
5	2.1	1.7	1.2	1.5	4.0	2.7	2.2
6	2.1	2.0	0.9	1.5	4.0	2.7	2.2
7	2.1	2.4	4.2	1.2	5.3	3.2	2.5
8	1.9	2.3	4.1	1.1	4.7	2.8	2.1
9	1.9	2.5	4.3	1.1	4.9	2.9	2.2
10	2.1	1.9	1.3	1.5	4.0	2.7	2.2
11	1.9	2.5	3.6	1.4	5.1	3.1	2.4

Table A- 11: RMSE observed for Lake EA Patterson ND (No. of days = 4)

Eddy diffusion model option no	Surface convection/evaporation model option no						
	1	2	3	4	5	6	7
1	0.7	1.0	3.1	2.5	4.8	1.4	0.9
2	0.8	1.4	3.2	2.3	5.3	1.7	1.2
3	0.8	1.3	3.2	2.4	5.2	1.7	1.2
4	0.8	1.1	3.2	2.5	4.9	1.4	1.0
5	0.8	1.3	3.2	2.4	5.2	1.7	1.1
6	0.8	1.3	3.2	2.4	5.2	1.7	1.1
7	0.8	1.4	3.2	2.4	5.3	1.7	1.2
8	0.8	1.2	3.2	2.5	5.0	1.5	1.0
9	0.8	1.4	3.2	2.3	5.3	1.7	1.2
10	0.8	1.3	3.2	2.4	5.2	1.7	1.1
11	0.8	1.3	3.2	2.4	5.2	1.7	1.2

Table A- 12: MBE observed for Lake EA Patterson ND (No. of days = 4)

Eddy diffusion model option no	Surface convection/evaporation model option no						
	1	2	3	4	5	6	7
1	0.6	0.7	2.9	2.4	4.6	1.2	0.6
2	0.7	1.0	3.0	2.2	5.1	1.5	0.9
3	0.7	1.0	2.9	2.2	5.0	1.5	0.9
4	0.7	0.9	2.9	2.4	4.7	1.2	0.7
5	0.7	1.0	2.9	2.3	5.0	1.4	0.8
6	0.7	1.0	2.9	2.3	5.0	1.4	0.8
7	0.7	1.0	3.0	2.2	5.1	1.5	0.9
8	0.7	0.9	2.9	2.3	4.7	1.2	0.8
9	0.7	1.0	3.0	2.2	5.1	1.5	0.9
10	0.7	1.0	2.9	2.3	5.0	1.4	0.8
11	0.7	1.0	2.9	2.2	5.0	1.4	0.8

Table A- 13: RMSE observed in epilimnion region for Lake Monona WI (No. of days = 5)

Eddy diffusion model option no	Surface convection/evaporation model option no						
	1	2	3	4	5	6	7
1	1.5	2.2	3.7	2.4	3.7	2.5	2.0
2	0.7	2.6	4.3	1.3	4.2	2.8	2.0
3	0.7	2.4	4.1	1.4	4.0	2.6	1.9
4	1.2	2.2	3.8	2.2	3.7	2.5	2.2
5	1.2	2.2	3.8	1.5	4.7	3.3	2.5
6	1.2	2.2	3.8	1.4	4.7	3.3	2.5
7	0.9	2.4	4.1	1.3	5.0	3.2	2.3
8	0.8	2.5	4.2	1.5	4.2	2.7	1.9
9	0.7	2.6	4.3	1.3	4.2	2.8	2.0
10	1.2	2.2	3.8	2.1	3.7	2.5	1.9
11	1.0	2.3	4.0	1.3	5.1	3.2	2.2

Table A- 14: RMSE observed in metalimnion region for Lake Monona WI (No. of days = 5)

Eddy diffusion model option no	Surface convection/evaporation model option no						
	1	2	3	4	5	6	7
1	4.7	4.7	4.3	4.8	3.4	5.0	4.7
2	4.4	5.9	7.5	2.6	7.8	6.1	5.6
3	2.4	3.0	3.6	1.4	3.9	3.1	3.0
4	4.1	4.3	4.1	2.9	3.7	4.5	7.3
5	1.1	3.8	3.9	0.7	3.9	2.9	2.5
6	0.8	4.1	4.1	0.7	3.8	2.5	2.3
7	2.7	0.6	0.9	2.0	1.4	1.7	2.3
8	1.9	2.5	3.3	0.9	3.7	2.5	2.4
9	4.4	5.9	7.5	2.6	7.8	6.1	5.6
10	3.8	3.8	3.9	2.9	3.4	4.1	3.8
11	3.0	0.6	0.6	2.1	2.9	3.5	3.3

Table A- 15: RMSE observed in hypolimnion region for Lake Monona WI (No. of days = 5)

Eddy diffusion model option no	Surface convection/evaporation model option no						
	1	2	3	4	5	6	7
1	2.7	2.5	2.1	3.5	1.6	2.7	2.4
2	5.7	6.6	8.0	4.3	8.2	6.8	6.5
3	2.4	2.5	2.7	2.5	3.1	2.5	2.5
4	3.1	2.8	2.1	3.5	1.8	2.7	6.1
5	3.2	2.8	2.0	1.5	2.6	3.0	3.0
6	3.2	2.8	2.1	1.2	2.7	3.1	3.4
7	1.6	1.0	0.8	1.7	1.3	1.6	1.6
8	0.9	1.0	1.4	1.0	1.7	1.0	1.0
9	5.7	6.6	8.0	4.3	8.2	6.8	6.5
10	3.0	2.8	2.1	3.4	1.8	2.7	2.8
11	1.4	2.0	1.5	1.7	1.6	1.7	1.9

Table A- 16: MBE observed in epilimnion region for Lake Monona WI (No. of days = 5)

Eddy diffusion model option no	Surface convection/evaporation model option no						
	1	2	3	4	5	6	7
1	1.4	1.9	2.8	1.9	3.0	2.2	1.8
2	0.6	2.3	4.1	1.3	4.0	2.6	1.8
3	0.7	2.2	4.0	1.2	3.9	2.5	1.8
4	1.2	1.8	3.1	1.8	3.2	1.9	2.1
5	1.0	1.9	3.1	1.3	4.4	3.1	2.4
6	1.0	1.9	3.1	1.3	4.5	3.2	2.4
7	0.8	2.2	3.9	1.1	4.9	3.1	2.2
8	0.7	2.3	4.1	1.2	4.1	2.6	1.8
9	0.6	2.3	4.1	1.3	4.1	2.6	1.8
10	1.2	1.9	3.1	1.7	3.2	2.0	1.5
11	0.9	2.1	3.9	1.1	5.0	3.0	2.2

Table A- 17: MBE observed in metalimnion region for Lake Monona WI (No. of days = 5)

Eddy diffusion model option no	Surface convection/evaporation model option no						
	1	2	3	4	5	6	7
1	4.2	4.2	3.8	4.5	2.9	4.6	4.1
2	4.0	5.4	7.0	2.2	7.4	5.6	5.1
3	2.0	2.6	3.2	1.1	3.6	2.7	2.6
4	3.5	3.7	3.4	2.6	3.1	3.7	6.9
5	0.9	3.3	3.3	0.5	3.1	2.3	2.0
6	0.8	3.5	3.4	0.5	2.9	2.0	1.8
7	2.4	0.6	0.8	1.6	1.3	1.6	2.1
8	1.6	2.1	2.9	0.7	3.4	2.2	2.0
9	4.0	5.4	7.0	2.2	7.4	5.6	5.1
10	3.3	3.2	3.3	2.5	2.9	3.5	3.2
11	2.6	0.5	0.6	1.7	2.5	2.9	2.7

Table A- 18: MBE observed in hypolimnion region for Lake Monona WI (No. of days = 5)

Eddy diffusion model option no	Surface convection/evaporation model option no						
	1	2	3	4	5	6	7
1	2.1	2.0	1.8	2.9	1.3	2.1	2.0
2	4.4	5.2	6.3	3.2	6.6	5.3	5.0
3	1.7	1.9	2.2	2.0	2.5	1.9	1.9
4	2.4	2.2	1.8	2.9	1.6	2.1	5.3
5	2.5	2.2	1.7	1.0	2.1	2.3	2.4
6	2.5	2.2	1.8	1.0	2.2	2.4	2.7
7	1.3	0.9	0.7	1.4	1.2	1.4	1.4
8	0.6	0.7	1.0	0.8	1.3	0.7	0.7
9	4.4	5.2	6.3	3.2	6.6	5.3	5.0
10	2.4	2.2	1.8	2.8	1.6	2.1	2.2
11	0.9	1.6	1.4	1.4	1.4	1.2	1.4

Table A- 19: RMSE observed in epilimnion region for Lake Sunapee NH (No. of days = 4)

Eddy diffusion model option no	Surface convection/evaporation model option no						
	1	2	3	4	5	6	7
1	3.1	6.1	7.7	1.2	5.6	6.6	4.2
2	4.1	8.2	10.9	2.2	7.5	8.6	5.9
3	3.6	7.5	9.9	1.8	6.8	7.9	5.3
4	3.5	7.2	9.2	1.4	6.7	7.7	5.2
5	3.5	7.2	9.3	1.4	6.7	7.7	5.1
6	3.5	7.2	9.2	3.4	6.8	7.7	5.2
7	4.5	8.7	10.7	2.4	7.8	9.2	6.3
8	3.8	7.7	10.0	1.9	7.0	8.1	5.5
9	4.1	8.2	11.0	2.2	7.5	8.6	5.9
10	3.7	7.2	9.1	1.6	6.7	7.7	5.2
11	3.9	8.0	9.9	2.0	7.0	8.4	5.6

Table A- 20: RMSE observed in metalimnion region for Lake Sunapee NH (No. of days = 4)

Eddy diffusion model option no	Surface convection/evaporation model option no						
	1	2	3	4	5	6	7
1	5.5	5.9	5.6	4.5	4.9	5.7	5.9
2	9.6	13.2	15.7	7.6	12.8	13.6	11.2
3	5.7	7.5	8.6	4.3	7.8	7.6	6.7
4	0.7	2.7	3.4	0.9	4.5	2.6	2.4
5	0.7	2.8	3.6	0.9	4.7	2.6	2.5
6	0.7	2.6	3.2	1.4	3.5	2.3	2.2
7	3.4	3.7	3.7	2.9	3.8	3.8	3.5
8	4.1	5.6	7.0	2.8	6.3	5.9	5.1
9	9.6	13.2	15.7	7.6	12.8	13.6	11.2
10	0.8	2.2	2.6	0.9	2.9	2.0	1.9
11	3.9	5.8	6.9	2.9	5.8	5.8	4.8

Table A- 21: RMSE observed in hypolimnion region for Lake Sunapee NH (No. of days = 4)

Eddy diffusion model option no	Surface convection/evaporation model option no						
	1	2	3	4	5	6	7
1	3.6	3.6	5.2	4.4	5.2	4.1	3.7
2	12.7	15.9	18.3	10.8	15.8	16.3	14.3
3	6.7	7.7	8.4	5.7	8.2	7.7	7.3
4	3.4	3.3	3.9	1.3	4.2	3.3	3.4
5	3.5	3.4	3.9	1.3	4.2	3.4	3.5
6	3.1	3.3	3.7	1.4	3.6	3.4	3.4
7	2.0	1.7	1.5	2.7	1.4	1.7	1.6
8	3.9	4.7	5.6	3.1	5.3	4.8	4.5
9	12.7	15.9	18.3	10.9	15.8	16.3	14.3
10	2.4	3.2	3.5	1.0	3.6	3.2	3.3
11	3.3	4.1	4.7	3.1	4.1	4.0	3.7

Table A- 22: MBE observed in epilimnion region for Lake Sunapee NH (No. of days = 4)

Eddy diffusion model option no	Surface convection/evaporation model option no						
	1	2	3	4	5	6	7
1	2.4	4.7	5.8	0.9	4.3	5.0	3.2
2	3.2	6.4	8.6	1.6	5.9	6.8	4.6
3	2.8	5.9	7.8	1.3	5.4	6.2	4.2
4	2.7	5.6	7.2	1.0	5.3	6.0	4.0
5	2.7	5.6	7.3	1.0	5.3	6.0	4.0
6	2.7	5.6	7.2	2.6	5.4	6.0	4.0
7	3.6	6.9	8.5	1.8	6.2	7.3	5.0
8	3.0	6.0	7.9	1.4	5.6	6.4	4.3
9	3.2	6.4	8.7	1.6	5.9	6.8	4.6
10	2.8	5.6	7.1	1.1	5.3	6.0	4.1
11	3.1	6.3	7.8	1.5	5.6	6.6	4.4

Table A- 23: MBE observed in metalimnion region for Lake Sunapee NH (No. of days = 4)

Eddy diffusion model option no	Surface convection/evaporation model option no						
	1	2	3	4	5	6	7
1	4.4	4.7	4.5	3.6	3.9	4.5	4.7
2	7.6	10.5	12.5	6.1	10.2	10.8	9.0
3	4.5	6.0	6.8	3.4	6.2	6.1	5.3
4	0.5	2.1	2.6	0.7	3.5	2.0	1.8
5	0.5	2.1	2.7	0.7	3.6	2.0	1.9
6	0.5	2.0	2.4	1.1	2.7	1.8	1.7
7	2.7	2.9	3.0	2.3	3.0	3.0	2.8
8	3.2	4.5	5.6	2.2	5.0	4.7	4.0
9	7.6	10.5	12.5	6.1	10.2	10.8	9.0
10	0.6	1.7	2.0	0.7	2.3	1.5	1.4
11	3.1	4.6	5.4	2.3	4.6	4.6	3.8

Table A- 24: RMSE observed in hypolimnion region for Lake Sunapee NH (No. of days = 4)

Eddy diffusion model option no	Surface convection/evaporation model option no						
	1	2	3	4	5	6	7
1	2.8	2.8	4.1	3.5	4.1	3.2	2.8
2	10.1	12.7	14.6	8.6	12.6	13.0	11.4
3	5.2	6.1	6.6	4.4	6.4	6.1	5.8
4	2.7	2.6	3.0	0.7	3.3	2.6	2.7
5	2.7	2.7	3.1	0.8	3.3	2.7	2.8
6	2.4	2.6	2.9	1.1	2.8	2.6	2.7
7	1.4	1.2	1.1	2.0	1.1	1.2	1.2
8	3.0	3.7	4.4	2.4	4.2	3.8	3.5
9	10.1	12.7	14.6	8.6	12.6	13.0	11.4
10	1.8	2.5	2.7	0.5	2.8	2.5	2.5
11	2.5	3.1	3.6	2.3	3.1	3.0	2.8

Table A- 25: RMSE observed in epilimnion region for Lake South Holston TN (No. of days = 3)

Eddy diffusion model option no	Surface convection/evaporation model option no						
	1	2	3	4	5	6	7
1	6.9	8.0	8.9	6.0	8.3	8.3	7.5
2	10.2	12.2	13.6	9.2	11.8	12.4	11.1
3	8.0	9.3	10.2	7.3	9.3	9.5	8.6
4	6.9	8.1	8.9	6.1	8.3	8.2	7.5
5	6.9	8.0	8.9	6.1	8.3	8.2	7.5
6	1.5	5.8	8.8	0.9	4.9	6.3	3.3
7	1.5	6.0	8.9	0.9	4.9	6.4	3.4
8	6.8	8.1	8.9	6.0	8.1	8.2	7.4
9	10.2	12.2	13.6	9.2	11.8	12.4	11.1
10	1.5	5.8	8.8	0.9	4.9	6.2	3.3
11	1.2	5.3	6.1	1.0	4.4	5.7	2.9

Table A- 26: RMSE observed in metalimnion region for Lake South Holston TN (No. of days = 3)

Eddy diffusion model option no	Surface convection/evaporation model option no						
	1	2	3	4	5	6	7
1	6.7	6.6	6.5	6.8	6.6	6.6	6.6
2	7.5	7.8	8.0	7.3	7.9	7.8	7.7
3	6.7	6.7	6.7	6.8	6.7	6.7	6.7
4	6.7	6.6	6.5	6.8	6.5	6.6	6.6
5	6.7	6.6	6.5	6.8	6.5	6.6	6.6
6	3.4	3.7	6.5	3.0	3.7	3.7	3.7
7	2.2	2.2	6.6	2.1	2.2	2.3	2.3
8	6.7	6.6	6.6	6.9	6.6	6.6	6.7
9	7.5	7.8	8.0	7.3	7.9	7.8	7.7
10	3.5	3.8	6.5	3.2	3.8	3.8	3.8
11	1.4	1.0	6.8	1.4	1.0	1.0	1.2

Table A- 27: MBE observed in epilimnion region for Lake South Holston TN (No. of days = 3)

Eddy diffusion model option no	Surface convection/evaporation model option no						
	1	2	3	4	5	6	7
1	1.5	1.4	1.6	1.3	1.8	1.6	1.5
2	-4.8	-5.8	-6.4	-4.4	-5.5	-5.8	-5.2
3	-2.1	-2.3	-2.5	-2.1	-2.1	-2.3	-2.2
4	1.4	1.4	1.6	1.2	1.7	1.4	1.5
5	1.4	1.4	1.6	1.2	1.7	1.5	1.5
6	-1.5	-5.7	1.4	0.7	-4.8	-6.2	-3.3
7	-1.5	-5.9	0.3	0.6	-4.9	-6.4	-3.4
8	-0.1	-0.3	-0.3	-0.1	-0.1	-0.2	-0.1
9	-4.8	-5.8	-6.4	-4.4	-5.5	-5.8	-5.2
10	-1.5	-5.7	1.3	0.7	-4.8	-6.1	-3.3
11	-1.2	-5.2	1.2	0.8	-4.4	-5.6	-2.9

Table A- 28: MBE observed in metalimnion region for Lake South Holston TN (No. of days = 3)

Eddy diffusion model option no	Surface convection/evaporation model option no						
	1	2	3	4	5	6	7
1	5.4	5.5	5.6	5.3	5.6	5.5	5.5
2	7.5	7.7	8.0	7.3	7.9	7.8	7.7
3	6.4	6.4	6.5	6.3	6.5	6.4	6.4
4	5.4	5.5	5.6	5.3	5.6	5.5	5.4
5	5.4	5.5	5.6	5.3	5.6	5.5	5.4
6	3.1	3.4	5.6	2.7	3.4	3.4	3.4
7	1.8	1.8	5.8	1.7	1.7	1.9	1.8
8	5.5	5.6	5.6	5.4	5.6	5.6	5.6
9	7.5	7.7	8.0	7.3	7.9	7.8	7.7
10	3.3	3.5	5.6	3.0	3.5	3.5	3.5
11	1.2	0.8	5.3	1.2	0.7	0.8	1.0

Table A- 29: RMSE observed in epilimnion region for Lake Maumelle AR (No. of days = 5)

Eddy diffusion model option no	Surface convection/evaporation model option no						
	1	2	3	4	5	6	7
1	1.2	1.8	3.9	2.8	4.4	2.2	1.8
2	0.4	2.3	4.6	1.9	4.9	2.8	2.0
3	0.5	2.3	4.6	1.9	4.9	2.8	2.0
4	0.6	2.5	4.1	2.0	5.1	2.9	2.2
5	0.6	2.4	4.0	1.9	5.1	2.9	2.1
6	0.6	2.5	4.1	2.0	5.1	2.9	2.2
7	0.6	2.4	4.3	1.8	5.1	2.9	2.1
8	0.5	2.2	4.4	1.9	4.8	2.7	2.0
9	0.4	2.3	4.6	1.9	4.9	2.8	2.0
10	0.6	2.4	4.0	1.9	5.1	2.9	2.1
11	0.6	2.4	4.3	1.8	5.1	2.9	2.2

Table A- 30: RMSE observed in metalimnion region for Lake Maumelle AR (No. of days = 5)

Eddy diffusion model option no	Surface convection/evaporation model option no						
	1	2	3	4	5	6	7
1	5.0	4.5	3.9	7.0	3.0	4.2	4.2
2	3.9	5.9	8.0	1.8	8.5	6.4	5.6
3	3.6	5.5	7.5	1.6	7.9	5.9	5.2
4	3.2	3.0	2.0	1.4	4.9	3.3	3.1
5	3.3	3.5	1.2	1.6	5.0	3.7	3.9
6	3.3	3.2	2.1	1.5	4.9	3.4	3.3
7	4.0	5.9	6.1	1.9	8.3	6.4	5.6
8	3.3	5.0	6.8	1.3	7.3	5.4	4.8
9	3.9	5.9	8.0	1.8	8.5	6.4	5.6
10	3.3	3.6	1.7	1.5	5.1	3.6	3.8
11	4.0	5.9	5.3	1.9	8.4	6.3	5.6

Table A- 31: RMSE observed in hypolimnion region for Lake Maumelle AR (No. of days = 5)

Eddy diffusion model option no	Surface convection/evaporation model option no						
	1	2	3	4	5	6	7
1	3.8	3.3	2.3	5.8	1.3	3.0	3.0
2	7.3	9.2	11.2	5.1	11.8	9.7	8.9
3	6.9	8.6	10.5	4.8	11.0	9.0	8.4
4	3.5	3.5	1.8	2.4	4.5	3.5	3.7
5	4.7	3.8	1.1	2.8	5.1	3.9	4.1
6	3.7	3.6	1.9	2.7	4.7	3.7	3.9
7	6.7	7.4	8.0	4.8	9.4	7.8	8.2
8	6.4	7.6	9.1	4.3	9.6	8.0	7.5
9	7.3	9.2	11.2	5.1	11.8	9.7	8.9
10	3.5	3.2	1.4	2.4	4.2	3.3	3.4
11	5.9	7.4	6.9	4.1	8.5	7.8	7.2

Table A- 32: MBE observed in epilimnion region for Lake Maumelle AR (No. of days = 5)

Eddy diffusion model option no	Surface convection/evaporation model option no						
	1	2	3	4	5	6	7
1	1.0	1.6	3.5	2.4	4.1	2.0	1.6
2	0.4	2.2	4.5	1.9	4.9	2.7	1.9
3	0.4	2.2	4.5	1.9	4.9	2.7	2.0
4	0.4	2.4	4.0	1.9	5.1	2.9	2.1
5	0.4	2.4	3.9	1.8	5.1	2.9	2.1
6	0.4	2.4	4.0	1.8	5.1	2.9	2.1
7	0.4	2.3	4.3	1.7	5.0	2.8	2.1
8	0.3	2.1	4.4	1.9	4.8	2.6	1.9
9	0.4	2.2	4.5	1.9	4.9	2.7	1.9
10	0.4	2.4	3.9	1.8	5.1	2.9	2.1
11	0.5	2.3	4.3	1.7	5.1	2.8	2.1

Table A- 33: MBE observed in metalimnion region for Lake Maumelle AR (No. of days = 5)

Eddy diffusion model option no	Surface convection/evaporation model option no						
	1	2	3	4	5	6	7
1	4.7	4.1	3.5	6.8	2.8	3.9	3.9
2	3.8	5.6	7.7	1.6	8.2	6.1	5.4
3	3.4	5.2	7.2	1.4	7.6	5.6	5.0
4	3.0	2.9	1.9	1.2	4.8	3.2	3.0
5	3.2	3.5	1.2	1.4	4.9	3.7	3.8
6	3.1	3.1	1.9	1.3	4.8	3.3	3.3
7	3.9	5.7	5.8	1.8	8.2	6.1	5.5
8	3.1	4.6	6.4	1.1	6.9	5.0	4.5
9	3.8	5.6	7.7	1.6	8.2	6.1	5.4
10	3.2	3.5	1.6	1.3	5.0	3.6	3.8
11	3.9	5.6	4.8	1.7	8.2	6.1	5.4

Table A- 34: MBE observed in hypolimnion region for Lake Maumelle AR (No. of days = 5)

Eddy diffusion model option no	Surface convection/evaporation model option no						
	1	2	3	4	5	6	7
1	4.7	4.0	2.7	7.4	1.5	3.7	3.7
2	9.2	11.5	14.1	6.4	14.8	12.1	11.2
3	8.7	10.8	13.2	6.1	13.9	11.3	10.6
4	3.4	3.3	2.2	2.3	4.2	3.3	3.5
5	4.6	3.7	0.7	2.7	5.0	3.9	4.0
6	3.6	3.5	2.3	2.6	4.4	3.5	3.8
7	6.4	7.2	10.3	4.5	9.1	7.5	7.8
8	8.1	9.7	11.7	5.5	12.4	10.2	9.6
9	9.2	11.5	14.1	6.4	14.8	12.1	11.2
10	3.9	3.4	1.7	2.5	4.5	3.5	3.7
11	6.3	7.8	8.7	4.2	9.2	8.2	7.6

Table A- 35: RMSE observed in epilimnion region for Lake Mendota WI (No. of days = 5)

Eddy diffusion model option no	Surface convection/evaporation model option no						
	1	2	3	4	5	6	7
1	0.9	2.6	4.3	1.3	4.4	2.9	2.3
2	1.1	2.7	4.4	0.8	4.3	3.0	2.3
3	0.8	2.4	4.0	1.0	4.0	2.6	2.0
4	0.9	2.5	4.3	1.2	4.2	2.8	2.2
5	1.1	2.7	4.2	1.0	4.2	3.0	2.3
6	1.1	2.7	4.3	1.0	4.2	3.0	2.4
7	1.0	2.6	4.3	0.9	4.1	2.9	2.3
8	0.7	2.3	4.1	1.1	4.1	2.6	2.1
9	1.1	2.7	4.4	0.8	4.3	3.0	2.3
10	1.0	2.7	4.2	1.0	4.2	2.9	2.3
11	0.9	2.4	4.0	1.1	3.8	2.6	2.1

Table A- 36: RMSE observed in metalimnion region for Lake Mendota WI (No. of days = 5)

Eddy diffusion model option no	Surface convection/evaporation model option no						
	1	2	3	4	5	6	7
1	2.9	2.8	2.7	3.7	1.5	2.6	2.6
2	5.0	6.0	7.3	3.5	7.6	6.2	5.9
3	3.7	4.4	5.3	2.9	5.6	4.5	4.3
4	3.7	3.7	2.7	3.5	2.0	3.4	3.4
5	4.2	5.9	2.6	3.7	5.3	5.9	5.4
6	4.3	6.1	2.7	3.9	5.1	6.0	5.8
7	2.1	3.3	1.0	1.9	3.4	3.1	3.4
8	2.5	2.7	3.2	1.9	3.3	2.8	2.7
9	5.0	6.0	7.3	3.5	7.6	6.2	5.9
10	4.2	5.9	2.5	3.7	5.2	5.8	5.4
11	2.9	4.5	2.1	2.9	3.6	4.2	4.2

Table A- 37: RMSE observed in hypolimnion region for Lake Mendota WI (No. of days = 5)

Eddy diffusion model option no	Surface convection/evaporation model option no						
	1	2	3	4	5	6	7
1	2.7	2.6	2.4	3.6	1.2	2.3	2.4
2	7.5	8.7	10.1	5.9	10.4	8.9	8.6
3	5.7	6.4	7.2	4.9	7.5	6.4	6.3
4	3.6	3.6	2.4	3.6	1.8	3.2	3.3
5	4.2	6.2	2.3	4.2	5.2	5.9	5.5
6	4.6	6.5	2.5	4.5	5.3	6.2	6.1
7	2.3	3.5	0.7	2.2	3.4	3.1	3.7
8	2.0	2.1	2.4	1.9	2.7	2.1	2.2
9	7.5	8.7	10.1	5.9	10.4	8.9	8.6
10	4.3	6.3	2.3	4.3	5.3	6.0	5.6
11	3.3	5.2	1.5	3.1	4.0	4.8	4.8

Table A- 38: MBE observed in epilimnion region for Lake Mendota WI (No. of days = 5)

Eddy diffusion model option no	Surface convection/evaporation model option no						
	1	2	3	4	5	6	7
1	0.8	2.2	3.7	1.2	4.0	2.5	2.0
2	1.0	2.3	4.1	0.8	4.1	2.7	2.1
3	0.7	2.1	3.8	0.9	3.8	2.3	1.8
4	0.8	2.2	3.8	1.2	3.9	2.4	1.9
5	0.9	2.4	3.7	1.0	3.6	2.6	2.1
6	0.9	2.4	3.8	1.0	3.6	2.6	2.1
7	0.8	2.2	3.9	0.9	3.4	2.4	2.0
8	0.6	2.0	3.8	1.0	3.9	2.3	1.9
9	1.0	2.3	4.1	0.8	4.1	2.7	2.1
10	0.9	2.4	3.7	1.0	3.5	2.6	2.1
11	0.8	2.1	3.6	1.1	3.3	2.3	1.8

Table A- 39: MBE observed in metalimnion region for Lake Mendota WI (No. of days = 5)

Eddy diffusion model option no	Surface convection/evaporation model option no						
	1	2	3	4	5	6	7
1	2.9	2.8	2.7	3.7	1.4	2.6	2.6
2	4.6	5.4	6.6	3.3	7.0	5.5	5.3
3	3.0	3.4	4.1	2.6	4.6	3.5	3.3
4	3.7	3.7	2.7	3.4	2.0	3.4	3.4
5	4.2	5.9	2.6	3.7	5.3	5.9	5.4
6	4.3	6.1	2.7	3.9	5.1	6.0	5.8
7	1.9	3.1	0.8	1.7	3.2	2.9	3.2
8	2.0	2.2	2.4	1.6	2.4	2.2	2.2
9	4.6	5.4	6.6	3.3	7.0	5.5	5.3
10	4.2	5.9	2.5	3.7	5.2	5.8	5.4
11	2.7	3.9	1.9	2.6	3.2	3.7	3.6

Table A- 40: MBE observed in hypolimnion region for Lake Mendota WI (No. of days = 5)

Eddy diffusion model option no	Surface convection/evaporation model option no						
	1	2	3	4	5	6	7
1	2.7	2.5	2.4	3.5	1.1	2.3	2.3
2	7.0	7.9	9.3	5.6	9.6	8.1	7.8
3	4.8	5.3	6.0	4.5	6.4	5.3	5.1
4	3.5	3.5	2.4	3.6	1.7	3.1	3.2
5	4.2	6.2	2.2	4.2	5.2	5.9	5.5
6	4.5	6.5	2.4	4.5	5.2	6.2	6.0
7	2.3	3.5	0.7	2.2	3.4	3.1	3.6
8	1.7	1.7	1.9	1.6	1.9	1.7	1.8
9	7.0	7.9	9.3	5.6	9.6	8.1	7.8
10	4.3	6.3	2.3	4.3	5.2	5.9	5.5
11	3.2	5.1	1.4	2.9	4.0	4.7	4.7

APPENDIX B

Design Tool for Surface Water Heat Pump Systems

User Documentation

School of Mechanical and Aerospace Engineering

Oklahoma State University

Introduction

Surface water heat pump (SWHP) systems utilize surface water bodies, such as ponds, lakes, rivers, and the sea, as heat sources and/or sinks. These systems may be open-loop, circulating water between the surface water body and a heat exchanger on dry land, or closed-loop, utilizing a submerged surface water heat exchanger (SWHE). If properly designed, SWHP systems can be one of the most efficient and economical alternatives used both for heating and cooling requirements. The design tool for surface water heat pump systems is used as an aid in the sizing of the SWHE used in a closed loop SWHP system. The procedure utilized by the design tool can be divided into three tasks:

- First, based on user input regarding the physical characteristics and location of the water body, the design tool simulates the lake and finds the daily water body temperatures[3] at the depth of the heat exchanger.

- Second, based on the water body temperatures at the depth where the heat exchanger is placed, the design tool calculates the heat transfer performance and determines the required size of the SWHE. The design tool can do this for four different SWHE configurations - spiral-helical, flat spiral, horizontal/vertical slinky and vertical flat plate heat exchangers. The design tool also determines the buoyancy force exerted on each heat exchanger if/when ice forms on the SWHE.

- Third, as a final check, the design tool simulates the lake considering the heat input and heat extraction of the SWHP system. Although, for most systems, the effect of the SWHP system on the lake will be negligible

The design tool uses a one-dimensional lake model to determine the daily average temperatures as a function of depth.

One of the major assumptions in the development of the lake model is that, the model does not consider the effect of inflows or outflows to the water body and assumes the water body depth to remain constant throughout the year. Water bodies especially reservoirs which exhibit high fluctuation in its depth, exhibit a different temperature phenomenon, which could not be reasonably predicted by the lake model. Since, the water body temperatures has a direct effect on predicting the heat transfer performance of a SWHE, the application of the design tool is limited to relatively stagnant water bodies.

Overview - using the design tool

1. The design tool is comprised of a Microsoft Excel spreadsheet and two executable files (LakeModel.exe) that contains the lake simulation and (SWHEmodel.exe) that contains the heat exchanger simulation model; originally written in Fortran 90. For the proper functioning of the design tool, both LakeModel.exe and SWHEmodel.exe must be in the same folder as the spreadsheet.

[3] These temperatures are the undisturbed temperatures; only in the last step is the effect of the heat exchangers on the lake temperature analyzed.

2. The spreadsheet makes extensive use of macros written in Excel's native programming language, Visual Basic for Applications. With default security settings, the user will have to allow these macros to run.

3. The design tool requires eight sets of input data, discussed in more detail in the next section.

    a. Hourly weather data.

    b. Lake morphometry - which describes the physical characteristics of the lake that are relevant to the lake simulation, specifically the bathymetry and turbidity.

    c. Undisturbed ground temperature and initial water body temperatures.

    d. Hourly or monthly and monthly peak total building heating and cooling loads.

    e. Surface water heat exchanger information.

    f. Type and percentage of concentration of antifreeze used, if any.

    g. Surface water heat pump characteristics.

    h. Surface water heat pump design temperatures.

    The"GetInputParameters" sheet acts as a main input sheet, directing the user to other input sheets where necessary.

4. The design tool has a default input unit option set to IP units. Users may also enter the input data in SI units by selecting the "SI units" option from the dropdown box. All input sheets except the "InputWeatherData" sheet contain a drop down input box, for the user to input the parameters in either IP (Inch-pound) or SI (Metric) units. The "InputWeatherData" sheet has an option which automates the weather data processing, if the input weather file selected is in the EnergyPlus weather (EPW) format .Since, the data in the EPW files are in SI units, for calculation purposes the design tool has this exception of only SI units for the "InputWeatherData" sheet.

5. All of the input data can be reviewed using the "View Input Data Summary" button on the "GetInputParameters" sheet, which creates and opens the "InputSummary" sheet.

6. In order to size the SWHE, the user presses the "Size SWHE" button on the "InputSummary sheet". The design tool runs LakeModel.exe to simulate the lake and size the SWHE. The output will be displayed in the "WriteOutput" sheet.

7. The user can also analyze the impact of the SWHP system on the lake temperatures by pressing the "Calculate change in lake temperatures" button in the "WriteOutput" sheet. The design tool simulates the lake considering the heat transfer effects from the sized SWHE and estimates change in lake temperatures. The results will be displayed in "Change in lake temperatures" sheet.

Input

I. Hourly weather data

1. The "Input Weather Data" button in the "GetInputParameters" sheet directs the user to the "InputWeatherData" sheet.
2. The user can input the weather file in either EnergyPlus weather format (.epw file) or in any other standard weather formats.
3. If the user opts to input the weather file in EnergyPlus weather format, the design tool has an automated procedure to process the data from the file, print the data in its respective columns and formulate the monthly statistical information. An Illustration of this procedure is shown in Figure B-1.
4. If the user chooses to input any other standard weather data, he/she may have to put in an additional effort to paste the hourly weather data parameters in SI units for the location in the respective columns provided.
5. The "Calculate Monthly Statistical Data" button enables the user to view/verify the statistical monthly data for air temperature and wind speed. This button becomes redundant when the user provides the design tool with the EnergyPlus weather file as the design tool automates this step.
6. EnergyPlus weather file is available for more than 2100 locations around the world; 1042 locations in the USA. The .epw weather files and can be downloaded from http://apps1.eere.energy.gov/buildings/energyplus/cfm/weather_data.cfm.
7. To clear the data, the user needs to select the "Reset" option from the dropdown menu. The option clears the current data in the sheet.
8. The design tool also computes and prints the annual average air temperature for the location. The annual average air temperature is used by the design tool as a default value for the undisturbed ground temperature (explained in detail in the Input Initialization section (section III)).

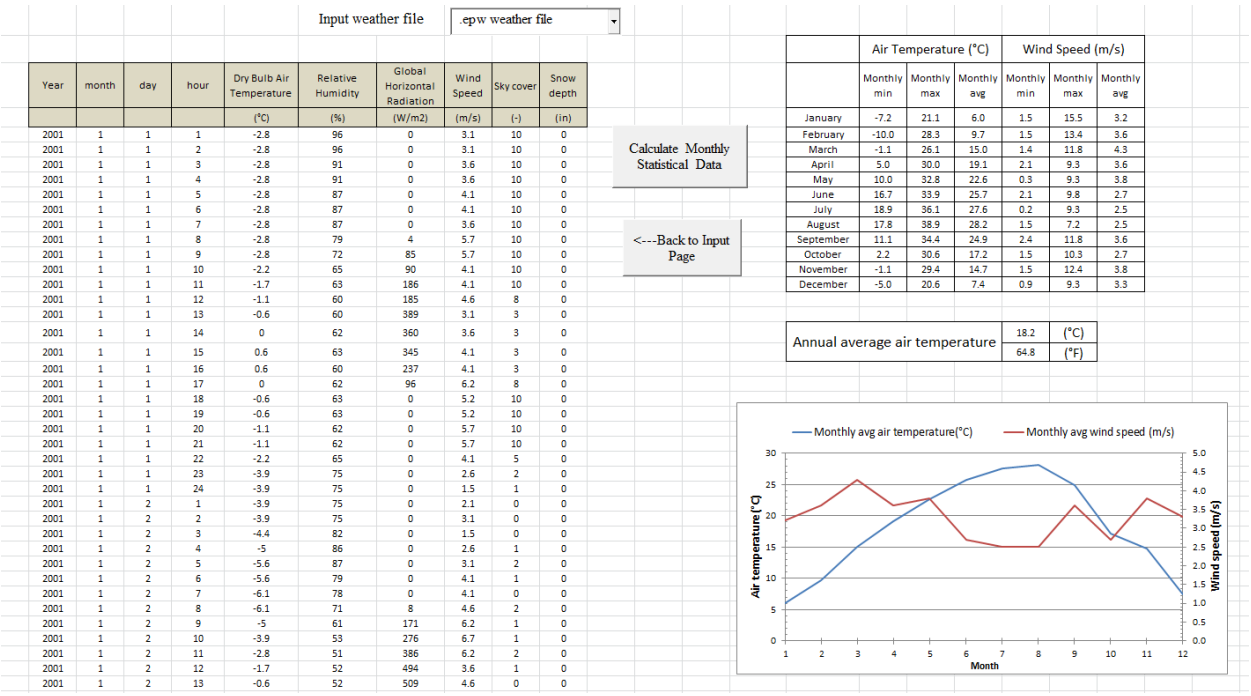

Year	month	day	hour	Dry Bulb Air Temperature	Relative Humidity	Global Horizontal Radiation	Wind Speed	Sky cover	Snow depth
				(°C)	(%)	(W/m2)	(m/s)	(-)	(in)
2001	1	1	1	-2.8	96	0	3.1	10	0
2001	1	1	2	-2.8	96	0	3.1	10	0
2001	1	1	3	-2.8	91	0	3.6	10	0
2001	1	1	4	-2.8	91	0	3.6	10	0
2001	1	1	5	-2.8	87	0	4.1	10	0
2001	1	1	6	-2.8	87	0	4.1	10	0
2001	1	1	7	-2.8	87	0	3.6	10	0
2001	1	1	8	-2.8	79	4	5.7	10	0
2001	1	1	9	-2.8	72	85	5.7	10	0
2001	1	1	10	-2.2	65	90	4.1	10	0
2001	1	1	11	-1.7	63	186	4.1	10	0
2001	1	1	12	-1.1	60	185	4.6	8	0
2001	1	1	13	-0.6	60	389	3.1	3	0
2001	1	1	14	0	62	360	3.6	3	0
2001	1	1	15	0.6	63	345	4.1	3	0
2001	1	1	16	0.6	60	237	4.1	3	0
2001	1	1	17	0	62	96	6.2	8	0
2001	1	1	18	-0.6	63	0	5.2	10	0
2001	1	1	19	-0.6	63	0	5.2	10	0
2001	1	1	20	-1.1	62	0	5.7	10	0
2001	1	1	21	-1.1	62	0	5.7	10	0
2001	1	1	22	-2.2	65	0	4.1	5	0
2001	1	1	23	-3.9	75	0	2.6	2	0
2001	1	1	24	-3.9	75	0	1.5	1	0
2001	1	2	1	-3.9	75	0	2.1	0	0
2001	1	2	2	-3.9	75	0	3.1	0	0
2001	1	2	3	-4.4	82	0	1.5	0	0
2001	1	2	4	-5	86	0	2.6	1	0
2001	1	2	5	-5.6	87	0	3.1	2	0
2001	1	2	6	-5.6	79	0	4.1	1	0
2001	1	2	7	-6.1	78	0	4.1	0	0
2001	1	2	8	-6.1	71	8	4.6	2	0
2001	1	2	9	-5	61	171	6.2	1	0
2001	1	2	10	-3.9	53	276	6.7	1	0
2001	1	2	11	-2.8	51	386	6.2	2	0
2001	1	2	12	-1.7	52	494	3.6	1	0
2001	1	2	13	-0.6	52	509	4.6	0	0

	Air Temperature (°C)			Wind Speed (m/s)		
	Monthly min	Monthly max	Monthly avg	Monthly min	Monthly max	Monthly avg
January	-7.2	21.1	6.0	1.5	15.5	3.2
February	-10.0	28.3	9.7	1.5	13.4	3.6
March	-1.1	26.1	15.0	1.4	11.8	4.3
April	5.0	30.0	19.1	2.1	9.3	3.6
May	10.0	32.8	22.6	0.3	9.3	3.8
June	16.7	33.9	25.7	2.1	9.8	2.7
July	18.9	36.1	27.6	0.2	9.3	2.5
August	17.8	38.9	28.2	1.5	7.2	2.5
September	11.1	34.4	24.9	2.4	11.8	3.6
October	2.2	30.6	17.2	1.5	10.3	2.7
November	-1.1	29.4	14.7	1.5	12.4	3.8
December	-5.0	20.6	7.4	0.9	9.3	3.3

Figure B- 1: Illustration of "InputWeatherData" sheet with ".epw weather file" option

II. Lake morphometry details

1. The "Input Lake Morphometry Data" button in the "GetInputParameters" sheet directs the user to the "LakeMorphometryInfo" sheet.
2. In all cases, the user inputs the surface area, maximum depth and average secchi depth of the lake. Secchi depth refers to the depth from the surface where the secchi disc becomes invisible (Michaud 1994). The lake turbidity is calculated based on the secchi depth (Hondzo and Stefan 1993a).
3. The user has three options for specifying the bathymetry of the lake – that is the area vs. depth profile. The first two options can be chosen by selecting "Basic input"; the last option is chosen by selecting "advanced input."
    a. The simplest option, which is suitable for lakes under 2470 acres or 1000 Hectares in surface area, is to simply specify the lake volume as zero, and a "typical bathymetry" will be specified based on the empirical correlation given by Hondzo and Stefan (1993b).
    b. The second simplest option, which is suitable for any size lake is to specify the volume of the lake, in which case, the design tool will estimate the lake bathymetry profile based on Johansson, et al. (2007).
    c. The last option is to specify the bathymetry by specifying the area at a range of depths. Methods for determining the area as a function of depth are described by(Håkanson 1981). In order to specify the bathymetry, the user clicks on the "advanced input" radio button and responds to the prompt for the number of area-depth pairs that will be specified. A new table is created and the user will fill that in, as shown in Figure B-2.

4. The lake bathymetry is best estimated with the advanced user input followed by Johansson, et al. (2007) correlation and Hondzo and Stefan (1993b) in that order. However, the sensitivity of lake temperature prediction and hence, its effect on the SWHE heat transfer performance to the bathymetry profile of the lake is yet to be determined.

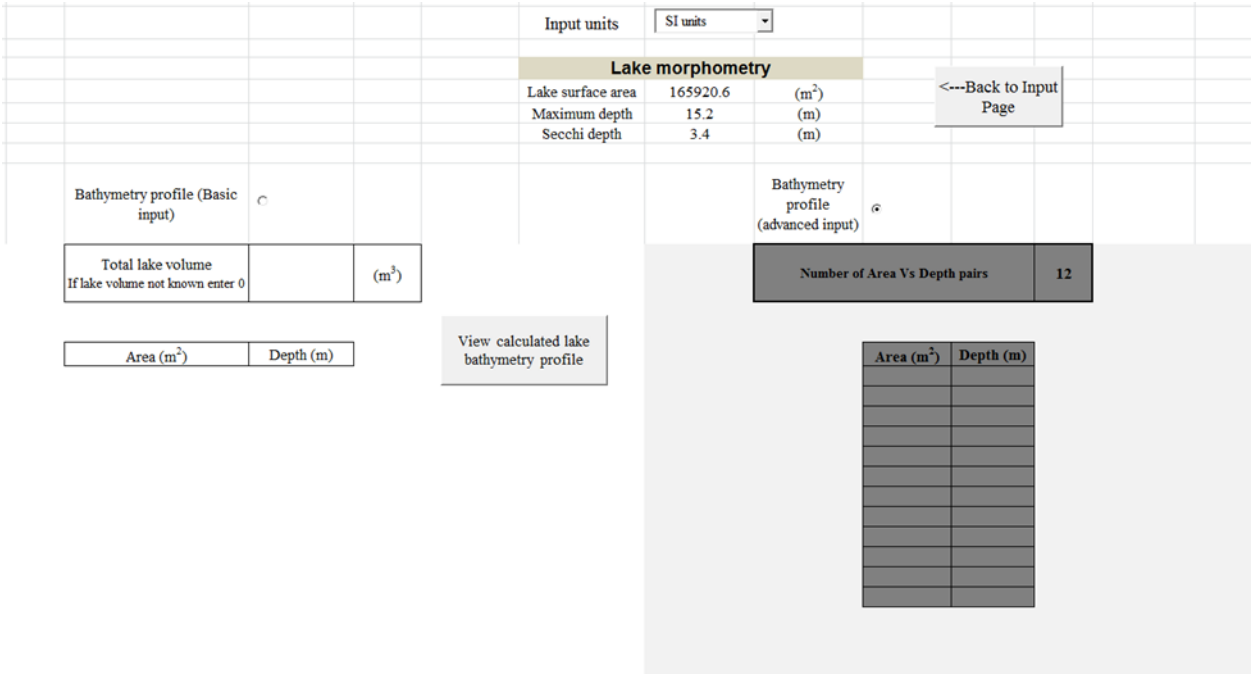

Figure B- 2: Screen shot image of the "LakeMorphometryInfo" sheet

III. Input Initialization

1. The "Initialize Temperature Data" button in the "GetInputParameters" sheet directs the user to the "TempInitialization" sheet.
2. The user is required to input the undisturbed ground temperature for the location and an initial temperature profile for the lake.
3. The design tool provides a default values for the undisturbed ground temperature and the initial uniform lake temperature as shown in Figure B-3.
    a. The default value for the undisturbed ground temperature is estimated approximately from the annual average air temperature (Signorelli and Kohl 2004), and the default initial uniform lake temperature value is estimated between 4°C (39.2°F) or the average air temperature obtained between December 15 to January 15, whichever is maximum.
    b. The user can also modify the default values.
4. The user also has an option to specify the initial lake temperature along the depth, if they could obtain the lake temperature profile from any historical experimental data. In order to specify the initial lake temperature profile, the user clicks on the "advanced input" radio button and responds to the prompt for the number of temperature-depth pairs that will be specified. A new table is created for the user to fill the data

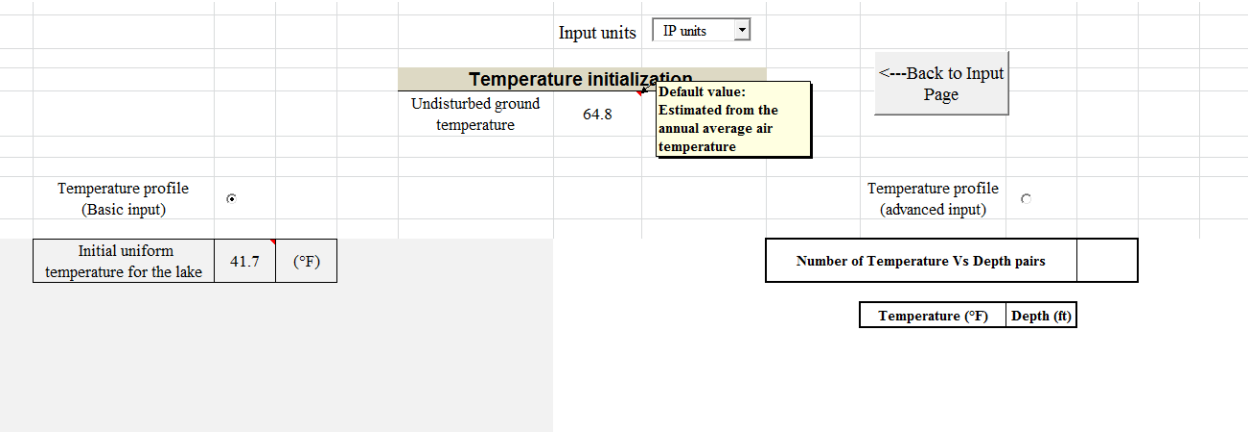

Figure B- 3: Screen shot of advanced bathymetry input option in the "LakeMorphometryInfo" sheet

IV. Building loads

1. The "Input Building loads" button in the "GetInputParameters" sheet directs the user to the "GetInputBuildingLoads" data sheet.
2. Building loads can be entered either as a monthly total load or in an hourly load format by selecting the appropriate option button.
3. The design tool reads the magnitude of the loads and hence, no specific sign convention needs to be followed for entering the cooling loads.

V. Surface Water Heat Exchanger (SWHE) parameters

The user can enter the SWHE parameters from the "GetInputParameters" sheet. The user has to select the type and material of the SWHE used from the respective drop down menus. The design tool can design SWHP systems with four SWHE configurations namely spiral-helical, flat spiral, vertical/horizontal slinky and vertical flat metal plate heat exchangers.

The following input parameters are required for every SWHE type.

a. **Spiral helical heat exchanger**.

- Outside tube diameter in mm (in)
- Inside tube diameter in mm (in)
- Length of the hydronic tubing per coil in m (ft)
- Outside coil diameter in m (ft)
- Horizontal spacing between adjacent tubes in mm (in)
- Vertical spacing between adjacent tubes in mm (in)
- Total system volumetric flow rate in L/s (GPM)

Figure B-4 shows the illustration of some of the input parameters for spiral helical heat exchanger.

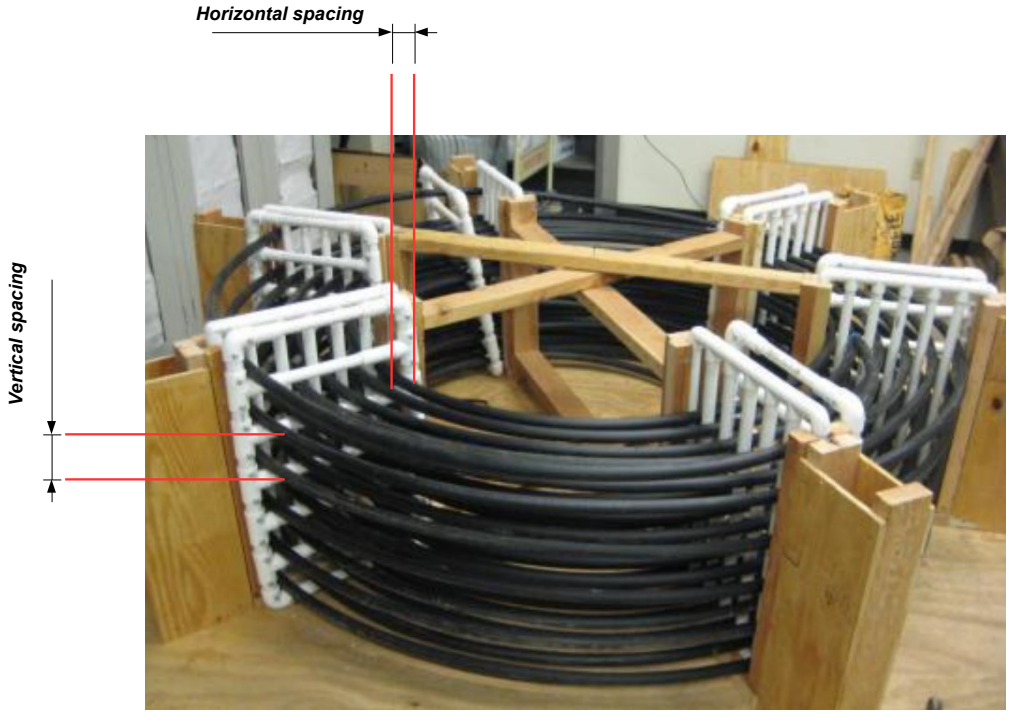

Figure B- 4: Spiral helical coil heat exchanger with illustrated input parameters (Courtesy: Hansen 2011)

- The correlation used by the design tool to calculate the heat transfer coefficients for spiral helical coil has been tested for certain range of input parameters. The user input should be within the correlation parameters.
- Effective range of input parameters
    - 26.7 mm(1.050 in) < outside tube diameter < 42.2 mm(1.660 in)
    - 21.8 mm(0.86 in) < inside tube diameter < 34.5 mm(1.358 in)
    - Length of the hydronic tubing <= 152.4 m (500 ft)
    - 38.1 mm(1.5 in) < horizontal spacing < 104.8 mm(4.125 in)
    - 38.1 mm(1.5 in) < vertical spacing < 104.8 mm(4.125 in)

b. Horizontal spiral heat exchanger.

- Outside tube diameter in mm (in)
- Inside tube diameter in mm (in)
- Length of the hydronic tubing per coil in m (ft)
- Outside coil diameter in m (ft)
- Horizontal spacing between adjacent tubes in mm (in)
- Total system volumetric flow rate in L/s (GPM)

Figure B-5 shows the illustration of some of the input parameters for horizontal spiral heat exchanger

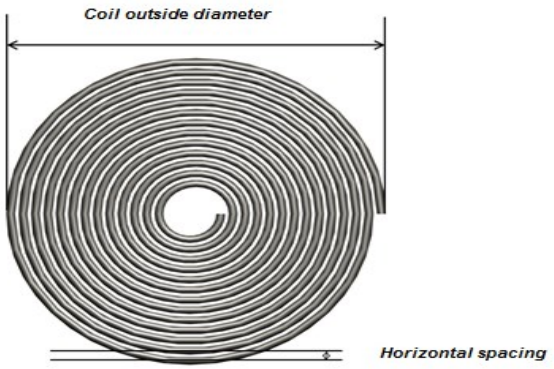

Figure B- 5: Illustration of a horizontal spiral coil and its input parameters

c. Vertical or horizontal slinky heat exchanger

- Outside tube diameter in mm (in)
- Inside tube diameter in mm (in)
- Total hydronic tubing length in m(ft)
- Outside coil diameter in m (ft)
- Total system volumetric flow rate in L/s (GPM)

Figure B-6 shows the illustration of some of the input parameters for vertical or horizontal slinky heat exchanger

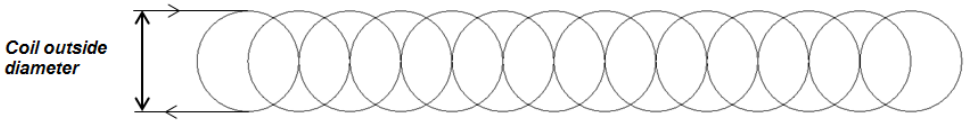

Figure B- 6: Illustration of the slinky coil input parameter

d. Flat plate heat exchanger

- Length of the plate in m (ft)
- Height of the plate in m (ft)
- Thickness of the plate in mm (in)
- Number of passes (-)
- Total system volumetric flow rate in L/s (GPM)

Figure B-7 shows the illustration of some of the input parameters for flat plate heat exchanger

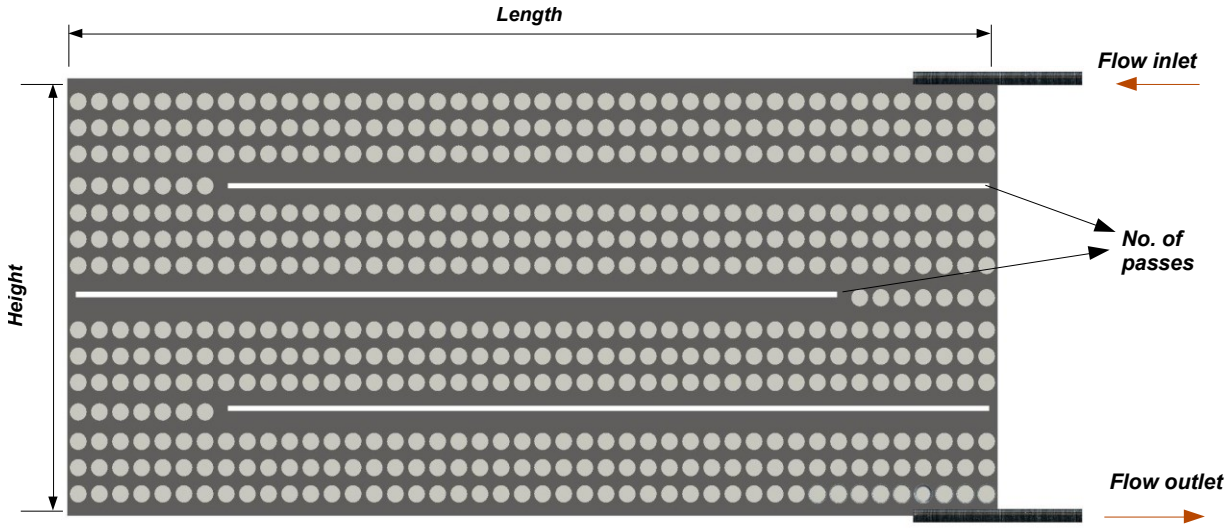

Figure B- 7: Illustration of a flat plate heat exchanger with input parameters

For every heat exchanger type, the user has to provide the minimum and maximum heat exchanger depth. Figure B-8 shows the illustration of the minimum and maximum heat exchanger depths.

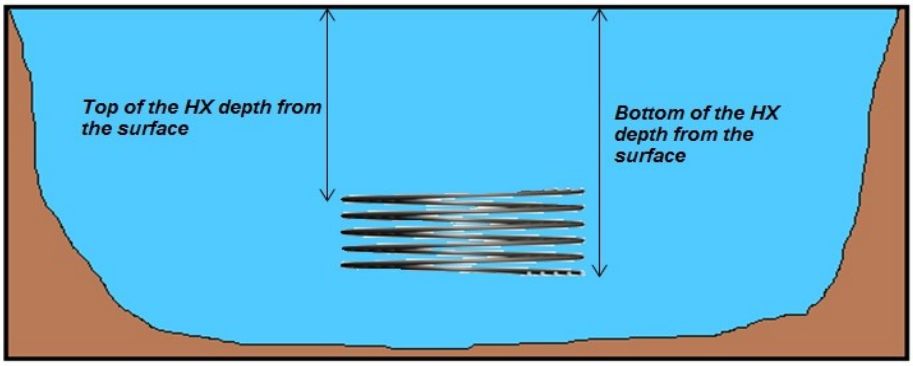

Figure B- 8: Illustration of the maximum and minimum heat exchanger depth

VI. Secondary coolant properties

1. The user can select the type of antifreeze mixture from the dropdown box and specify its percentage of concentration as shown in Figure 9.
2. The design tool has four antifreeze mixture types specified; they are propylene glycol, ethylene glycol, ethyl alcohol and methyl alcohol. If no antifreeze mixture is used, the user can select the option “None” from the dropdown box.

Step 6 - Secondary coolant properties		
Type of antifreeze	Propylene glycol	
Percentage of Concentration	15	% by volume

Figure B- 9: Screen shot image of the secondary coolant property input

VII. Heat pump coefficients

The design tool uses two curve fit equations to describe the performance of the heat pump. The user needs to specify some of the heat pump performance parameters from the manufacturer's catalogue for the design tool to compute the heat pump coefficients.

1. The user has to enter the following data from the heat pump manufacturer's catalogue.
    a. Entering fluid temperature
    b. Heat rejection rate
    c. Total cooling rate or cooling capacity
    d. Heat extraction rate
    e. Total heating rate or heating capacity
2. The number of data points for the cooling and heating loads should be entered in their respective input boxes as shown in Figure B-10.

Input units: IP units

Cooling loads	
Enter number of data points	11

Heating loads	
Enter number of data points	8

EFT (°F)	Total cooling (MBTU/hr)	Heat rejected (MBTU/hr)
30.0	40.0	45.5
40.0	39.9	45.6
50.0	39.2	45.3
60.0	38.0	44.7
70.0	36.4	43.9
80.0	34.5	42.9
85.0	33.4	42.3
90.0	32.2	41.7
100.0	30.1	40.8
110.0	27.6	39.6
120.0	25.4	38.9

EFT (°F)	Total heating (MBTU/hr)	Heat extracted (MBTU/hr)
30.0	27.5	18.2
40.0	32.4	22.3
50.0	37.3	26.4
60.0	42.0	30.4
70.0	46.4	34.2
80.0	50.3	37.6
85.0	52.0	39.0
90.0	53.7	40.5

Figure B- 10: Heating and cooling mode performance data

3. The "Calculate HP Coefficients" button calculates the heat pump coefficients using the quadratic fit equations. The calculated heat pump coefficients and the curve fits are displayed in the "CalcHPCoeff" sheet as shown in Figure B-11.

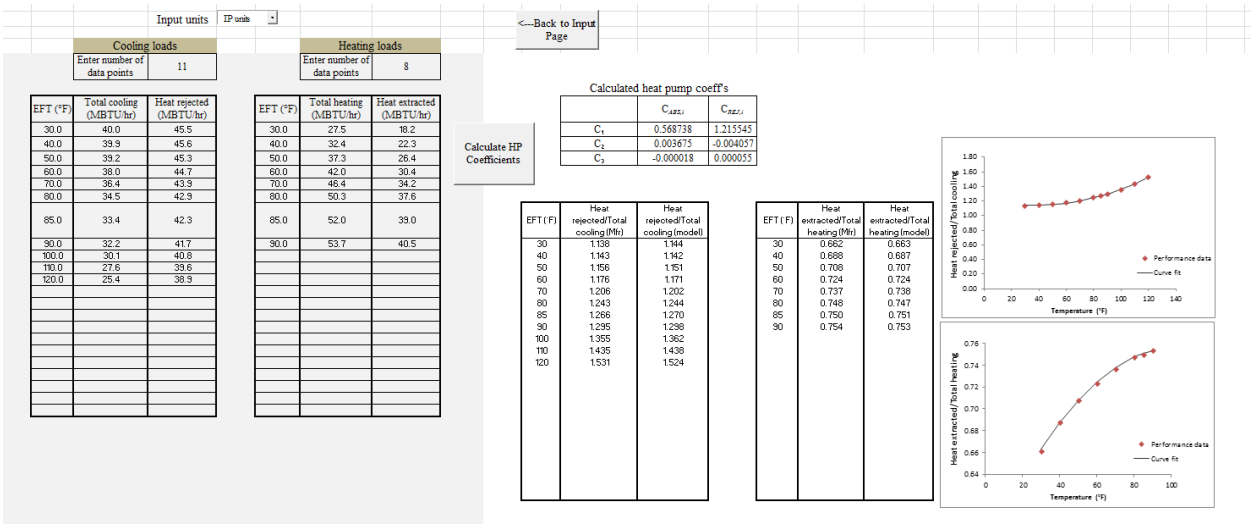

Figure 11: Calculated heat pump coefficients and corresponding curve fits displayed in "CalcHPCoeff" sheet

4. The design tool uses the following curve fit equations to compute the heat pump coefficients.
   a. For the cooling mode:

$$Heat\ Rejection\ Rate = Cooling\ Rate[C_{rej,1} + C_{rej,2}(EFT) + C_{rej,3}(EFT^2)] \quad (2.45)$$

   b. For the heating mode:

$$Heat\ Extraction\ Rate = Heating\ Rate[C_{abs,1} + C_{abs,2}(EFT) + C_{abs,3}(EFT^2)] \quad (2.46)$$

Where, EFT = Temperature of the fluid entering the heat pump
$C_{abs,i}$ = heat pump coefficients determined by quadratic curve fit function for heating mode
$C_{rej,i}$ = heat pump coefficients determined by quadratic curve fit function for cooling mode

VIII. Heat pump design temperatures

1. Specify the required minimum and maximum heat pump design temperatures.

IX. Verify data and run simulation

1. The "Verify Input Data Summary" button creates and activates the "InputSummary" data sheet, which displays the all the input parameters entered by the user in a consolidated format.
2. This sheet is for final verification purposes only. Changes in the input parameters should be made in their respective input sheets.
3. The "Size SWHE" button triggers the executable file to simulate the lake temperatures. The design tool runs the yearly lake simulation twice or thrice so that the lake temperatures reach a

steady state. Then, with the predicted lake temperatures at the heat exchanger depth, the design tool estimates the number of SWHE coils/plates and runs the SWHE model multiple times, until an optimum number of coils/plates to satisfy the design condition is obtained.

4. The SWHP design tool on an average takes about 10-15 minutes to perform one complete run, although the design tool run time may vary with the user input conditions.

X. Design tool output

1. Once the design calculations are performed, the design tool directs the user to the "WriteOutput" sheet.
2. The "WriteOutput" sheet displays the following outputs.
    a. The number of heat exchanger coils/plates required for the design conditions
    b. Tabulated values and a plot comparison on the average, minimum and maximum lake temperature and the average, minimum and maximum heat pump entering fluid temperatures.
    c. Plot showing the buoyancy force experienced by each heat exchanger coil/plate during icing conditions.
3. The user can also analyze the impact of SWHE on the water body temperatures by pressing the "Calculate Change in Lake Temperatures" button in the "WriteOutput" sheet.
4. The design tool simulates the lake temperatures by also considering the heat transfer effects from the SWHE. "ChangeinLakeTemperatures" sheet displays both a plot comparing the daily lake temperatures with and without the effect of surface water heat exchangers at the heat exchanger depth and also the maximum observed change in the lake temperature.

Design tool error messages:

The design tool exhibits the following error messages if the simulation conditions exceed beyond the design parameters.

1. If input lake bathymetry calculation is beyond correlation parameters:

The design tool has a provision to approximately estimate the lake bathymetry using Hondzo and Stefan (1993a) correlation if the lake volume is not known. The correlation is limited for lakes whose surface area is less than 1000 Ha (2470 acres). Hence, for lakes surface area is beyond this limit, the user has to specify an approximate logical value for the total lake volume; else, the design tool displays an error message box as shown in Figure B- 11.

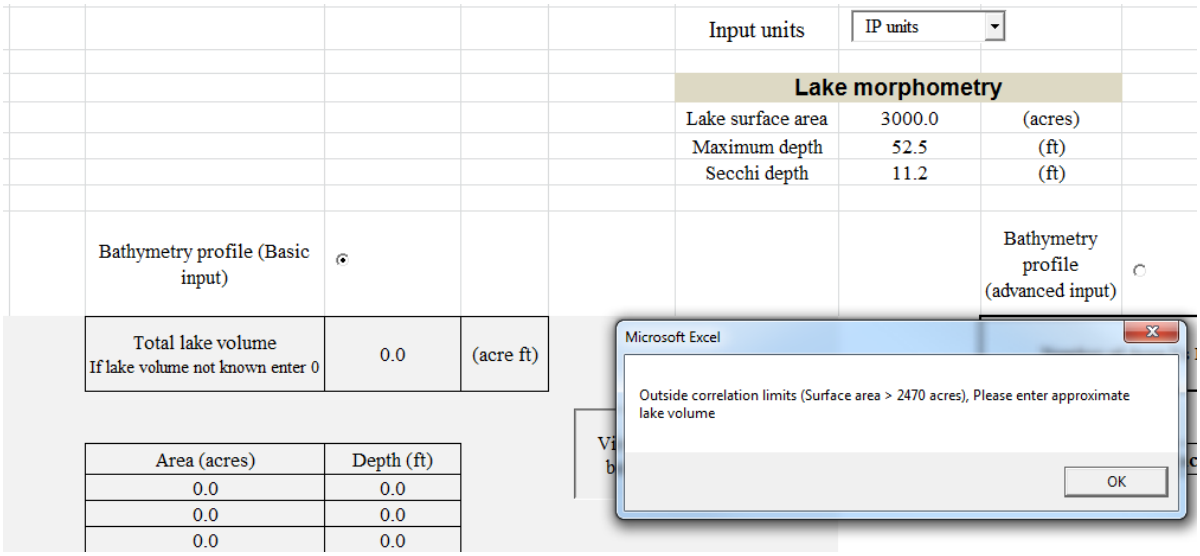

Figure B- 11: Error message display for lake bathymetry calculation beyond correlation parameters

2. **If the heat pump design temperature inputs are beyond maximum heat transfer capacity of the lake:**

If the entered maximum heat pump entering fluid temperatures are less than maximum lake temperatures at the heat exchanger depth the design tool displays the error message in the "GetInputParameters" sheet as shown in Figure B- 12.

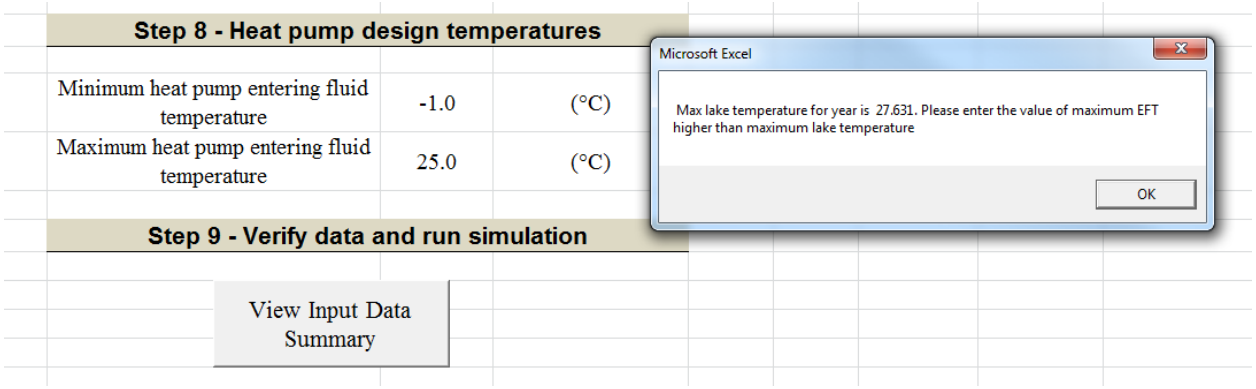

Figure B- 12: Error message display if heat pump design temperature inputs are beyond maximum heat transfer capacity of the lake

Similar message is displayed if the minimum heat pump entering fluid temperatures are greater than minimum lake temperatures at the heat exchanger depth.

3. **If the spiral helical coil input are beyond correlation parameters:**

If the user inputs for the spiral helical coil are beyond the parameters used in developing the correlation, the design tool displays the error message as shown in Figure B- 13 in the "InputSummary" sheet.

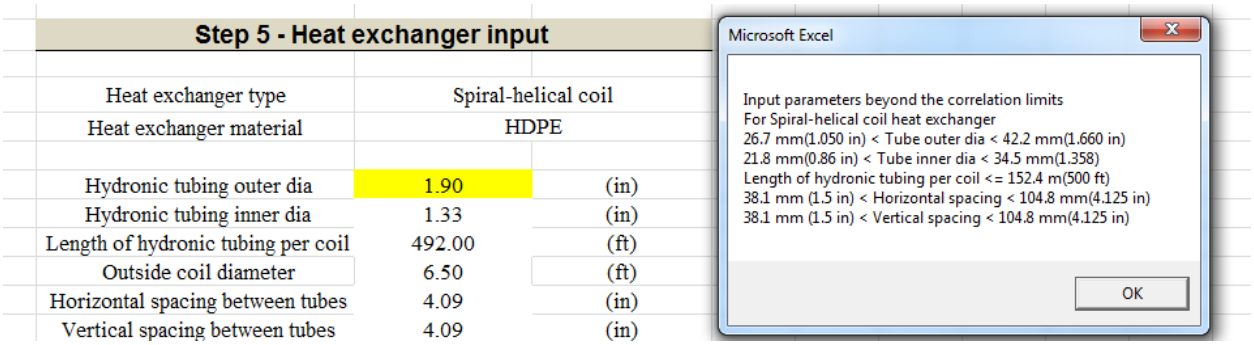

Figure B- 13: Error message if the spiral helical coil inputs are beyond the correlation parameters

4. **If the simulation predicts large amount ice formation around the surface water heat exchanger**

   For the given input conditions if the design tool predicts large amount of ice formation around the surface water heat exchanger(SWHE) coil/plate, the error message as shown in Figure B- 14 is displayed in the "GetInputParameters" sheet.

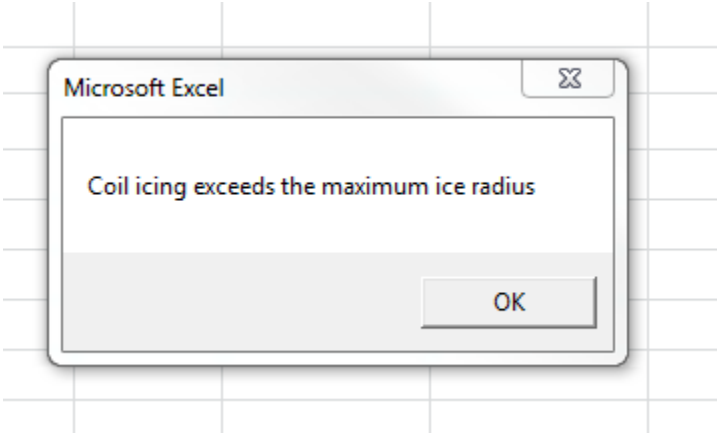

Figure B- 14: Error message if the design tool predicts heat exchanger ice formation

For adverse design conditions, where in the SWHE are subjected to very high heating loads and/or the water body temperatures at the heat exchanger depth are close to freezing temperatures, the ice formation predicted around the SWHE coils/plates would be large enough, the entire SWHE would form a solid ice block. When this condition is reached, the design tool displays the error message.

APPENDIX C

Design Tool for Surface Water Heat Pump Systems

Example of Usage

School of Mechanical and Aerospace Engineering

Oklahoma State University

Introduction:

The design tool can be used as an aid in the sizing of surface water heat exchangers (SWHE) used in surface water heat pump (SWHP) systems. This document provides a detailed description on the procedures involved in using the design tool. The example presented here is about using the design tool to estimate the number of spiral-helical coil heat exchangers required for a SWHP to satisfy the heating and cooling requirements for a small apartment building located in Grand Rapids, Minnesota. The SWHP system is installed in a 41 acre lake located in Grand Rapids, Minnesota.

Design Tool Inputs

The design tool requires the following set of inputs

1. Hourly weather data
2. Lake morphometry- that describes the physical characteristics of the lake that are relevant to the lake simulation, specifically the bathymetry and turbidity.
3. Undisturbed ground temperature and initial water body temperatures.
4. Hourly or monthly and monthly peak total building heating and cooling loads
5. Surface water heat exchanger information.
6. Type and percentage of concentration of antifreeze used, if any.
7. Surface water heat pump characteristics.
8. Surface water heat pump design temperatures.

Step 1: Hourly weather data

EnergyPlus weather file (.epw file) for Grand Rapids, Minnesota is entered by selecting the ".epw weather file" option from the dropdown box in the "InputWeatherData" sheet. The .epw weather files and can be downloaded from http://apps1.eere.energy.gov/buildings/energyplus/cfm/weather_data.cfm. Selecting the ".epw weather file" option prompts a dialogue box to specify the path of the EnergyPlus file as shown in Figure C-1. Once, the path of the EnergyPlus file is provided, the design tool automatically loads the required weather data input in the respective columns and displays the monthly statistical data for air temperature and wind speed. Figure C-2 shows the screen shot image of the "InputWeatherData" sheet after the .epw file for Grand Rapids, MN has been processed.

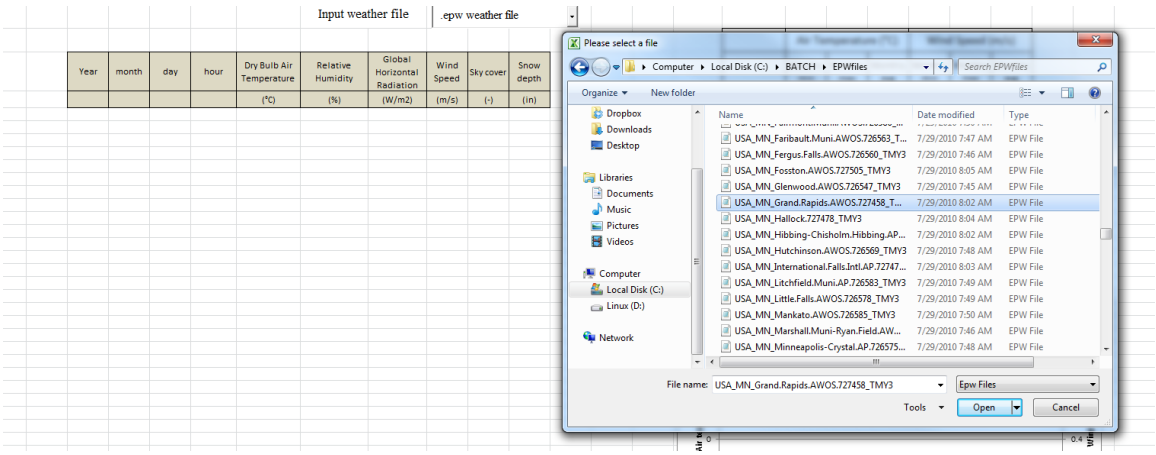

Figure C- 1: Specifying the path of the EnergyPlus weather file

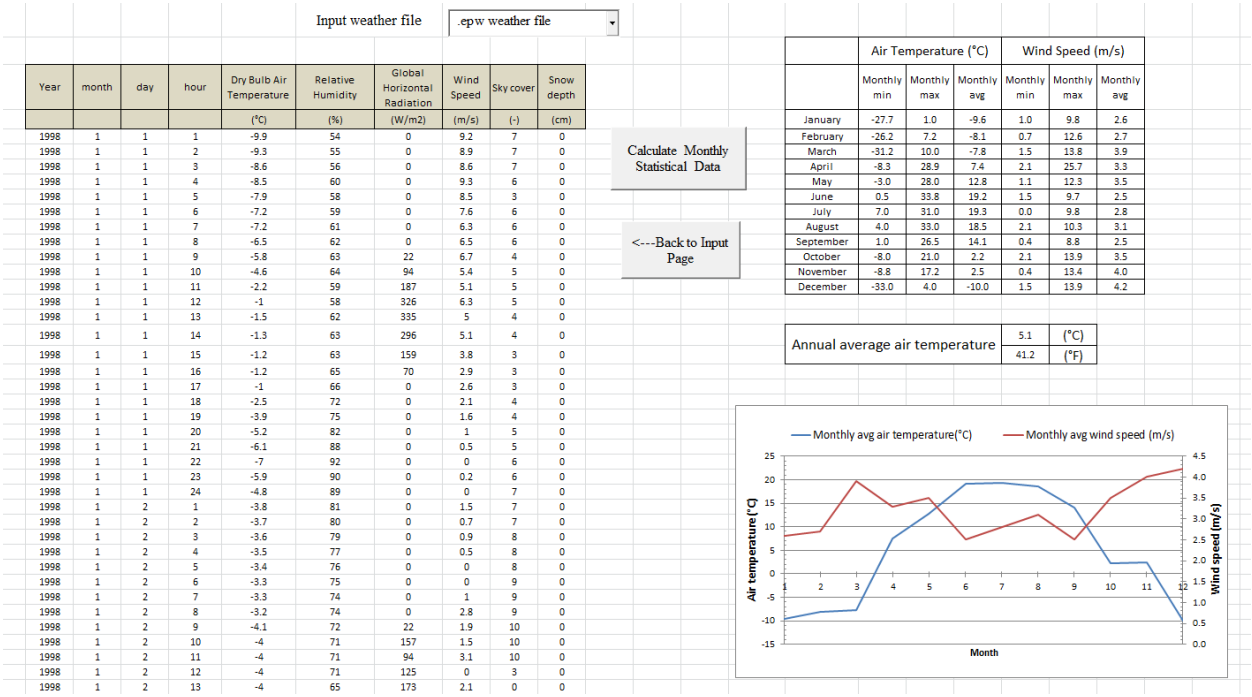

Figure C- 2: Screen shot image of the "InputWeatherData" sheet with processed EnergyPlus weather file for Grand Rapids, Minnesota

Step 2: Lake morphometry details:

Ice Lake is a small lake situated in the city of Grand Rapids in Minnesota. The morphometry data for Ice Lake is obtained from "Water on the Web" (WOW 2012). The details are given below.

Surface area : 41 acres

Maximum depth : 52.5 ft

Total lake volume : 940 acre-ft

Average secchi depth : 11 ft

The morphometry details for Ice Lake are entered in the respective input cells in the "Input Lake Morphometry Data" sheet as shown in Figure C-3. "Bathymetry profile (basic input)" option button is selected to enter the total volume for Ice Lake. "View calculated lake bathymetry profile" button estimates the bathymetry profile for Ice Lake, based on the given input parameters.

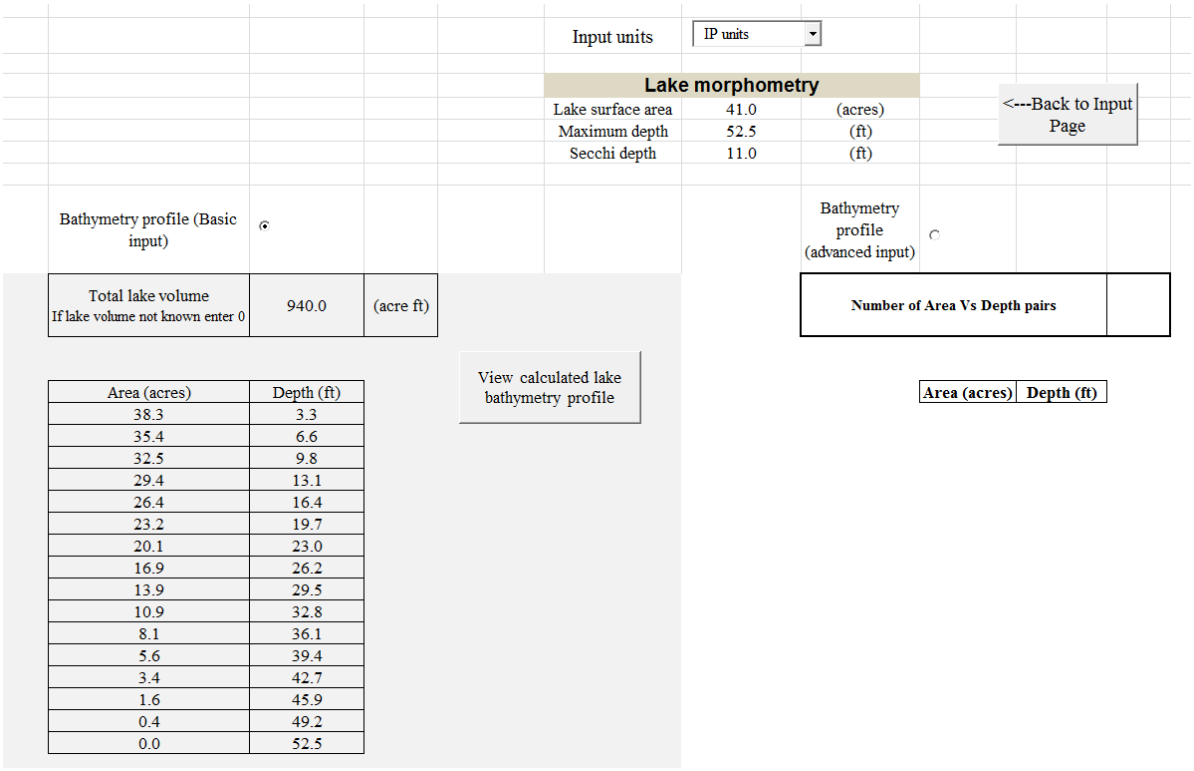

Figure C- 3: Screen shot image of "Input Lake Morphometry Data" sheet with the morphometry details for Ice Lake in Minnesota

Step 3: Temperature initialization

The undisturbed ground temperature data for taken from the design tool default value as 5.1°C (41.2°F). An initial temperature values along the depth is given as input by selecting the "Temperature profile (advanced input)" radio button. Figure C-4 displays the screen shot image of "TempInitialization" data sheet.

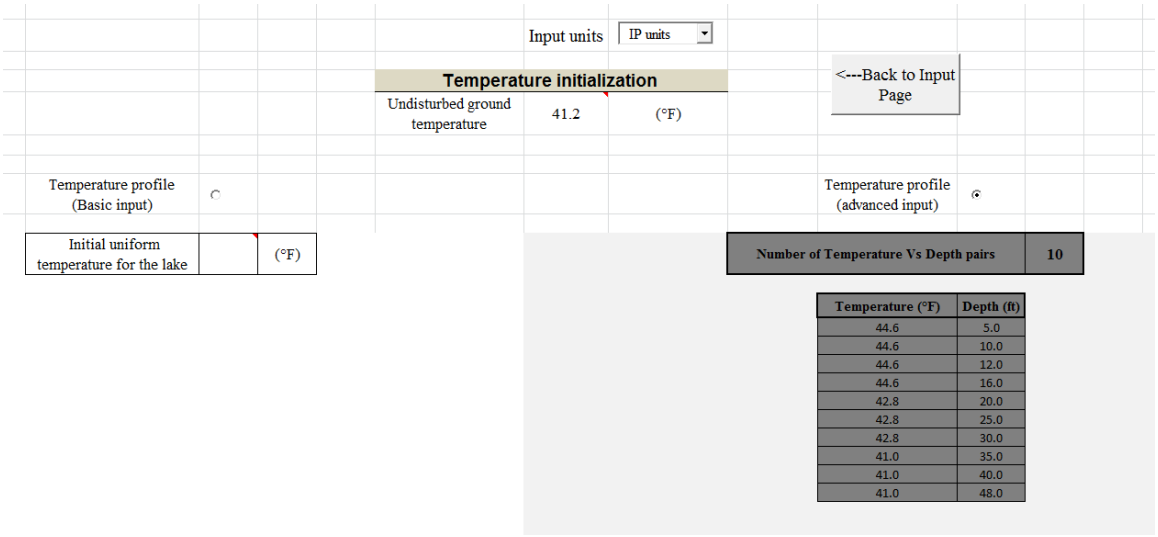

Figure C- 4: Initial temperature details of Ice Lake

Step 4: Building heating and cooling loads:

The hourly heating and cooling load data for a small apartment building is entered after selecting the "Hourly loads" option button in the "GetInputBuildingLoads" sheet. Figure C- 5 shows the entered hourly load data.

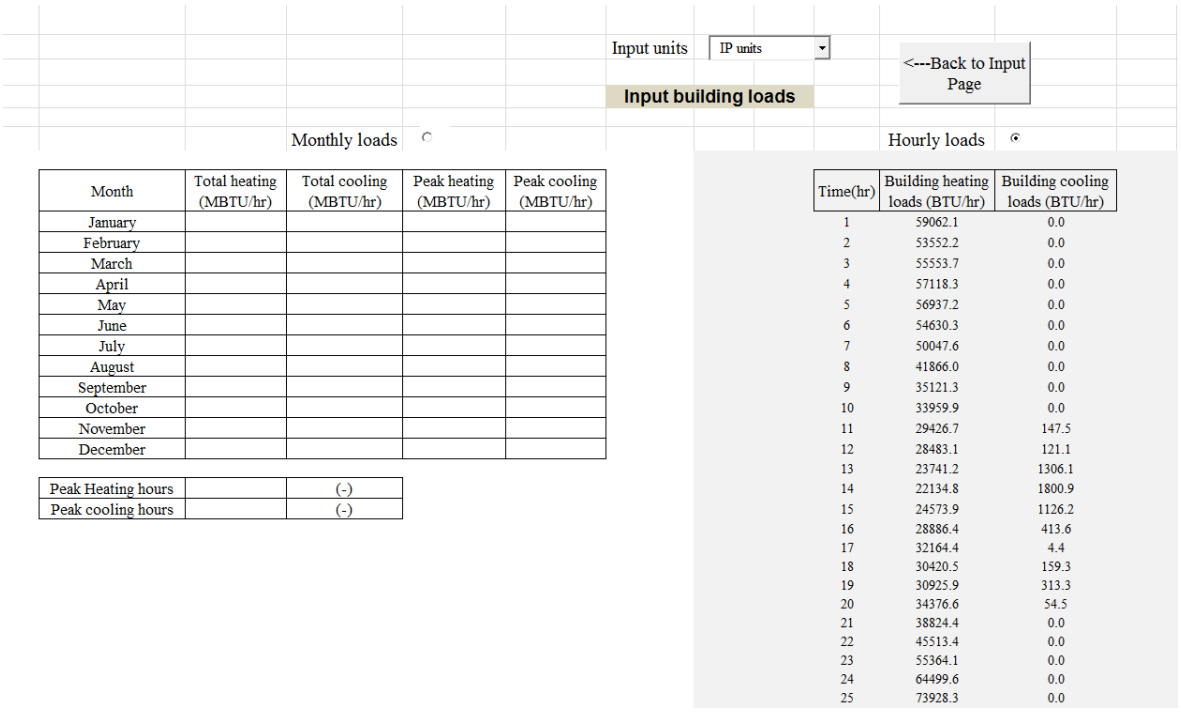

Figure C- 5: Hourly building heating and cooling load data

Step 5: Surface water heat exchanger (SWHE) parameters:

The design tool can perform heat transfer calculations and sizing on four surface water heat exchanger types namely spiral helical, horizontal spiral, vertical – horizontal slinky and flat plat plate heat exchangers. The heat exchanger type and material can be selected from the dropdown menu in the "GetInputParameters" sheet. Once the heat exchanger type is selected, the required inputs need to be entered as shown in Figure C- 6. For this example, a spiral helical coil heat exchanger is used. For this example it is assumed that the spiral-helical coil heat exchanger is submerged in the lake between the depths 5-6m (16.4 – 19.7 ft) from the surface.

Step 5 - Heat exchanger input		
Heat exchanger type	Spiral-helical coil	
Heat exchanger material	HDPE	
Hydronic tubing outer dia	1.05	(in)
Hydronic tubing inner dia	0.90	(in)
Length of hydronic tubing per coil	492.00	(ft)
Outside coil diameter	6.50	(ft)
Horizontal spacing between tubes	4.09	(in)
Vertical spacing between tubes	4.09	(in)
Total system volumetric flow rate	100.00	(GPM)
Minimum heat exchanger depth	16.40	(ft)
Maximum heat exchanger depth	19.70	(ft)

Figure C- 6: Heat exchanger inputs

Step 6: Secondary coolant properties

The user needs to specify the type and percentage of concentration of antifreeze used in the heat exchanger fluid. In this example as shown in Figure C-7, the SWHE fluid is considered to be a mixture of water and propylene glycol with concentration of 15% by volume.

Step 6 - Secondary coolant properties		
Type of antifreeze	Propylene glycol	
Percentage of Concentration	15	% by volume

Figure C- 7: Secondary coolant properties

Step 7: Calculating heat pump coefficients:

The **"**Calculate Heat Pump Coefficients" button in the "GetInputParameters" sheet directs the user to "CalcHPCoeff" data sheet. The user needs to specify some of the heat pump performance parameters from the manufacturer's catalogue for the design tool to compute the

heat pump coefficients. The performance data extracted from a commercially available 3-ton heat pump unit is shown in Table C- 1. In cooling mode, the performance sheet contains data for eleven different entering water temperatures, and in the heating mode, data is listed for eight different entering water temperatures. The number of data points to be entered in the cooling and heating mode is first provided in their respective input cells. The performance data for the heat pump in the heating and cooling modes are then entered.

Table C- 1: Performance data extracted from a commercially available 3-ton heat pump

EFT (°F)	Total cooling (MBTU/hr)	Heat rejected (MBTU/hr)	Total heating (MBTU/hr)	Heat extracted (MBTU/hr)
30.0	40.0	45.5	27.5	18.2
40.0	39.9	45.6	32.4	22.3
50.0	39.2	45.3	37.3	26.4
60.0	38.0	44.7	42.0	30.4
70.0	36.4	43.9	46.4	34.2
80.0	34.5	42.9	50.3	37.6
85.0	33.4	42.3	52.0	39.0
90.0	32.2	41.7	53.7	40.5
100.0	30.1	40.8	-	-
110.0	27.6	39.6	-	-
120.0	25.4	38.9	-	-

"Calculate HP coefficients" button calculates the heat pump coefficients and displays in the "CalcHPCoeff" sheet. Plots comparing the manufacturer performance data with the calculated curve fit are also displayed. Figure C- 8 shows the screen shot of the "CalcHPcoeff" sheet with the calculated heat pump coefficient data.

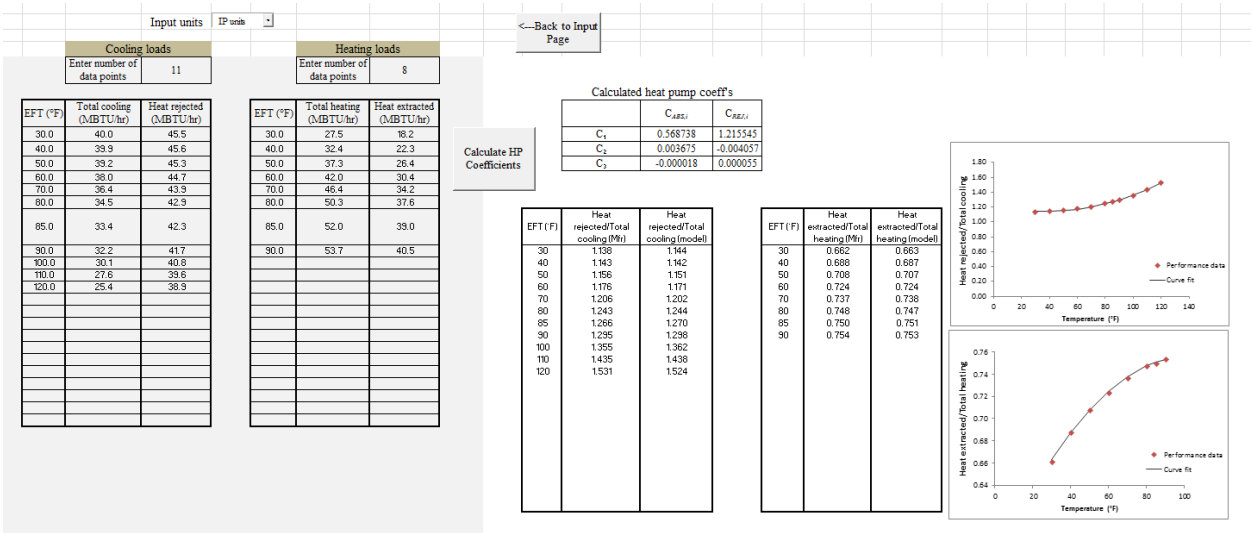

Figure C- 8: Screen shot image of the "CalcHPCoeff" sheet with the input data and calculated heat pump coefficients

Step 8: Heat pump design temperatures

For this example, the spiral helical heat exchanger coil is sized for the design minimum and maximum heat exchanger exit fluid temperatures of -1°C (30.2°F) and 30°C (86°F) as shown in Figure C- 9.

Step 8 - Heat pump design temperatures		
Minimum heat pump entering fluid temperature	30.2	(°F)
Maximum heat pump entering fluid temperature	86.0	(°F)

Figure C- 9: Heat pump design temperature input

Step 9: Verify input data and run simulation

The "View Input Data Summary" button in the "GetInputParameters" sheet directs the user to the "InputSummary" sheet. The "InputSummary" sheet displays the consolidated input data provided in the above 8 steps. Figure C- 10 displays a part of the "InputSummary" sheet.

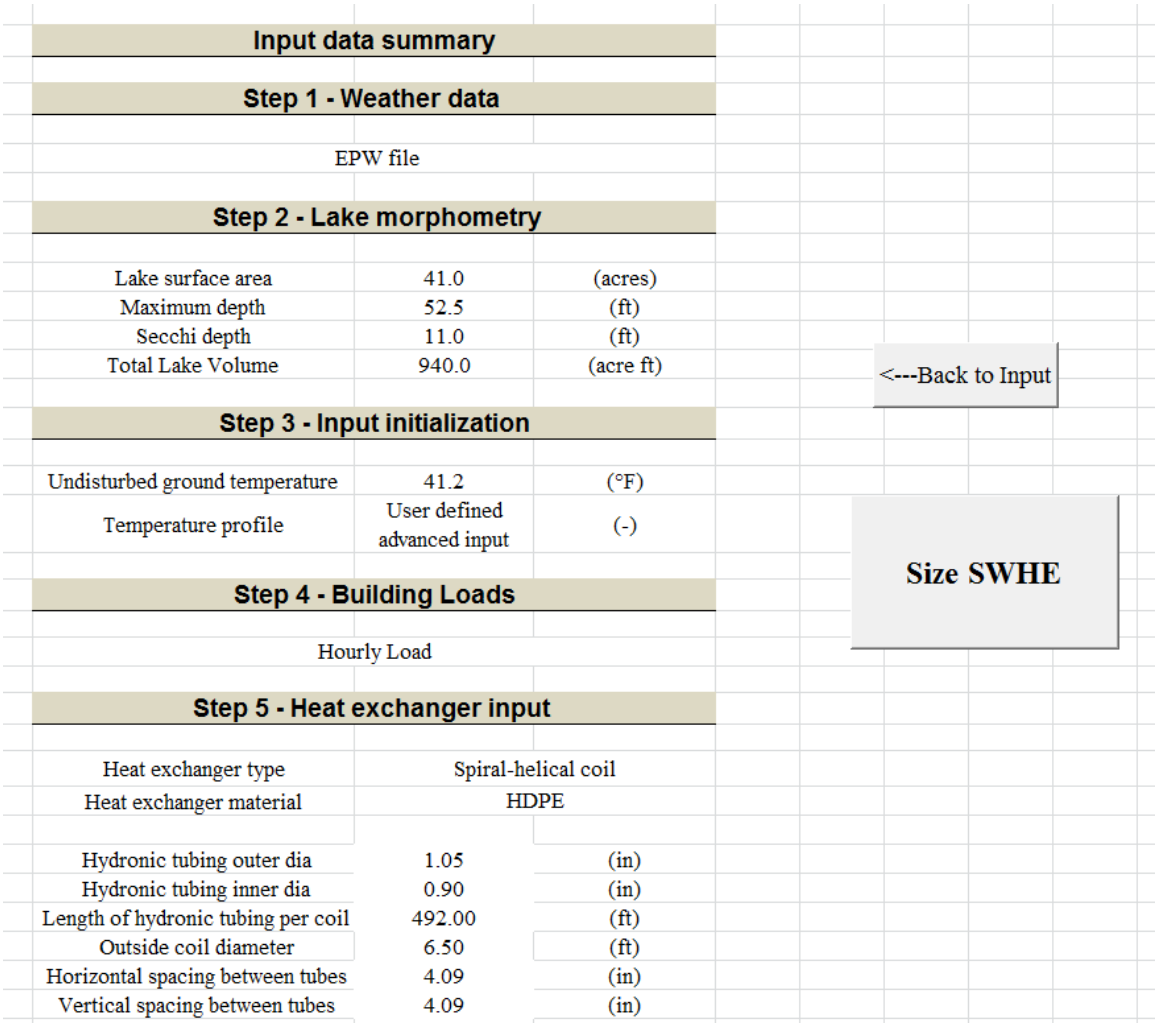

Input data summary		
Step 1 - Weather data		
EPW file		
Step 2 - Lake morphometry		
Lake surface area	41.0	(acres)
Maximum depth	52.5	(ft)
Secchi depth	11.0	(ft)
Total Lake Volume	940.0	(acre ft)
Step 3 - Input initialization		
Undisturbed ground temperature	41.2	(°F)
Temperature profile	User defined advanced input	(-)
Step 4 - Building Loads		
Hourly Load		
Step 5 - Heat exchanger input		
Heat exchanger type	Spiral-helical coil	
Heat exchanger material	HDPE	
Hydronic tubing outer dia	1.05	(in)
Hydronic tubing inner dia	0.90	(in)
Length of hydronic tubing per coil	492.00	(ft)
Outside coil diameter	6.50	(ft)
Horizontal spacing between tubes	4.09	(in)
Vertical spacing between tubes	4.09	(in)

Figure C- 10: Screenshot image of the "InputSummary" sheet

"←Back to Input page" button directs the user back to the "GetInputParameters" sheet to make any changes and "Run Simulation" button prompts the executable file to simulate lake temperatures and the design tool to size the number of SWHE coils/plates required based the input design conditions. The output will be displayed in the "WriteOutput" sheet.

Design tool output

The design tool displays the sized number of coil output in the "WriteOutput" sheet. Other output data's such as daily heat exchanger entering fluid temperatures, exit fluid temperatures and buoyancy force exerted per heat exchanger coil are also printed in the sheet as shown in Figure C- 11.

Hour	Heat Exchanger EFT(°F)	Heat Exchanger ExFT(°F)	Hx Buoyancy Force/ coil (Lbs)
1	33.2	34.6	0.0
2	32.6	34.2	0.0
3	32.1	34	0.0
4	31.9	33.9	0.0
5	32.3	34.3	0.0
6	31.9	34	0.0
7	31.9	34	0.0
8	31.8	33.8	0.0
9	29.3	32.8	0.0
10	32.4	34.4	0.0
11	34.6	35.4	0.0
12	37	37	0.0
13	38.4	38	0.0
14	39.2	38.5	0.0
15	37.6	37.4	0.0
16	37	37	0.0
17	37	37	0.0
18	35.3	35.8	0.0
19	33.7	34.9	0.0
20	37	37	0.0
21	36.8	36.8	0.0
22	35.5	35.9	0.0

Sizing of coils output

Required no of coils =	18	(-)

Month	Average Lake Temperature (°F)	Min Lake Temperature (°F)	Max Lake Temperature (°F)	Average HP EFT (°F)	Min HP EFT (°F)	Max HP EFT (°F)
January	37.56	37.32	37.47	35.61	32.01	40.21
February	37.42	37.17	37.32	36.21	32.09	41.74
March	37.25	37.03	37.17	35.92	31.45	41.68
April	39.45	36.97	48.13	39.60	33.42	51.28
May	52.78	46.87	57.14	52.78	44.00	60.23
June	56.24	53.25	61.08	56.40	52.28	63.11
July	64.79	61.10	65.90	64.69	60.36	69.00
August	64.28	59.32	67.44	64.19	58.54	71.06
September	57.54	53.14	59.75	57.50	51.46	63.46
October	41.40	37.43	50.33	40.89	33.20	52.77
November	37.76	37.58	37.59	37.08	33.19	43.06
December	37.70	37.48	37.57	35.66	31.29	40.26

Figure C- 11: Part of the "WriteOutput" sheet displaying the sized number of heat exchanger coils

Figure C- 12 shows the other part of the "WriteOutput" data sheet where the plots on the monthly minimum, maximum and average lake temperature and heat pump entering fluid temperature data and the buoyancy force exerted by a heat exchanger coil during ice formation around the coil surface are displayed.

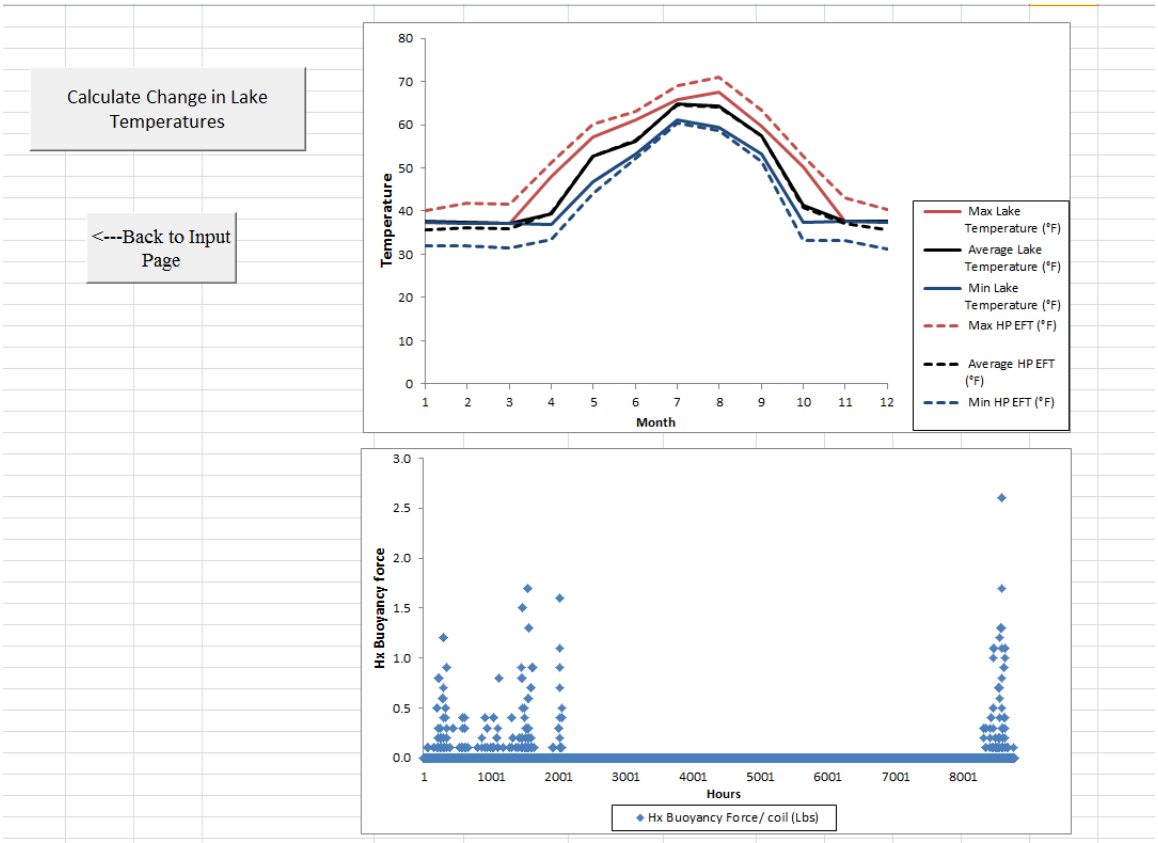

Figure C- 12: Part of the "WriteOutput" sheet displaying the plots on monthly lake and heat pump temperature data and heat exchanger buoyancy force exerted per coil

"←Back to Input page" button takes the user to the "GetInputParameters" page, if the user wants to begin a new simulation. "Calculate Change in Lake Temperatures" button calculates the effect of the sized heat exchanger coils on the lake temperatures. The calculated change in lake temperatures is displayed in the "Change in Lake Temperatures" sheet as shown in Figure C- 13. The design tool displays a plot comparing the change in lake temperatures with and without the surface water heat exchangers at the depth where the heat exchanger coils are placed.

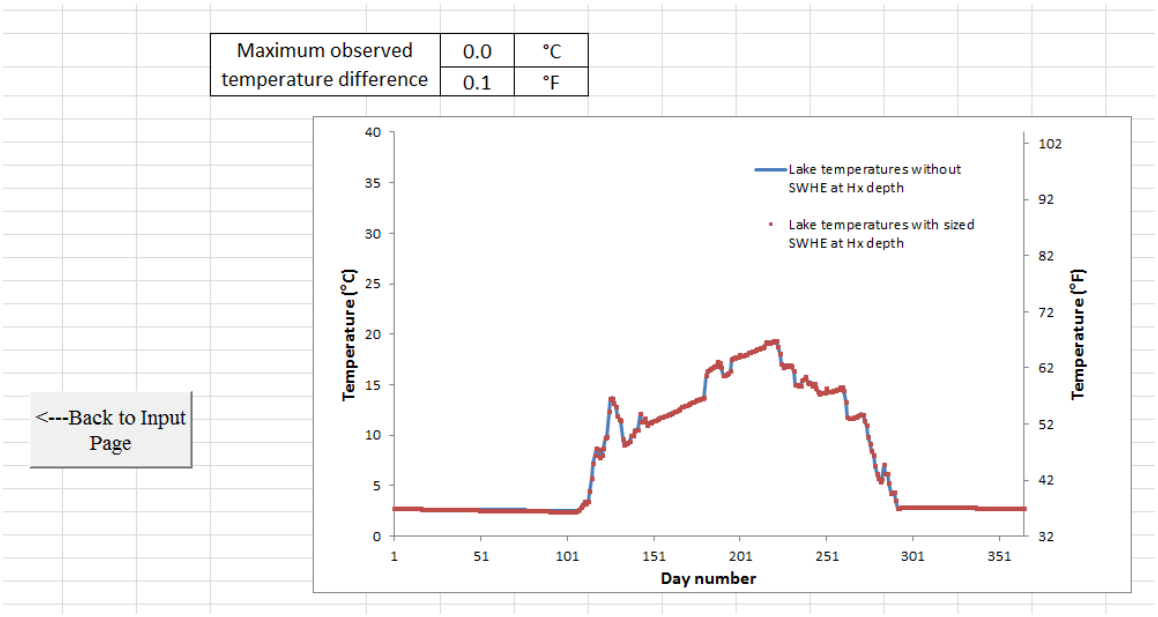

Figure C- 13: Comparison of lake temperatures at the depth where the heat exchangers are placed

APPENDIX D

ENERGY IMBALANCE STUDY

The effect of lake temperatures due to the slight imbalance in the governing equation is studied with the following example. Please note that temperatures and enthalpy values in this section are given to a higher precision that can be otherwise justified. This allows us to check the small differences.

A lake of surface area 41 acres (16.6 ha) which has a maximum depth of 20 m (65.6 ft) is used for this example study. The lake is assumed to be completely isolated from all the input energy sources (solar, longwave, sediment, heat exchangers).The lake is also assumed to have two distinct temperature zones initially. The temperature zones are divided equally based on the maximum depth of the lake as illustrated in Figure D-1. Mixing of water layers in the two temperature zones is only by means of convective mixing due to temperature-density gradient. Hence, with all these assumptions, it is possible to have a completely mixed temperature zone over a period of time.

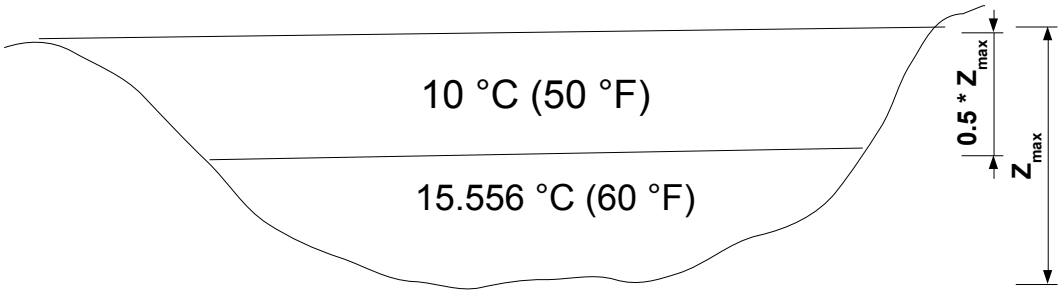

Figure D- 1: Illustration of the initial temperature assumption

It is also analytically possible to calculate the completely mixed lake temperature. The analytically calculated temperature is compared with the temperature values by simulating the lake model by using the governing equation with constant and variable water properties.

Analytical method:

The properties of water in the "Top" and "Bottom" thermal zone are given in Tables D-1. The water properties obtained from ASHRAE (2009).

Table D- 1: Water properties at the temperature zones

Water temperature zone	Water temperature °C (°F)	Water properties	
		Density kg/m^3 (lb/ft^3)	Specific enthalpy kJ/kg (BTU/lb)
Top	10.000 (50)	999.7 (62.41)	42.1 (18.1)
Bottom	15.556 (60)	999.1 (62.37)	65.1 (28.0)

The volume of water in the top zone (V_{top}) owing to the lake bathymetry is calculated as 1.179*10^6 m^3 and the volume of the lake in the bottom zone (V_{bottom}) is calculated to be 2.585 *10^5 m^3. The mass of water in the top zone (m_{top}) is calculated as 1.178*10^9 kg, and the mass of water in the bottom zone (m_{bottom}) is calculated as 2.583*10^8 kg.

The enthalpy for the lake water temperature when it is completely mixed (h_{mixed}) is calculated using the energy balance equation.

$$(m_{top} + m_{bottom})h_{mixed} = m_{top}h_{top} + m_{bottom}h_{bottom} \qquad \text{D.1}$$

Where, h_{top} and h_{bottom} are the specific enthalpy of water at the initial temperature conditions.

From these conditions the h_{mixed} is calculated as 46.242 kJ/kg (19.880 BTU/lb) and the corresponding mixed temperature value is obtained as 11.249 °C (52.248 °F).

Simulation method:

The lake model for this example study is simulated for two cases

1. Simulating the lake model with constant water properties in the governing equation

2. Simulating the lake model with variable water properties in the governing equation

For case 1, water properties at 10 °C (50 °F) are used in the governing equation. To simulate the lake for the given example condition, the input energy to the lake from solar, long wave radiation, sediment and heat exchangers are set to zero. In addition, the exchange of energy from the lake surface to the atmosphere by evaporation and convection are also set to zero. The lake model is simulated for both the cases and the total enthalpy of the lake for the first and the last day of the simulation are calculated as shown in Table D-2. Since, no energy is added or removed from this hypothetical lake example; the total enthalpy of the system is expected to remain constant throughout the simulation. However, the simulation with both constant and variable water properties in the governing equation resulted in slight increase in the net energy of the lake.

Table D- 2: Mean enthalpy and temperature comparison for the initial and final simulation day

Method	Initial mean enthalpy kJ/kg (BTU/lb)	Corresponding initial mean water temperature °C (°F)	Final mean enthalpy kJ/kg (BTU/lb)	Corresponding final mean water temperature °C (°F)
Analytical	46.217 (19.870)	11.038 (51.868)	46.217 (19.870)	11.038 (51.868)
Simulation (constant properties)	46.054 (19.800)	10.998 (51.796)	46.139 (19.836)	11.224 (52.203)
Simulation (variable properties)	45.222 (19.802)	11.004 (51.807)	46.134 (19.834)	11.223 (52.201)

From Table D-2, for this example study it is observed that the water temperatures obtained from both the simulation cases does not accurately match with the temperature estimated analytically. There seems to be a slight imbalance even when simulated with constant properties in the governing equation. The exact reason for this phenomenon could not be ascertained yet. The major reasons for not identifying the exact cause for the imbalance are the time limitations in this project and also due to the fact that it is difficult to validate this phenomenon using an

experimental setup. It is to be noted that the authors are the first to address this phenomenon and we do wish to address the possibilities of small errors in the numerical scheme which might contribute to the overall energy imbalance. However, since the imbalance affects the water temperatures only in the order of a 100^{th} of a degree, it results in negligible effects in the calculation of the heat transfer performance of surface water heat pump systems.

VITA

Krishna Conjeevaram Bashyam

Candidate for the Degree of

Master of Science

Thesis: SIMULATION OF LAKES AND SURFACE WATER HEAT EXCHANGERS FOR DESIGN OF SURFACE WATER HEAT PUMP SYSTEMS

Major Field: Mechanical Engineering

Biographical:

Education:

Completed the requirements for the Master of Science in Mechanical Engineering at Oklahoma State University, Stillwater, Oklahoma in May, 2013.

Received Bachelor of Engineering in Mechanical Engineering at Anna University - B.S.A Crescent Engineering College, Chennai, Tamil Nadu, India in 2009.

Experience:

Employed as a Research assistant in the School of Mechanical and Aerospace Engineering, Oklahoma State University, Stillwater, Oklahoma from July 2011 to May 2013.

Employed as a Teaching Assistant in the School of Mechanical and Aerospace Engineering, Oklahoma State University, Stillwater, Oklahoma from August 2010 to June 2011.

Certifications:

Engineer in Training (FE/EIT)

Professional Memberships:

Associate member - American Society of Heating, Refrigerating, and Air Conditioning Engineers (ASHRAE)